EXPLORATION OF ACYCLIC DIAMINOCARBENES AS TRANSITION METAL LIGANDS

By

DAVID ROBINSON SNEAD

A DISSERTATION PRESENTED TO THE GRADUATE SCHOOL
OF THE UNIVERSITY OF FLORIDA IN PARTIAL FULFILLMENT
OF THE REQUIREMENTS FOR THE DEGREE OF
DOCTOR OF PHILOSOPHY

UNIVERSITY OF FLORIDA

2010

To Stephanie

ACKNOWLEDGMENTS

Pursuit of the PhD and the opportunity to completely immerse myself into research endeavors was a dream of mine, only made possible through the efforts and allowances of others. To forget their help would be arrogant and inaccurate.

First and foremost, I would like to express my total and awe-filled gratitude to my wife, Stephanie. At many times, I spent incredible amounts of time away from home at the laboratory. This was a sacrifice not only on my part, but also and maybe mostly on her part. I thank her for giving so much of herself, and for supporting me after long days with understanding, conversation, or a meal. I am grateful not only for the allowance, but for the encouragement to follow this pursuit which at times might seem incomprehensible. She made it possible to get through this when I was discouraged and tired. I will always be thankful.

Secondly, I would like to thank my parents who steadfastly invested in their children's success. Without all the preparation, wisdom, education, and love they bestowed, fulfillment of the PhD would be impossible. I especially would like to thank my father for pushing and challenging me in adolescence to instill a dogmatic sense of ambition, which I value and believe to be a great asset.

I would like to thank my mentor, Sukwon Hong, for providing an exciting project to explore, belief in my abilities, and the good character to help me fulfill my career aspirations. I would also like to thank all of our wonderful Gainesville friends who enriched our lives with smiles, jokes, and conversation. You will be the most memorable part of our Florida experiment.

TABLE OF CONTENTS

page

LIST OF TABLES

LIST OF FIGURES

Abstract of Dissertation Presented to the Graduate School
of the University of Florida in Partial Fulfillment of the
Requirements for the Degree of Doctor of Philosophy

EXPLORATION OF ACYCLIC DIAMINOCARBENES AS TRANSITION METAL LIGANDS

By

David Robinson Snead

August 2010

Chair: Sukwon Hong
Major: Chemistry

Carbenes are an important class of spectator ligands, the most common of which are *N*-heterocyclic carbenes (NHCs). Lesser explored carbene ligands are acyclic diaminocarbenes(ADCs), which possess a degree of intrigue due to significant variations in electronic and steric parameters from NHCs. In this work, ADCs are explored, with a special emphasis on methods of complexation to metal centers.

ADC ligands were built from chiral *C_1*-symmetric pyrrolidine subunits. Ureas **2-1** through **2-4** were synthesized from 2-substituted pyrrolidines, and X-ray analysis was obtained for these compounds. The location of the chiral substituents proximal to the oxygen atom of the carbonyl led to a reasonable hypothesis that these ADCs might be useful asymmetric ligands. Palladium complexes **2-15** and **2-18** were formed through oxidative addition of chloroamidinium precursors; however steric crowding created by the phosphine ligands caused the chiral groups to orient themselves away from the metal center, as observed by X-ray analysis. ADCs with substituents larger than benzyl were not able to be isolated with palladium, likely as a result of steric constraints. Complexes **2-15**, **2-18**, and **2-26** were tested in Suzuki reactions, but as the degree of ligand substitution increased, reactivity decreased.

Access to a diversity of metal complexes from chloroamidiniums was restricted based on use of the oxidative addition methodology and also required the use of electron rich ligands like phosphines. As such, a new more general method of carbene generation was developed. Lithium-halogen exchange was applied to chloroamidiniums to give carbenoid intermediates. 13^C-NMR of the carbene in solution and formation of thiourea constitute proof, and after generation, Rh, Ir, Pd, and B complexes were produced. Interestingly, X-ray analysis of Rh-ADC complex **3-5** based on chiral *C_1*-symmetric pyrrolidine subunits demonstrated a change in conformational preference from the palladium compounds, as the methyl substituents were located proximal to the rhodium center. Rh-ADC complex **3-5** was tested in catalytic reactions and showed good reactivity in 1,4 conjugate addition of aryl boronic acids to cyclohexenone and in 1,2 addition of aryl boronic acids to aryl aldehydes. Notably, the ADC ligand performed better than NHC in 1,2 addition.

CHAPTER 1
INTRODUCTION

Acyclic Diaminocarbenes

N-heterocyclic carbenes (NHCs) are of the most ubiquitous class of ligands, and their presence has only grown since the discovery of isolable carbenes by Arduengo in 1991.[1] The emergence of NHCs is attributed to their ability to act as a more robust alternative to phosphines. Many metal complexes incorporating NHCs are more stable against heat, moisture and oxygen than their phosphine counterparts.

Carbenes, similarly to phosphines, show strong σ-donor capacity, creating an analogy between the two classes of ligands,[2] but an advancement in the understanding of carbenes has shown these ligands have a rich breadth of chemistry all their own and are much more than simple "phosphine mimics".[3] Carbenes are more basic than even the most electron-donating phosphines.[4] Additionally, they are less labile, and the lower lability is most likely due to bond dissociation energies that are practically double that of even the most electron rich trialkyl phosphines.[3a,4a] In some notable cases, carbene complexes have demonstrated higher activity than even the best phosphine systems.[5]

Typically, carbenes used as ancillary ligands are located on a heterocyclic scaffolding such as **1-1** shown below. Rare cases feature acyclic diaminocarbenes (ADCs) in which the carbene ring has been dissolved (**1-2** to **1-4**). ADCs are a promising variant of NHCs possibly representing the next generation of carbenes. ADCs feature a larger carbene N—C—N bond angle with respect to regular NHCs, leading to a more basic carbene lone pair (Table 1).[6] The carbene's move toward linearity decreases the singlet triplet energy gap of the carbene frontier molecular orbitals,[1j] and bis(diisopropylamino) carbene **1-2** is the most basic carbene known to date.

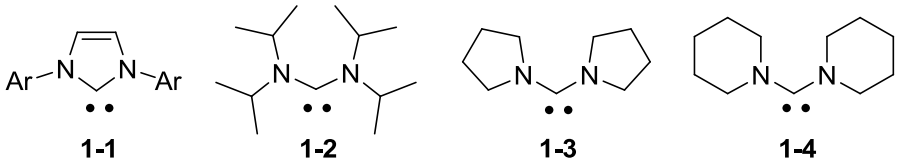

Figure 1-1. An *N*-heterocyclic carbene and some acyclic diaminocarbenes.

In addition to the increased donor capacity of ADCs, it is envisioned that ADCs could be quite useful in asymmetric catalysis. The larger bond angle of these carbenes should place chiral centers closer to metal coordination spheres than traditional NHCs, leading to a more efficient transfer of chirality. Thus far, only one example of a chiral ADC complex exists.[7a] The goal of this research was to explore novel chiral ADCs.

Table 1-1. Calculated values of N—C—N bond angle and proton affinity (PA) for select carbenes

	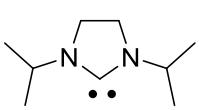 1-5	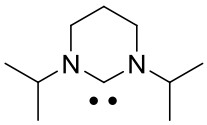 1-6	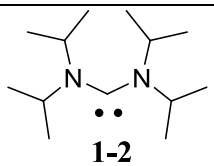 1-2
N—C—N Bond Angles (°)	106.0	116.3	121.0
Proton Affinity (kcal/mol)	271.4	278.9	282.9

ADCs have been relatively unexplored with respect to NHCs, and relatively few examples of catalysis with ADCs exist. Slaughter and Fürstner have both isolated metal complexes with ADCs and then used them catalytically, and Thadani has shown in situ generation of metal complexes with ADCs to be useful.[7] The lack of proliferation is partially caused by the difficulties associated from working with ADCs. Since they are more basic and sterically hindered than the usual NHCs, extension of common methods for the preparation of metal compounds do not always translate. Therefore, non-traditional modes of complexation are sometimes necessary.

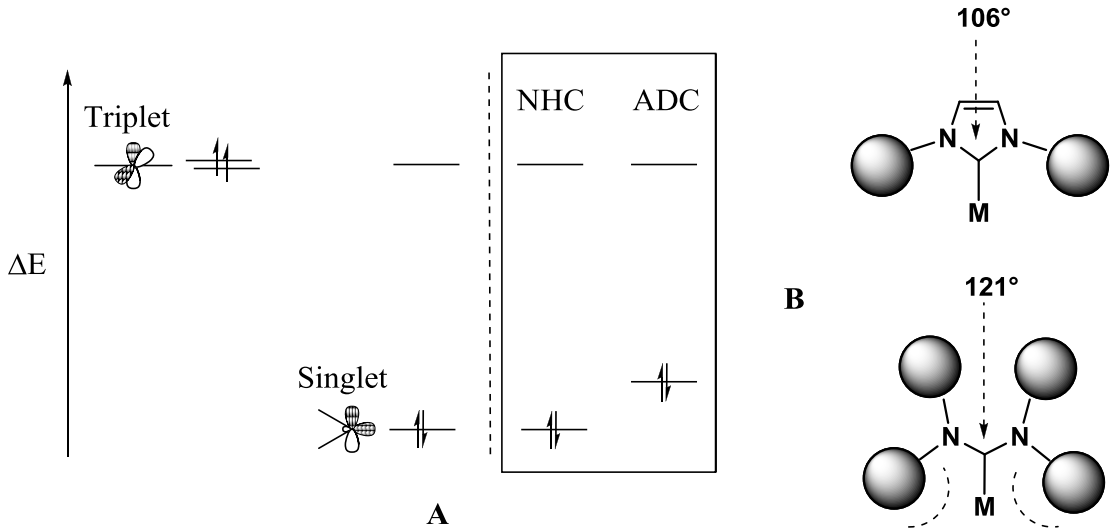

Figure 1-2. A comparison of electronic and steric parameters for NHC and ADC ligands. A) Frontier molecular orbitals of carbenes. Triplet carbenes adopt a linear geometry whereas singlet carbenes take on a bent geometry with 120° angles. An NHC is a typical singlet carbene, but an ADC has a larger carbene bond angle. As it moves toward a more linear state, the HOMO rises in energy with the lone pair becoming more donating as a result. B) The greater carbene bond angle of the ADC places the *N*-substituents in closer proximity to the metal center.

Fürstner and co-workers utilized chloroamidinium ions in a novel way to initiate formation of metal complexes with ADCs.[7c,d] This route relied on three tasks: formation of ureas, generation of chloroamidinium ions, and the ability to metalate chloroamidinium salts. The chloroamidinium ions were formed by reacting ureas with oxalyl chloride, and the chlorinated product underwent oxidative addition to electron-rich, palladium phosphine species. NHC and ADC complexes were synthesized through this route, and the products were demonstrated as useful in Suzuki Coupling, Heck Coupling, and Buchwald-Hartwig amination. Previous research by Stone and Cavell gave precedent for this work.[8]

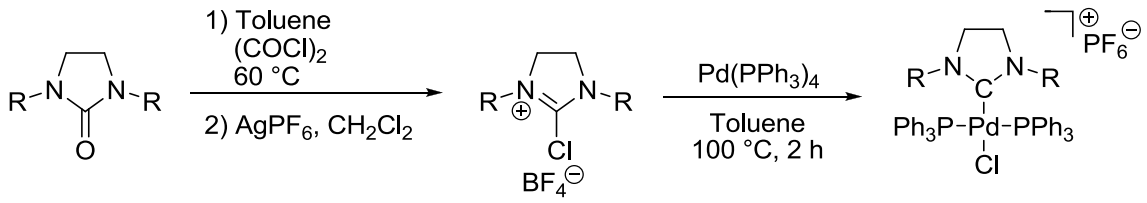

Figure 1-3. General method of preparation of carbene metal complexes via Fürstner's route.

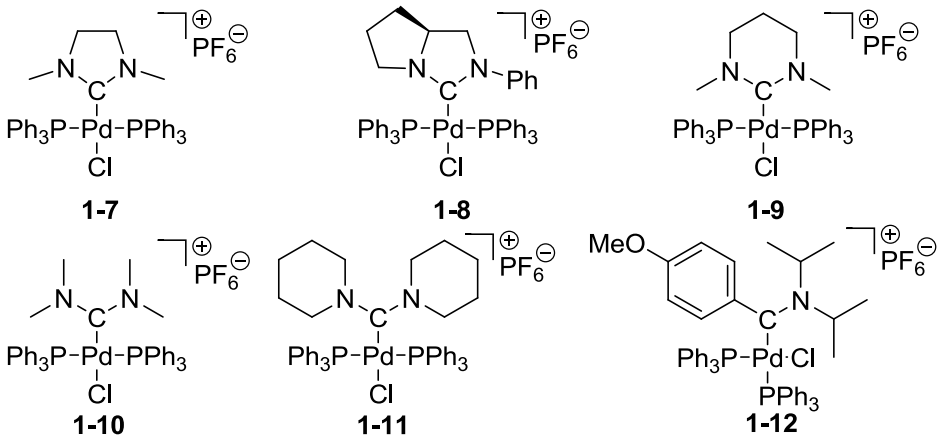

Figure 1-4. Some carbene metal complexes formed by oxidative addition of chloroamidinium ions.

CHAPTER 2
BIS(2-ALKYLPYRROLIDIN-1-YL)METHYLIDENES AS CHIRAL ACYCLIC DIAMINOCARBENE LIGANDS

Introduction

Potentially, ADCs based upon a 2-substituted pyrrolidine framework might demonstrate interesting properties. Depending on the conformational preference of the chiral substituents, the ligands might show an ability to influence stereochemical outcomes in catalysis. Alternatively, potential rotation about the N—C bond of the carbene would provide a ligand capable of drastic alterations in its steric profile (Figure 2-1). Complexes capable of conformational flexibility can

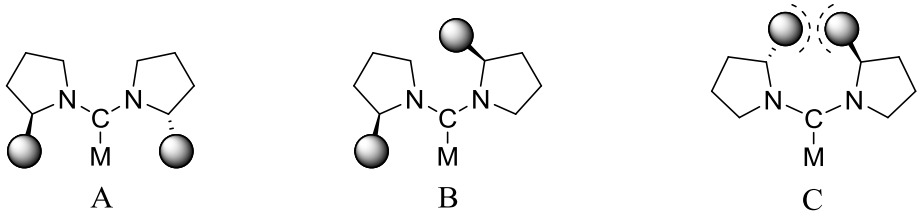

Figure 2-1. Potential conformers associated with carbenes designed about 2-substituted pyrrolidines. A) Adoption of a conformer with chiral groups situated close to the metal center might afford a catalyst capable of displaying high enantioselectivities and additionally is quite sterically hindered. B) A conformer with one chiral group proximal to the metal center might promote some selectivity in catalytic reactions, and is less intruding into the metal coordination sphere. C) The rotamer with both substituents positioned away from the metal center is expected to display the lowest levels of selectivity in catalysis and exhibits the least steric hindrance.

lead to high catalytic activity, as illustrated by Glorius and co-workers, since a transition metal promoted transformation might require both an unhindered (open) or congested (closed) environment during a catalytic cycle (Figure 2-2).[9] For example oxidative addition is facilitated by a non-crowded coordination sphere, whereas reductive elimination is promoted by a sterically congested environment around the metal. Both processes are often important within the same catalytic cycle, such as that known for the Suzuki cross-coupling reaction, and while the needs of oxidative addition and reductive elimination appear to be at odds, they can be met with the use of a conformationally flexible ligand.

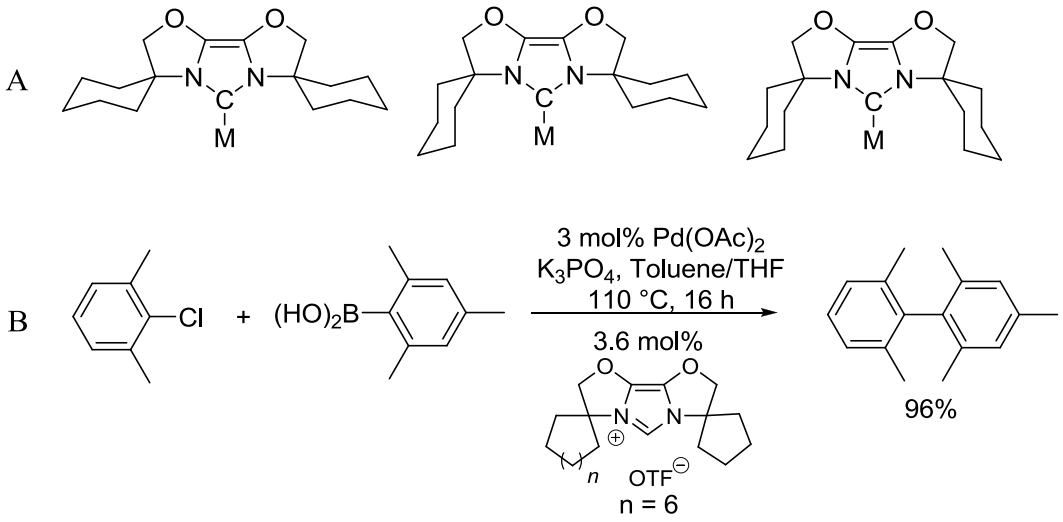

Figure 2-2. Unique abilities of conformationally flexible ligands. A) Potential conformers of a bis-oxazoline based NHC where the leftmost structure is relatively non-hindered and the structure on the right is most hindered. B) High catalytic activity of conformationally flexible ligand.

Ureas Stemming from 2-Substituted Pyrrolidine

Commercially available amines such as (*S*)-(+)-2-methyl-pyrrolidine and (*R*)-(+)-2-(diphenylmethyl)pyrrolidine were used along with (*R*)-(+)-2-isopropyl-pyrrolidine and (*R*)-(+)-2-benzyl-pyrrolidine to give symmetrically substituted ureas stemming from 2-substituted pyrrolidine derivatives. The mono-substituted pyrrolidines easily afforded ureas **2-1** to **2-4** (Figure 2-3).

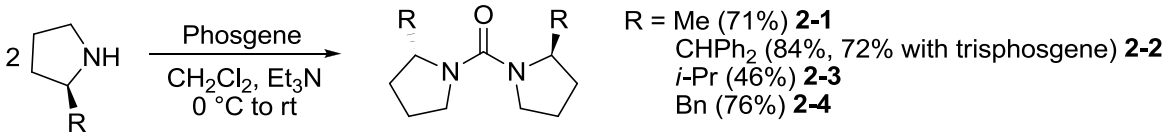

Figure 2-3. Ureas from 2-substituted pyrrolidine derivatives.

(*R*)-(+)-2-isopropyl-pyrrolidine was synthesized from valine, and amide **2-9** was prepared by a known procedure (Figure 2-4).[10] The carbonyl functionality of **2-9** was reduced with $LiAlH_4$ and protected in situ with Boc_2O because of volatility of the corresponding amine. Protected amine **2-10** was deprotected with 4M HCl in dioxane, the excess HCl was removed *in*

vacuo, and a phosgene solution was added to give urea **2-3**. (*R*)-(+)-2-benzyl-pyrrolidine was synthesized following the same procedure and leading to the related urea **2-4**.

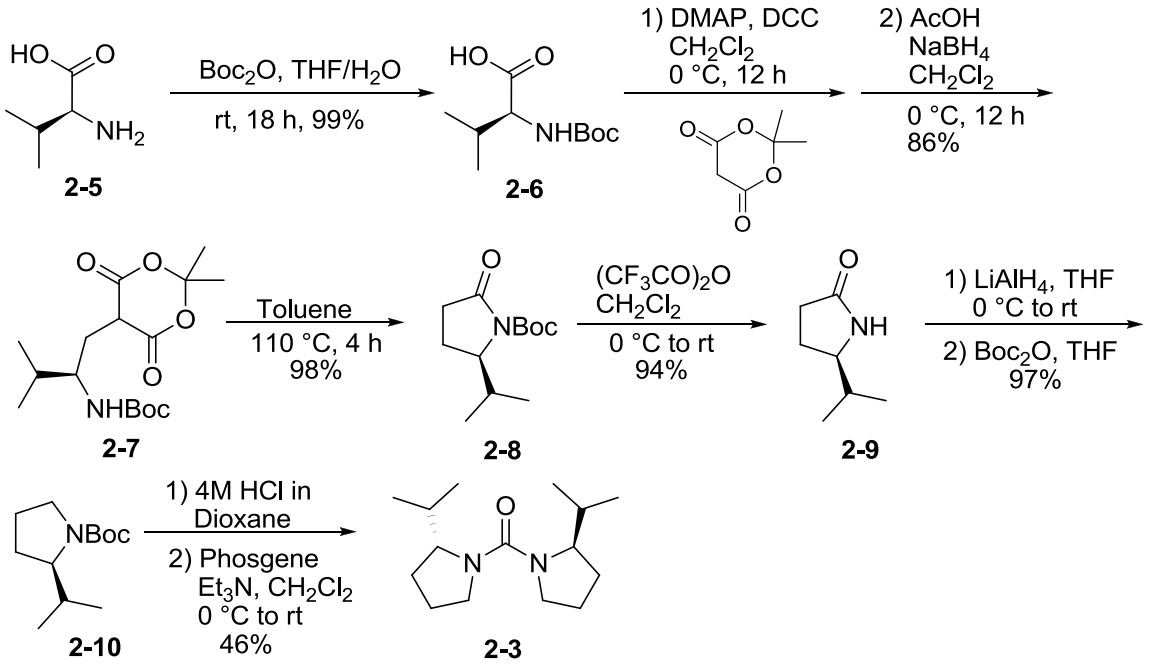

Figure 2-4. Synthesis of urea **2-3** from condensation of (*R*)-(+)-2-isopropyl pyrrolidine.

Urea Crystal Structures

Crystal structures of ureas **2-1** and **2-2** were obtained to better understand conformational preference of the alkyl substituents and to discern whether the ensuing carbenes might be suitable as chiral ligands. Three different conformers, **A**, **B**, and **C**, are attainable as rotation about the amide bond is possible (Figure 2-5). Conformer **A** places the aliphatic substituents in a *syn*-relationship proximal to the carbonyl functionality. This isomer was expected to predominate over **B** and **C** as it relieves steric hindrance associated with an alkyl substituent located distal to the carbonyl group. Indeed, when a single crystal was obtained for ureas **2-1** and **2-2**, isomer **A** was observed (Figures 2-6 and 2-7). Notably, the two pyrrolidine ring systems are not coplanar. In the solid state, **2-1** demonstrates a dihedral angle of ~ 34° for N(2)-

C(1)- N(1)-C(2) and N(1)-C(1)-N(2)-C(7), and in urea **2-1** these dihedral angles are larger at ~ 40°.

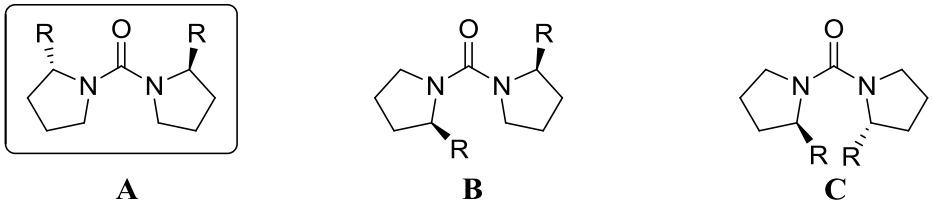

Figure 2-5. Potential conformers of ureas **2-1** to **2-4**.

This twisting of the ring systems seems to indicate steric repulsion at carbons C(2)-C(7) and C(2)-C(19) for **2-1** and **2-2** respectively and growing strain in the molecule. It also indicates a lack of conjugation. The growing strain in the bulkier molecule becomes even more evident when viewing the N(1)-C(1)-N(2) bond angle. The less hindered **2-1** possesses an N—C—N bond angle of 116.57(9)°, but for urea **2-2** this value shrinks to 113.3(5)°, further deviating from the ideal 120° and pushing the methylene groups adjacent to nitrogen closer together.

If a similar conformational preference is assumed with carbenes, acyclic carbenes stemming from 2-substituted pyrrolidines might make good asymmetric ligands. In the solid state the ureas show a conformational preference for **A** over **B** and **C**, and there seems to be a degree of repulsion between C(2) and C(7) in **2-1** and C(2) and C(19) in **2-2**. An isomer of type **A** should be even more favorable in the case of a carbene since the carbene generally shows a higher level of conjugation due to the empty p-orbital centered on C(1). This increase in conjugation and flatness of the carbene should decrease the twisting in the pyrrolidine ring system, and therefore it should be less able to accommodate the strain induced from conformations such as **B** and **C**.

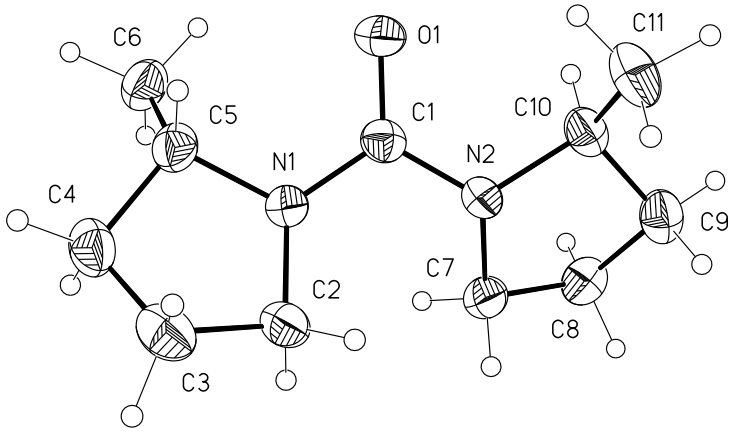

Figure 2-6. Molecular structure of urea **2-1**. Selected bond lengths (Å) and angles (°): O(1)-C(1) 1.2349(13), N(1)-C(1) 1.3733(13), N(2)-C(1) 1.3739(13), N(1)-C(1)-N(2) 116.57(9), N(2)-C(1)-N(1)-C(2) 34.66(15), N(1)-C(1)-N(2)-C(7) 33.61(15).

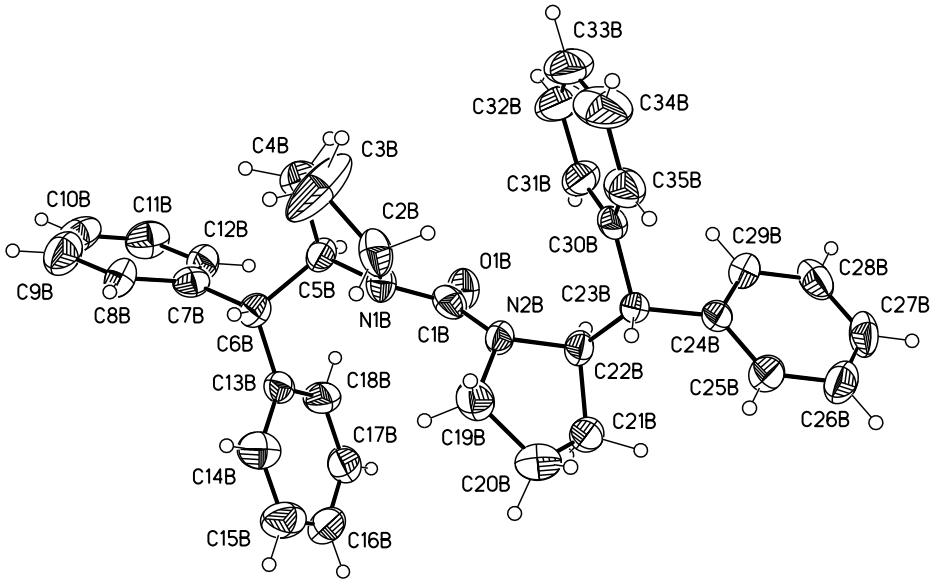

Figure 2-7: Molecular structure of urea **2-2**. Selected bond lengths (Å) and angles (°): O(1)-C(1) 1.242(6), N(1)-C(1) 1.372(6), N(2)-C(1) 1.373(7), N(1)-C(1)-N(2) 113.3(5), N(2)-C(1)-N(1)-C(2) 40.0(8), N(1)-C(1)-N(2)-C(19) 43.0(8).

Table 2-1. Crystal data and structure refinement for **2-1**.

Empirical formula	C11 H20 N2 O	
Formula weight	196.29	
Temperature	173(2) K	
Wavelength	0.71073 Å	
Crystal system	Orthorhombic	
Space group	$P2_12_12_1$	
Unit cell dimensions	a = 8.9984(7) Å	α= 90°.
	b = 10.1229(8) Å	β= 90°.
	c = 12.283(1) Å	γ = 90°.
Volume	1118.86(15) $Å^3$	
Z	4	
Density (calculated)	1.165 Mg/m^3	
Absorption coefficient	0.075 mm^{-1}	
F(000)	432	
Crystal size	0.20 x 0.20 x 0.18 mm^3	
Theta range for data collection	2.61 to 27.50°.	
Index ranges	$-11\leq h\leq 11$, $-13\leq k\leq 13$, $-15\leq l\leq 12$	
Reflections collected	7612	
Independent reflections	2561 [R(int) = 0.0312]	
Completeness to theta = 27.50°	100.0 %	
Absorption correction	Integration	
Max. and min. transmission	0.9904 and 0.9851	
Refinement method	Full-matrix least-squares on F^2	
Data / restraints / parameters	2561 / 0 / 127	
Goodness-of-fit on F^2	0.961	
Final R indices [I>2sigma(I)]	R1 = 0.0321, wR2 = 0.0744 [2149]	
R indices (all data)	R1 = 0.0399, wR2 = 0.0763	
Absolute structure parameter	-0.4(11)	
Largest diff. peak and hole	0.165 and -0.264 $e.Å^{-3}$	

Table 2-2. Crystal data and structure refinement for **2-2**.

Empirical formula	C35 H36 N2 O
Formula weight	500.66
Temperature	173(2) K

Wavelength	0.71073 Å	
Crystal system	Monoclinic	
Space group	P2(1)	
Unit cell dimensions	a = 16.0406(14) Å	α= 90°.
	b = 10.8168(9) Å	β= 90.539(1)°.
	c = 56.512(5) Å	γ = 90°.
Volume	9804.9(14) $Å^3$	
Z	14	
Density (calculated)	1.187 Mg/m^3	
Absorption coefficient	0.071 mm^{-1}	
F(000)	3752	
Crystal size	0.19 x 0.11 x 0.05 mm^3	
Theta range for data collection	1.08 to 25.00°.	
Index ranges	$-9\leq h\leq 19$, $-12\leq k\leq 12$, $-67\leq l\leq 64$	
Reflections collected	40889	
Independent reflections	28710 [R(int) = 0.0496]	
Completeness to theta = 25.00°	94.7 %	
Absorption correction	None	
Refinement method	Full-matrix least-squares on F^2	
Data / restraints / parameters	28710 / 1 / 2413	
Goodness-of-fit on F^2	0.841	
Final R indices [I>2sigma(I)]	R1 = 0.0555, wR2 = 0.0884 [10696]	
R indices (all data)	R1 = 0.1757, wR2 = 0.1230	
Absolute structure parameter	0.8(10)	
Largest diff. peak and hole	0.151 and -0.185 $e.Å^{-3}$	

Formation of Palladium-ADC Complexes

Ureas were treated with a chlorinating agent such as oxalyl chloride or $POCl_3$ to generate the chloroamidinium salts (Figure 2-8). Anion exchange was performed on these salts to make them less hygroscopic, and the chloride anion was substituted with a tetrafluoroborate anion. The isolated chloroamidinium salts were then reacted with $Pd(PPh_3)_4$ in toluene at 100 °C for two hours, and the product was purified by recrystallization (Figure 2-9).

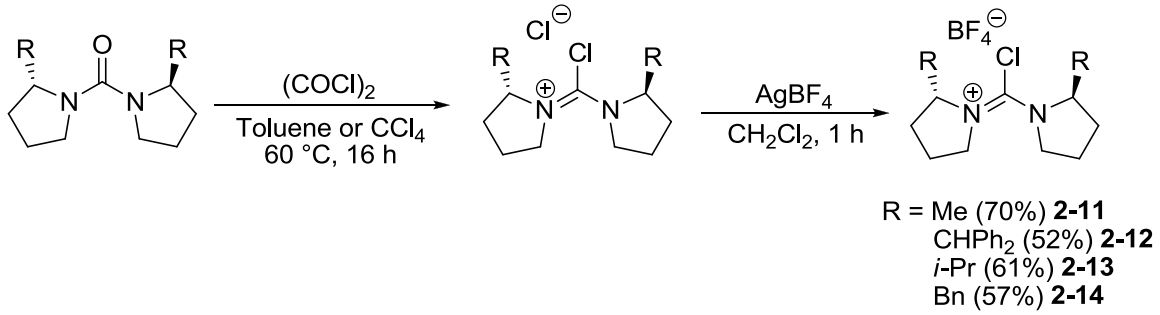

Figure 2-8. Chlorination of ureas with oxalyl chloride.

Chloroamidiniums featuring primary alkyl substituents such as **2-11** (methyl group) and **2-14** (benzyl group) afforded ADC-Pd complexes in good yield. However, more congested secondary alkyl substituted carbene precursors **2-12** ($CHPh_2$) and **2-13** (*i*-Pr) did not afford the desired complex as an isolable substance.

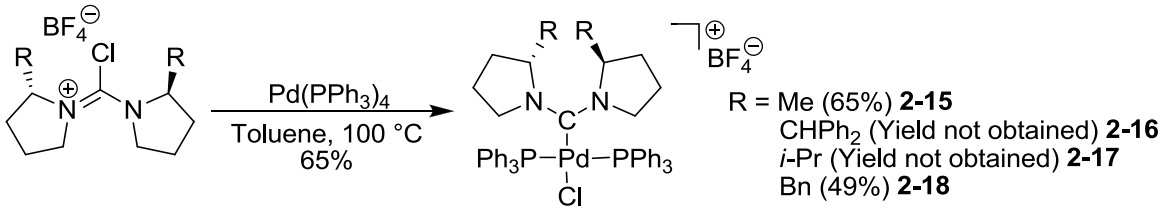

Figure 2-9. Complexation of chloroamidiniums to palladium.

The metal complexes of **2-15** and **2-18** were fully characterized by mass spectroscopy and NMR, and a crystal structure of **2-15** was obtained as well. Unfortunately, conclusive NMR and mass spectroscopy were not obtained for complexes **2-16** and **2-17**.

The X-ray crystal structure of complex **2-15** provides several key insights and depicts an image of a somewhat strained molecule (Figure 2-10). In contrast to the urea crystal structure, the methyl groups are positioned away from the metal center, apparently reducing steric repulsions with the triphenyl phosphine ligands. Thus the phenyl rings of triphenyl phosphine are staggered with respect to the chloride ligand yet eclipsed with regards to the carbene. This

close proximity and resulting repulsion certainly plays a role in the orientation of the methyl groups.

Similarly to crystal structures obtained by Fürstner's group,[7c] the plane of the carbene created by N(1)-C(1)-N(2) is nearly orthogonal to the metal coordination plane defined by the four ligands P(1), P(2), Cl(1), and C(1). The dihedral angles of N(2)-C(1)-N(1)-C(5) and N(1)-C(1)-N(2)-C(10) are less than those observed with the corresponding urea. They are 12.6(5)° and 14.8(5)° respectively, still showing a slight divergence from coplanarity and complete conjugation; however, this is not unusual for acyclic diaminocarbenes.[6c]

The increased carbene bond angle [N(1)-C(1)-N(2)] is of the highest interest, and its value is 123.7(2)°. This is one of the largest diaminocarbene bond angles known, and to the best of my knowledge only one metal carbene complex shows a larger angle.[6a,d] The chromium complex **2-19** has an N—C—N bond angle of 125°, although it is bound in η^2-fashion, and the author states this increased hapticity enlarges the angle (Figure 2-11). The carbene bond angle of complex **2-15** is ~ 1.5 to 2.0° greater than analogous achiral complexes such as **1-10** prepared by Fürstner and co-workers. While small, this value is certainly not insignificant. The increase is most likely caused by the increased repulsion due to methyl groups close proximity. The palladium carbene bond length is 2.021(2) Å.

An analysis and comparison to crystal structures from the work of Fürstner and co-workers leads to interesting conclusions. Larger bond angles lead to longer metal carbene bonds. The longer bond is possibly caused by greater intrusion into the metal coordination sphere which commonly promotes lower bond dissociation energies in NHCs.[3a] It is also possible the increase in bond length comes from a carbene that is increasing in triplet character and that is potentially destabilized by this change.

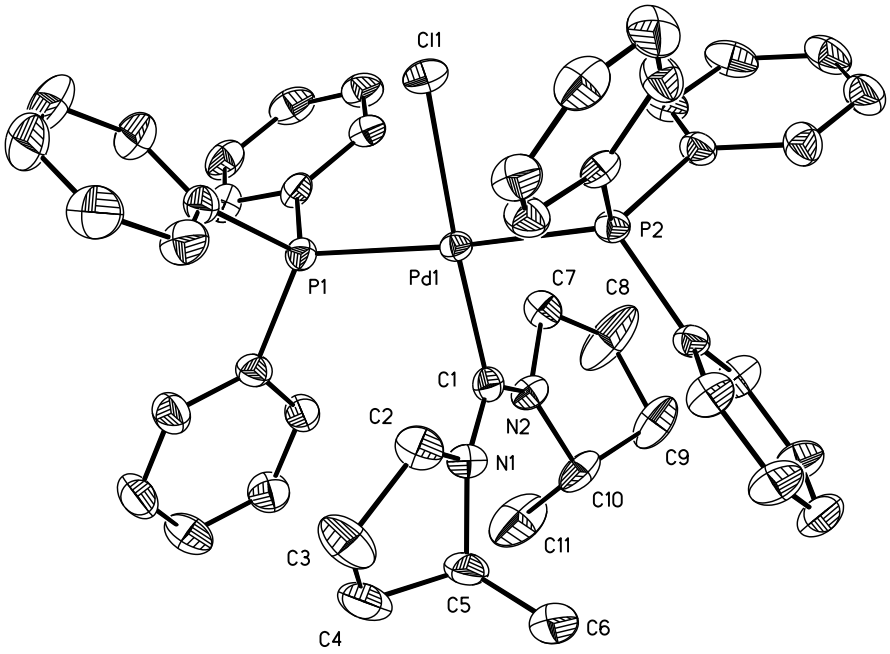

Figure 2-10. Molecular structure of complex **2-15**. Selected bond lengths (Å) and angles (°): Pd(1)-C(1) 2.021(2), N(1)-C(1) 1.329(3), N(2)-C(1) 1.342(3), N(1)-C(1)-N(2) 123.7(2), N(2)-C(1)-N(1)-C(5) 12.6(5), N(1)-C(1)-N(2)-C(19) 14.8(5).

Table 2-3. Crystal data and structure refinement for **2-15**.

Empirical formula	C47 H50 B Cl F4 N2 P2 Pd	
Formula weight	933.49	
Temperature	173(2) K	
Wavelength	0.71073 Å	
Crystal system	Orthorhombic	
Space group	P212121	
Unit cell dimensions	a = 16.0636(8) Å	α= 90°.
	b = 16.2605(8) Å	β= 90°.
	c = 19.0326(9) Å	γ = 90°.
Volume	4971.4(4) $Å_3$	
Z	4	
Density (calculated)	1.247 Mg/m_3	
Absorption coefficient	0.538 mm^{-1}	

F(000)	1920
Crystal size	0.19 x 0.13 x 0.11 mm^3
Theta range for data collection	1.65 to 26.68°.
Index ranges	$-19 \leq h \leq 19$, $-20 \leq k \leq 15$, $-23 \leq l \leq 23$
Reflections collected	28914
Independent reflections	9381 [R(int) = 0.0550]
Completeness to theta = 25.00°	99.9 %
Absorption correction	Integration
Max. and min. transmission	0.9245 and 0.8844
Refinement method	Full-matrix least-squares on F^2
Data / restraints / parameters	9381 / 7 / 529
Goodness-of-fit on F^2	1.068
Final R indices [I>2sigma(I)]	R1 = 0.0311, wR2 = 0.0818 [8716]
R indices (all data)	R1 = 0.0337, wR2 = 0.0828
Absolute structure parameter	0.017(18)
Largest diff. peak and hole	0.370 and -1.869 $e.Å^{-3}$

When bulky chloroamidiniums such as **2-12** and **2-13** are used, the corresponding carbene ligands should exhibit N—C—N bond angles greater than that observed for complex **2-15** with the relatively small methyl substituents. The larger carbene bond angles probably increase the potential metal carbene bond length accounting for the difficulty in obtaining the more complex compounds **2-16** and **2-17**.

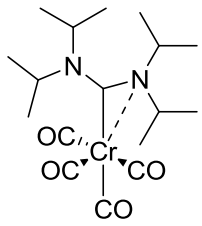

2-19

Figure 2-11. Chromium-ADC complex prepared by Herrmann.

Table 2-4. N—C—N bond angles and Pd-C bond lengths for select carbenes.

	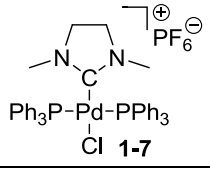 **1-7**	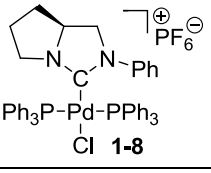 **1-8**	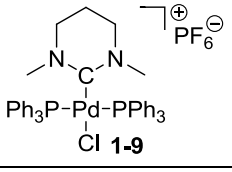 **1-9**	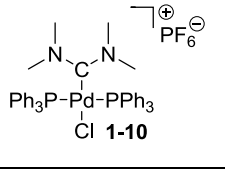 **1-10**
N—C—N Angles (°)	109.70	108.95	119.6	121.6
Pd—C Bond Lengths (Å)	1.9805	1.9687	2.005	2.003

	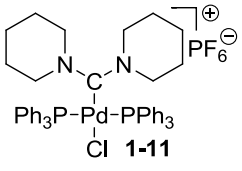 **1-11**	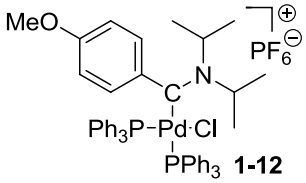 **1-12**	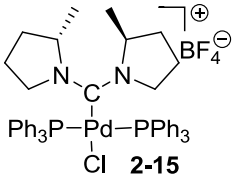 **2-15**
N—C—N Angles (°)	122.3	124.0	123.7
Pd—C Bond Lengths (Å)	2.023	2.047	2.021

Suzuki Cross-Coupling

Palladium complexes of electron-rich, sterically demanding phosphines or NHC ligands are effective catalysts for sterically demanding Suzuki couplings, and those ligands are believed to stabilize a putative monoligated Pd complex.[11] It is known that the oxidative addition step is promoted by a highly σ-donating ligand to stabilize the Pd^{II} oxidation state whereas the reductive elimination step can be accelerated by a sterically demanding ligand. Therefore, the highly σ-donating and bulky ADC ligand is perfect, meeting those exact requirements. In fact, Thadani and co-workers reported that ADC-Pd complexes efficiently catalyze demanding Suzuki couplings, and therefore application of chiral ADC-Pd complexes in the asymmetric Suzuki coupling reaction is promising.[7b] Prior to our studies, Fürstner and co-workers conducted some preliminary work with the cationic palladium complexes in the Suzuki reaction. Using 1 mol % of **1-7**, phenyl boronic acid and 4-bromoacetophenone were coupled in 79% yield (Equation 2-1). With catalyst **1-8**, that yield improved to 89%.

In our work, application of the reported conditions led to low to moderate yields in the coupling of simple substrates such as **2-20** and **2-21** and **2-20** and **2-22** with ADC complexes

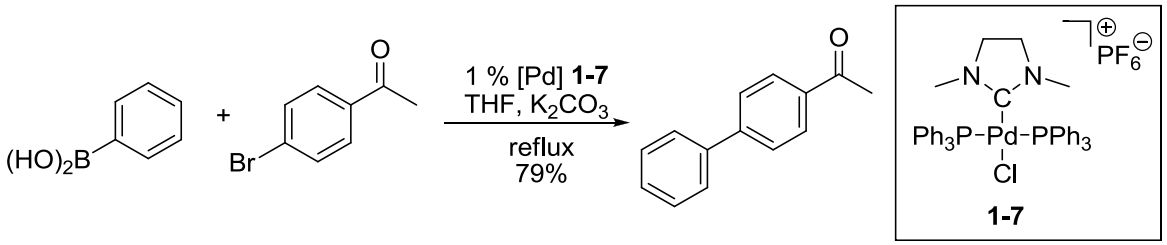

(2-1)

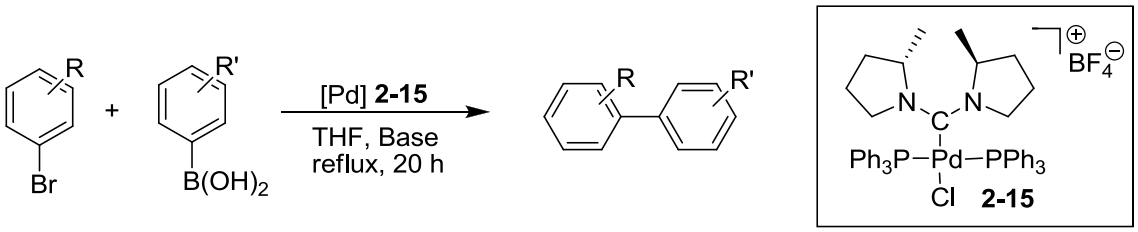

(2-2)

Table 2-5. Optimization of Suzuki cross-coupling reaction.

Entry	Boronic Acid	Aryl Bromide	Base	Mol %	Yield (%)
1	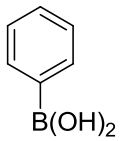 **2-20**	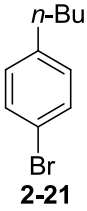 **2-21**	K_2CO_3	1	24
2	**2-20**	 **2-22**	K_2CO_3	1	50
3	**2-20**	**2-22**	CsF	3	100

(Entries 1 and 2, Table 2-5). Optimizing the conditions by changing the base and increasing the amount of catalyst resulted in significant gains in yield. Thus, the conformationally flexible, chiral ADC-Pd complexes are active catalysts for sterically demanding Suzuki coupling reactions. Hindered di-*ortho* and tri-*ortho*-substituted biaryls were produced in excellent yields with catalysts **2-15** and **2-31**. Attempting the very challenging synthesis of tetra-*ortho*-substituted biaryls did not result in product formation (Entries 4 and 5, Table 2-7).

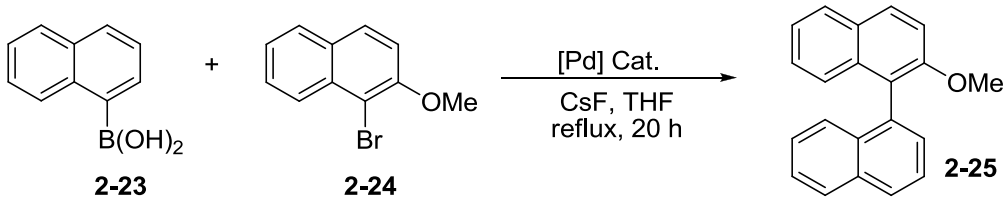

(2-3)

Table 2-6. Suzuki cross-coupling of **2-23** and **2-24** with a variety of catalysts.[a]

Entry	Boronic Acid	Aryl Bromide	Catalyst	Yield (%)	Ee (%)
1	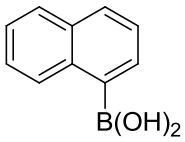 **2-23**	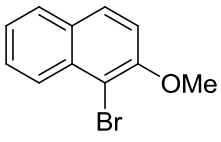 **2-24**	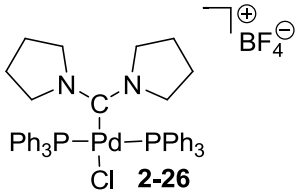 **2-26**	99	N.A.
2	**2-23**	**2-24**	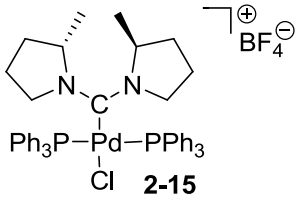 **2-15**	95	4
3	**2-23**	**2-24**	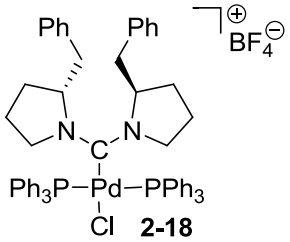 **2-18**	85	4
4	**2-23**	**2-24**	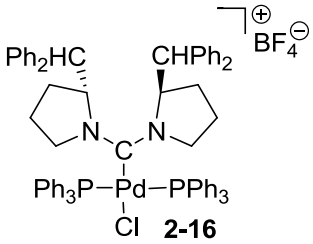 **2-16**	64[b]	3
5	**2-23**	**2-24**	$Pd(PPh_3)_4$	45	N.A.

[a] Conditions: 3 mol % [Pd], 1 equiv ArBr, 1.2 equiv $ArB(OH)_2$, 2.8 equiv CsF, THF, 100 °C. [b] Complex generated in situ and used without further purification.

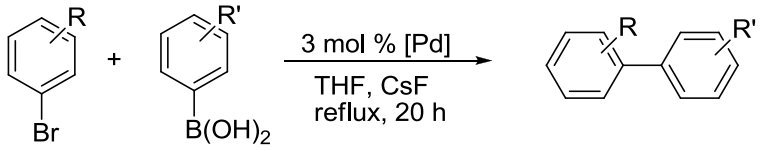

(2-4)

Table 2-7. Exploration of substrate scope in Suzuki cross-coupling reaction.

Entry	Boronic Acid	Aryl Bromide	Catalyst	Yield (%)
1	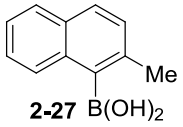 **2-27**	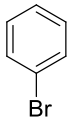 **2-28**	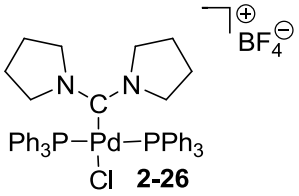 **2-26**	98
2	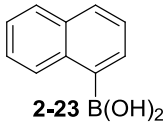 **2-23**	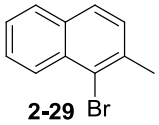 **2-29**	**2-26**	93
3	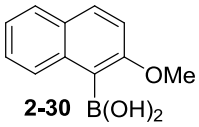 **2-30**	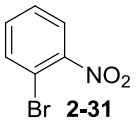 **2-31**	**2-26**	75
4	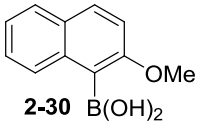 **2-30**	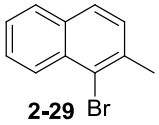 **2-29**	**2-26**	NR
5	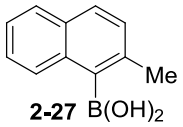 **2-27**	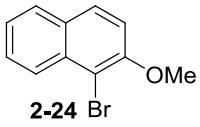 **2-24**	**2-26**	NR
6	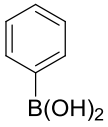 **2-20**	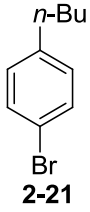 **2-21**	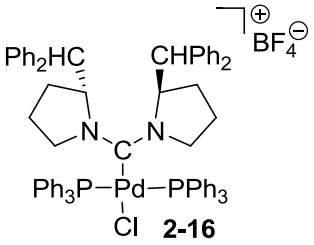 **2-16**	95

The catalyst was varied when producing biaryl **2-25**, and it is interesting to note that the carbenes showing the most steric hindrance provided the lowest yields in Suzuki cross-coupling reactions. This might be attributed to the observation that more hindered carbenes exhibit longer Pd to carbene bonds, perhaps causing the ligands to become more labile. Although difficult to isolate, catalyst **2-16** was generated in situ from chloroamidinium and $Pd(PPh_3)_4$ and tested in

catalysis resulting in 64% yield of **2-25** (Entry 4, Table 2-6). $Pd(PPh_3)_4$ was tested separately in the Suzuki reaction, to ensure catalysis with **2-16** was not solely a result of residual $Pd(PPh_3)_4$ (Entry 5, Table 2-6).

A major goal of this program is to develop an asymmetric version of the Suzuki reaction.[12] Using chiral catalysts such as **2-15**, **2-16**, and **2-18** substrates **2-23** and **2-24** were combined to form a tri-*ortho*-substituted product, and the enantiomeric excess (ee) was determined by chiral HPLC using a Chiralcel OJ-H column.[12] The observed ee's were low and ranged from 3-4 %. While this might be rationalized by the location of the chiral substituents, it was hoped that upon dissociation of the phosphines at elevated temperature, the chiral centers might reposition themselves proximal to the metal center in order to relieve steric strain.

C_2-Symmetric Pyrrolidine Moieties and Attempts at Symmetrically Substituted Ureas

A potential problem associated with chiral ADCs made from 2-substituted pyrrolidine subunits involved rotation about the bond linking nitrogen and the carbenoid carbon. Based on the low enantioselectivities observed in the Suzuki cross-coupling, we focused on the synthesis of ureas with a C_2-axis of symmetry to minimize difficulties caused by rotation. Design of ureas centered on the use of (2*S*,5*S*)-*trans*-diphenylpyrrolidine **2-37** as the chiral moiety.

The chiral amine was easily produced following a known procedure (Figure 2-12).[13] Friedel-Crafts arylation of fumaryl chloride leads to enone **2-33**, and the olefin is subsequently hydrogenated using $SnCl_2$. Excellent enantioselectivity was observed for the CBS-catalyzed reduction of the dione to a diol. Following reduction, the diol is cyclized to the amine in one-pot with allyl amine. At this stage, the diastereomers were separated using column chromatography, and the chiral tertiary amine was deprotected by refluxing in an acetonitrile-water mixture with Wilkinson's Catalyst to afford enantiomerically pure amine **2-37**.

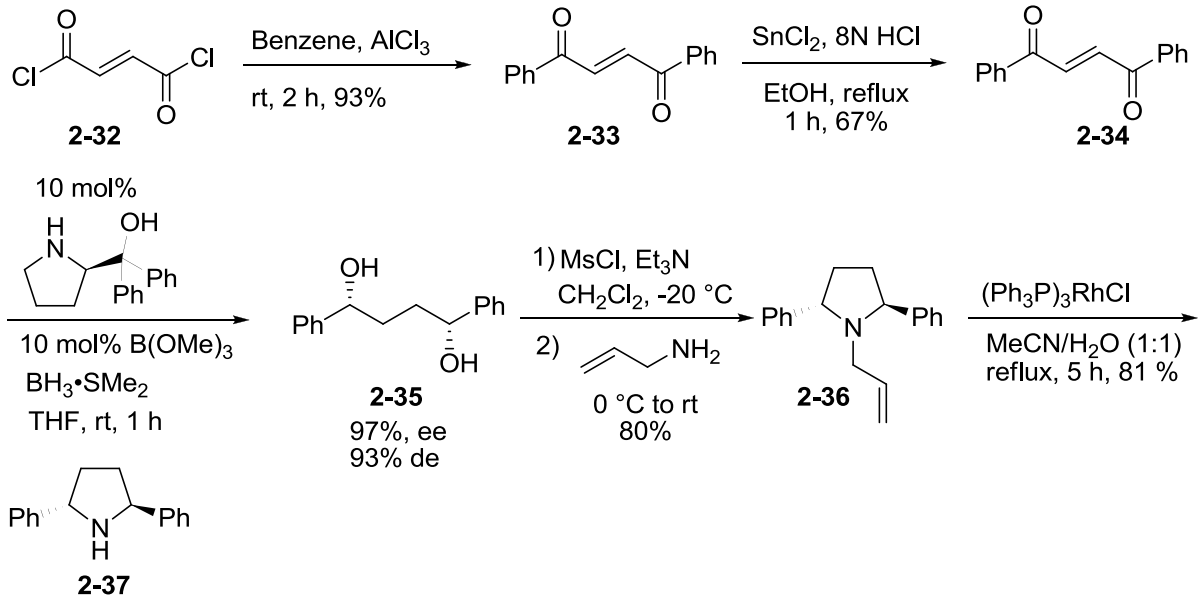

Figure 2-12. Preparation of (2*S*,5*S*)-*trans*-diphenylpyrrolidine

Urea formation was attempted in a condensation reaction using two equivalents of chiral amine **2-37** with phosgene (Equation 2-3), but the simple condensation reaction did not give urea. A product with 286 amu was recovered, which corresponds to carbamoyl chloride **2-38**. Changing the solvent to toluene and heating at temperatures up to 200 °C were ineffective in changing the outcome, and various strategies were undertaken to produce urea **2-39** (Figure 2-13). For example, amine **2-37** was deprotonated with *n*-BuLi and reacted with **2-38**. Also, ferric chloride was added to a solution of carbamoyl chloride **2-38** and chiral amine **2-37** in an effort to help activate the electrophile. At one point, a phosgene derivative, carbonyl diimidazole (CDI), was utilized to replace phosgene (Figure 2-14). None of these strategies led to the desired

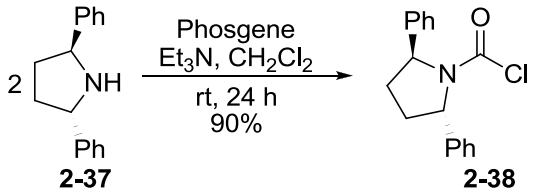

(2-3)

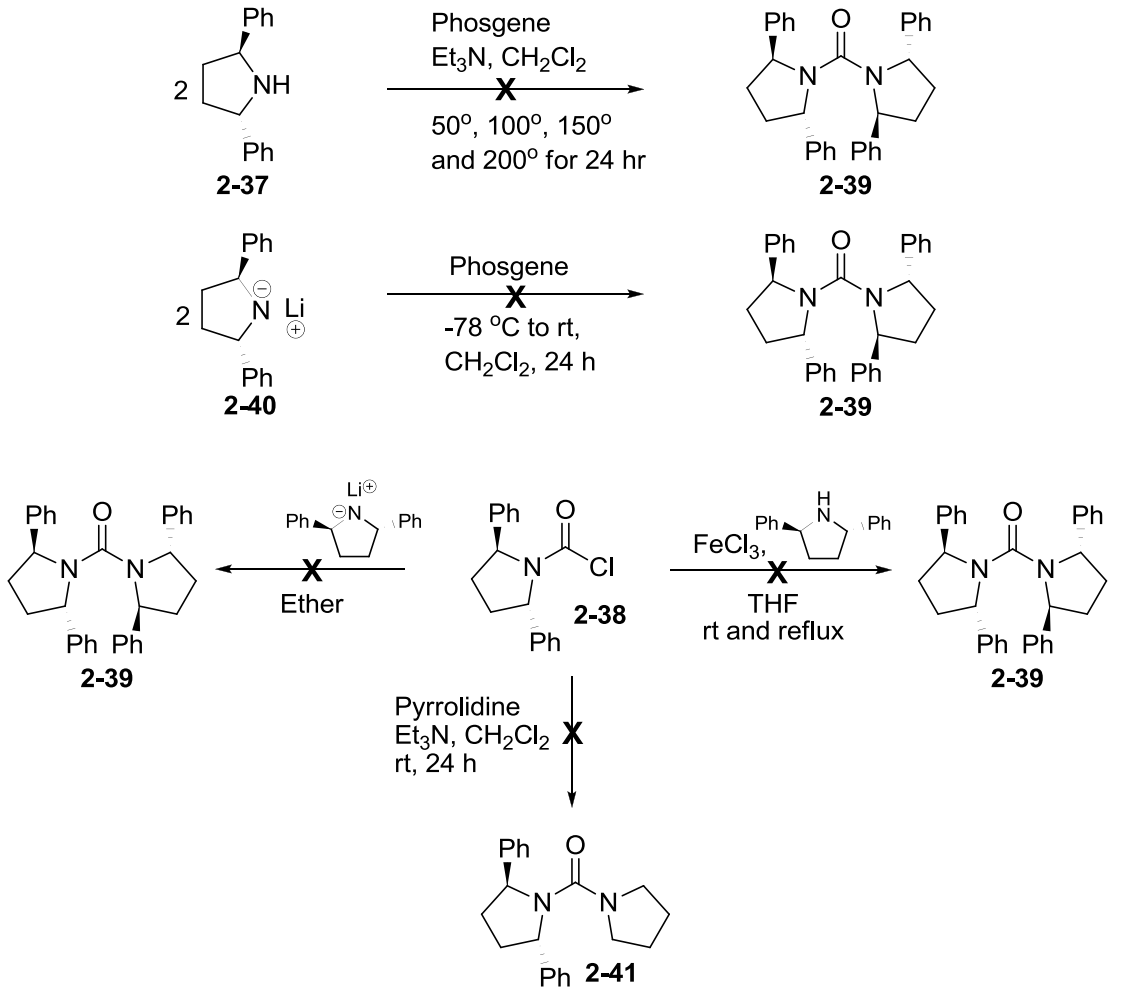

Figure 2-13. Some attempts at urea formation with (2*S*,5*S*)-*trans*-diphenylpyrrolidine.

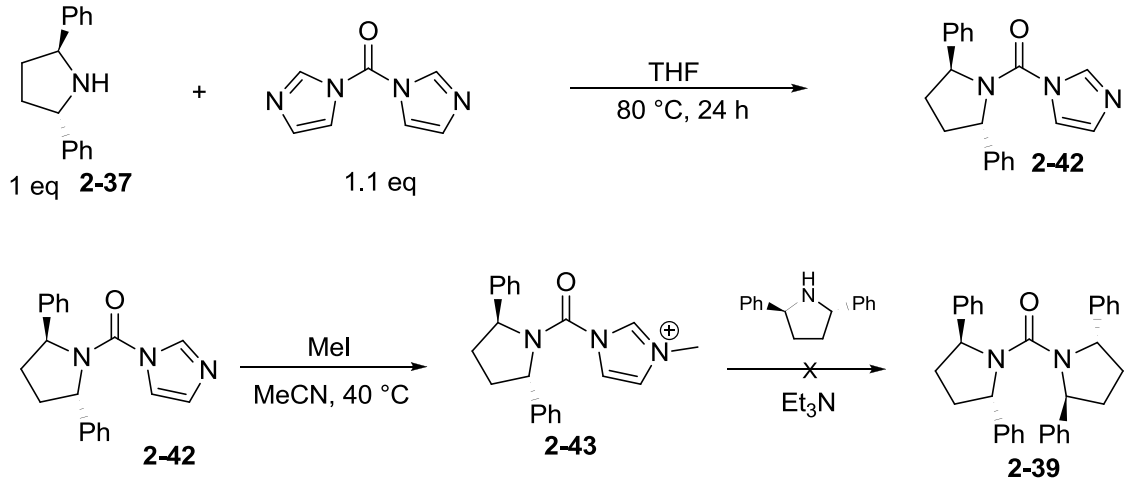

Figure 2-14. Synthetic attempt aimed at urea **2-39** using CDI.

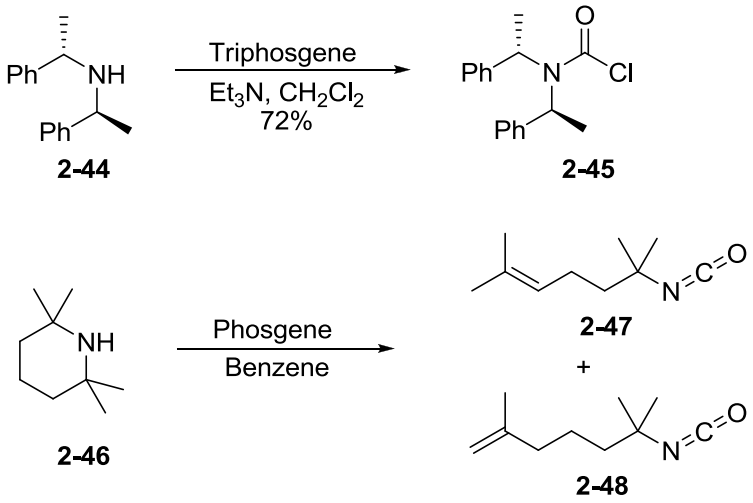

Figure 2-15. Challenging secondary amines in desired urea production.[14]

product **2-39**, and it is believed that the hindered nature of the carbamoyl chloride caused a second condensation to be difficult, as production of hindered ureas is known to be difficult (Figure 2-15).[14]

Ureas with Non-Identical Amine Moieties Featuring (2*S*,5*S*)-*trans*-diphenylpyrrolidine

Carbenes incorporating 2-substituted pyrrolidine moieties showed a preference for placement of the chiral substituents away from the metal center. Since the conformers could not be effectively controlled, a C_2-symmetric amine was needed, rendering rotation about the nitrogen carbene bond insignificant. As a result, **2-37** was featured in the synthesis of several ureas constructed from non-identical secondary amines.

Chiral amine **2-37** can be combined with a variety of electrophiles to make ureas. Figure 2-16 below shows reaction sequences where the pyrrolidine derivative is mixed with carbamoyl chlorides, acyl halides, and isocyanates to form ureas. Ureas **2-41** and **2-49** were made from carbamoyl chlorides; however, some hindered molecules such as diisopropyl carbamoyl chloride failed to react with **2-37**. Isocyanates react best with **2-37** leading to tri-*N*-substituted ureas

which can easily be methylated in high yield, as seen in the formation of **2-52** and **2-54**. Also, the amide precursor to a Bertrand type carbene, **2-50**, was made from *p*-anisoyl chloride.[15]

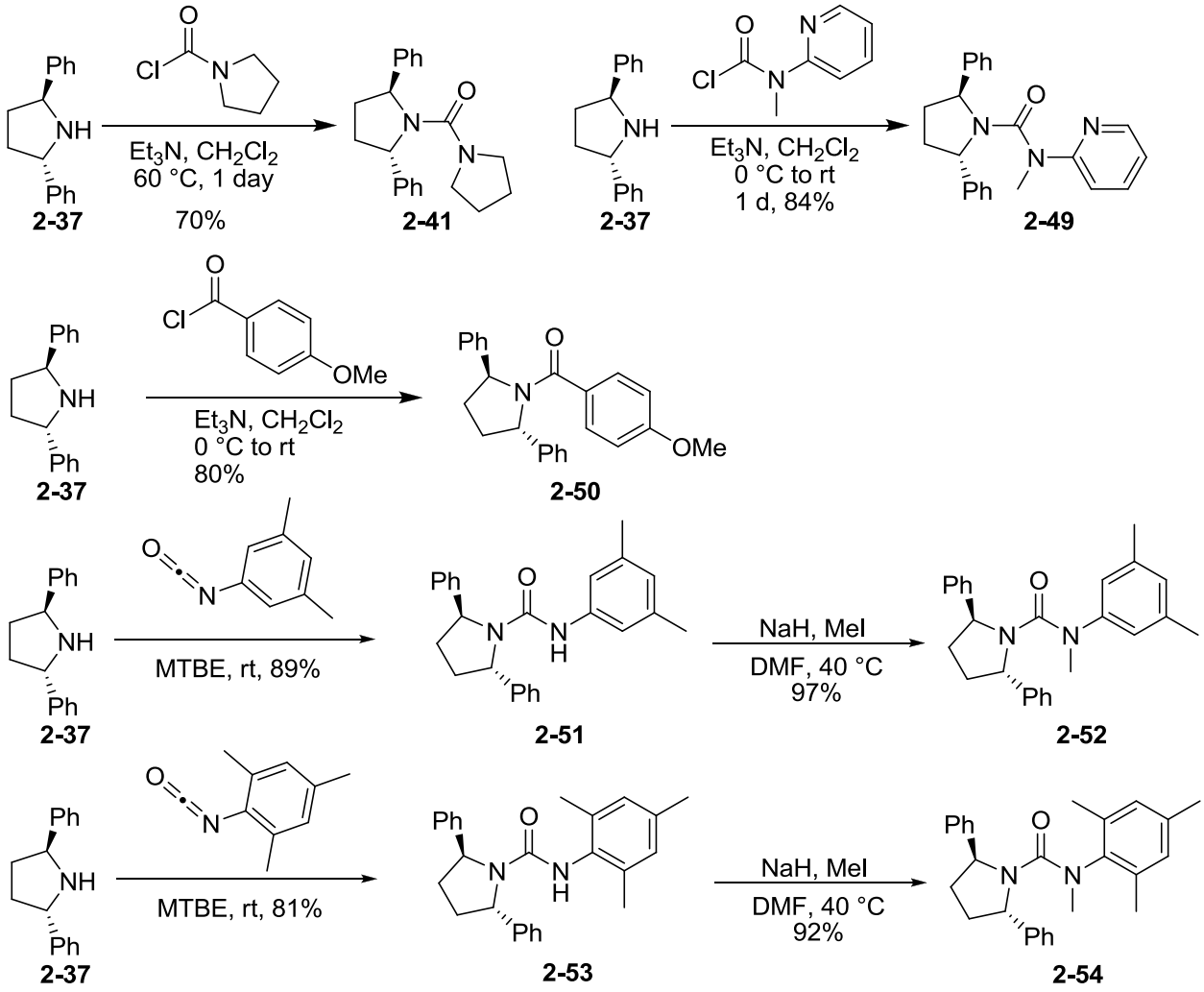

Figure 2-16. Ureas from carbamoyl chlorides, acyl chlorides, and isocyanates.

Chlorination and Metalation of Ureas Based on (2*S*,5*S*)-*trans*-Diphenylpyrrolidine

Chlorination was conducted with the newly made ureas (Figure 2-17). Unlike ureas **2-1**-**2-4**, not all of the urea based on **2-37** chlorinated smoothly. Compound **2-41** took five days to complete reaction, and the NMR spectrum of the product was difficult to reproduce. Urea **2-50** fragmented under the reaction conditions, and pieces of the molecule were isolated upon workup. The mesityl substituted urea **2-54** did not provide the chlorinated product to an appreciable

extent either, but the slightly less hindered **2-52** chlorinates after several days at 60 °C. Urea **2-49** chlorinates with exceeding ease in comparison to the other reagents, and after stirring overnight, a nice, white, isolable solid is obtained. The desired ADC-Pd compound was not isolated under oxidative addition conditions, however.

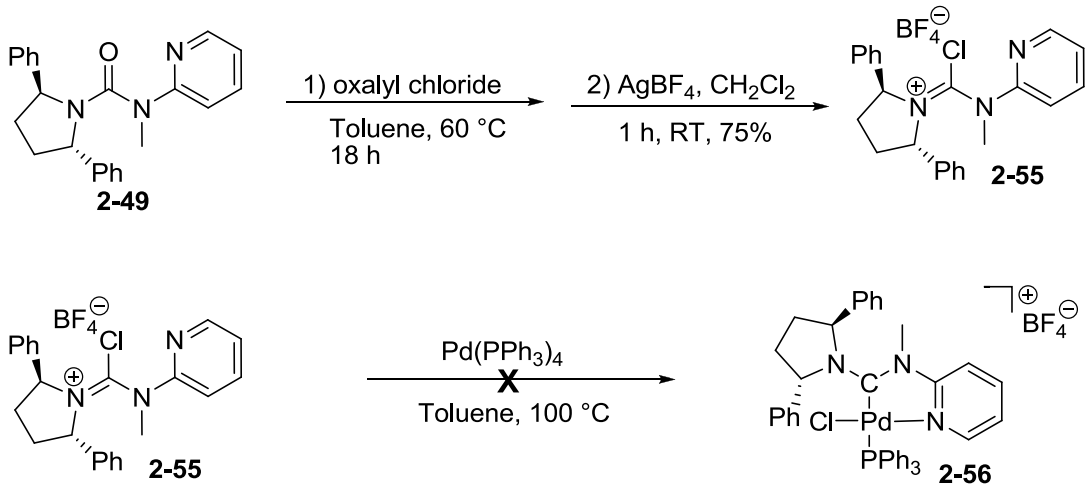

Figure 2-17. Chlorination of urea **2-49** and attempt at cationic ADC-Pd compound **2-56**.

Conclusion and Summary

Ureas are a logical entry point from which to reach acyclic diaminocarbenes. Ureas are purified with relative ease and their synthesis is relatively straightforward. Amidinium salts on the other hand can be difficult to purify and are sometimes difficult to make for non-simple structures.[6e] Based on others' work, oxidative addition was taken advantage of to form ADC-Pd complexes with the incorporation of triphenyl phosphine ligands.[7c,d]

Simple ureas constructed from 2-substituted chiral pyrrolidines were converted to chloroamidinium salts and then bound to palladium. Interest in these ligands lay in their potential for heightened activity and selectivity. The potential for conformational flexibility did not improve the catalytic ability of the ADCs. Conversely, as the 2-position became more highly

substituted, catalyst activity decreased. Whether the substituents ever actually shift to create a more sterically crowded environment under catalytic reaction conditions is unknown.

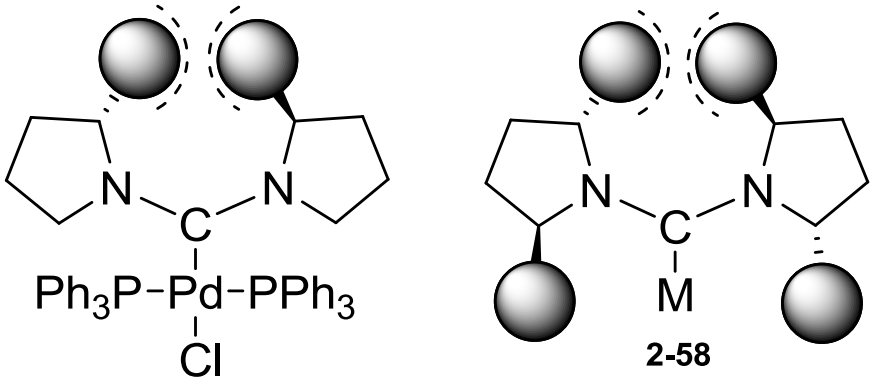

Figure 2-18. ADC-Pd complexes with 2-substituted pyrrolidines as mimics for ADC ligands with C_2-symmetric pyrrolidines. The steric interaction of the substituents toward the back of the catalyst are detrimental.

We can presume that ureas of the type depicted in Figure 2-18 incorporating two C_2-symmetric pyrrolidine units would not be feasible ligands if the substituent has any significant bulk. They can not avoid the detrimental interaction of substituents located distal to the metal center that seems to account for the difficulty in isolating **2-16** and **2-17** and the also decreased catalytic activity of complexes with increasing ADC substitution.

CHAPTER 3
LITHIUM-HALOGEN EXCHANGE: A NEW METHOD FOR DIAMINOCARBENE FORMATION

Introduction

While the previously described methodology led to palladium complexes with carbenes, several non-desirable features present themselves. Most importantly, the oxidative addition procedure necessitates the use of electron donating ligands like phosphines and restricts the diversity of catalysts that can be synthesized. Primarily, NHC chemistry was developed as an alternative to phosphine use, but the insertion of Pd into the C—Cl bond of the chloroamidinium does not take place in the absence of phosphines. The second drawback is that formation of catalysts incorporating sterically demanding substituents such as those seen in chloroamidiniums **2-12** and **2-13** was not feasible. The difficulty arises from the intrusion of the triphenyl phosphine ligand into the space occupied by ADC ligands, and it is manifested in the strained orientation of the chiral substituents. In a related manner, the direction of the chiral substituents of 2-substituted pyrrolidines is problematic. In being located distal to the metal center, the ability of these directing groups to transfer chirality to substrate is minimized.[16]

The direct conversion of chloroamidiniums **2-11** to **2-14** into carbene synthons is ideal, and it was envisioned that lithium-halogen exchange might accomplish this goal through a reduction of the C—Cl bond (Figure 3-1).

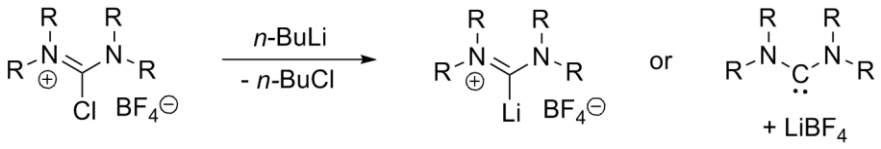

Figure 3-1. Envisioned synthesis of carbene intermediates through Li-X exchange.

Organolithium reagents have played an important role in organic synthesis,[17] and the formation of these reagents proceeds through a number of routes including reduction with

metallic lithium,[18] deprotonation with a lithiated base,[19] lithium-halogen exchange,[20] and transmetalation.[21] It is important to note that lithiation has been speculated to generate carbenoid intermediates in reaction with R_2CBr_2 and in the Fritsch-Buttenberg-Wiechell rearrangement.[22,23] Nevertheless, to the best of my knowledge, there have been no examples using lithium-halogen exchange to form diaminocarbenes from chloroamidiniums.

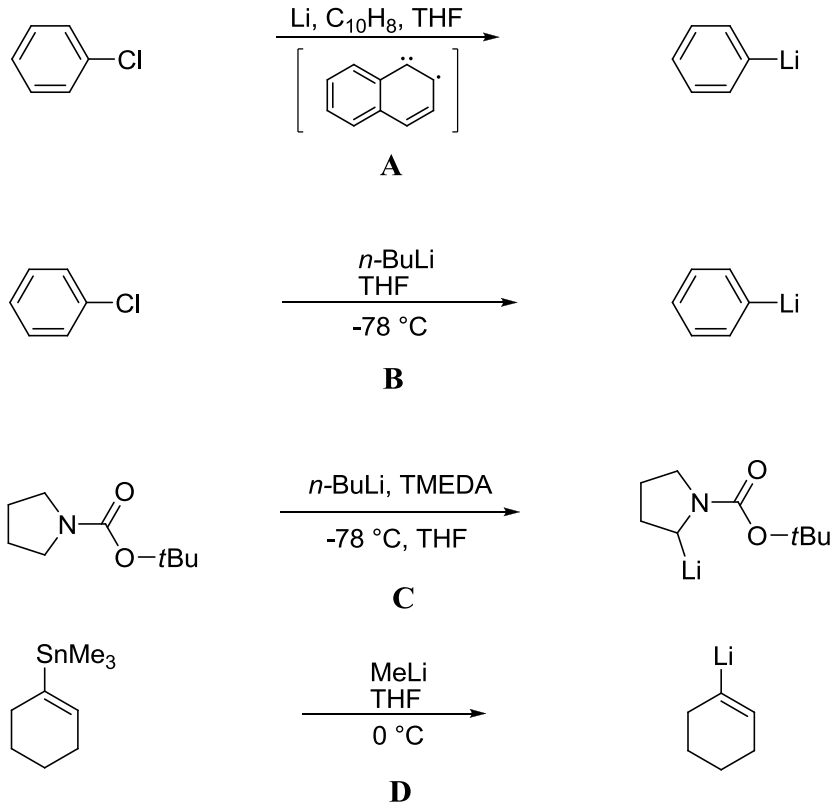

Figure 3-2. Classic methods to form organolithium species. A) Reduction with metallic lithium. B) Lithium-halogen exchange. C) Deprotonation. D) Transmetalation.

Carbene Formation and Proof

As shown in Figure 3-1, formation of diaminocarbenes through lithium-halogen exchange with chloroamidiniums is easily imagined. In his seminal research, Arduengo demonstrated that diaminocarbenes react with elemental sulfur (S_8) to form thioureas (Figure 3-3), and the formation of thioureas can be taken as a simple proof of carbene intermediates.

In the attempted formation of a putative carbene species, chloroamidinium **3-1** was added

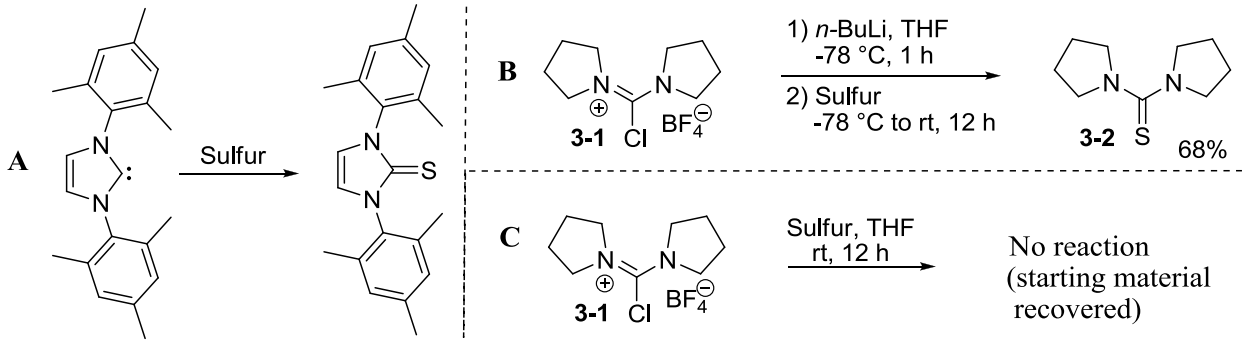

Figure 3-3. Tentative proof of carbene intermediacy via lithium-halogen exchange. A) As demonstrated by Arduengo and co-workers NHCs react with sulfur to produce thioureas. B) Production of bis(pyrrolidine)thiourea through lithium-halogen exchange. C) Control reaction showing that chloroamidinium does not react with sulfur.

to a Schlenk flask under an argon atmosphere, and THF was added. The suspension was cooled to -78 °C, and at this point, 1.05 equivalents of *n*-BuLi was added. After approximately five minutes the white precipitate disappeared, resulting in a clear suspension, indicating consumption of the chloroamidinium salt and the possibility of a soluble carbene intermediate. The reaction mixture was stirred for one hour at -78 °C before elemental sulfur was introduced to the solution. The yellowish suspension was allowed to slowly warm to room temperature and was stirred for twelve hours. Upon purification, thiourea **3-2** was obtained in 68% yield, suggesting ADC formation under lithium-halogen exchange conditions (Figure 3-3). Since the chloroamidinium potentially could serve as an electrophile to be attacked by sulfur, a control reaction was established without the presence of *n*-BuLi. In this case, thiourea **3-2** was not obtained (Figure 3-3).

NMR studies were enlisted to further probe the nature of the intermediate generated in situ (Equations 3-1 to 3-3). The lithium-halogen exchange reaction with chloroamidinium **3-1´** was carried out under an inert atmosphere of argon in THF-d_8 in a sealed NMR tube. Data was

collected at -30 °C because the carbene decomposed too quickly at room temperature (within five minutes). Both 1D and 2D techniques were utilized, where the 2D carbon trace was obtained through indirect detection of the proton nucleus. Both spectra showed a strong signal at 232.9 ppm clearly indicating the presence of carbene and nicely corresponding to the known value for the lithiated carbenoid species (Figures 3-4 and 3-5).[24]

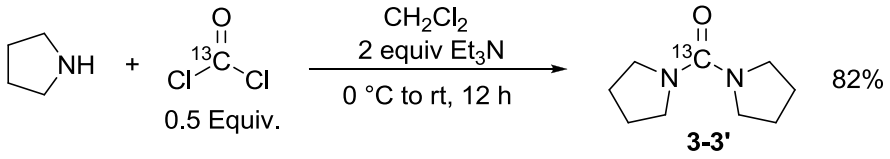

(3-1)

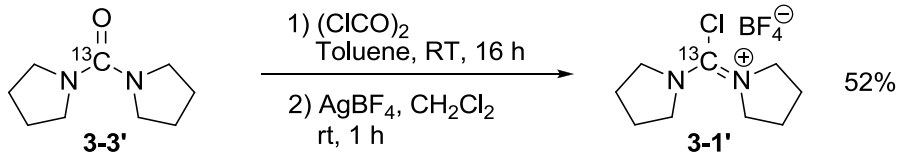

(3-2)

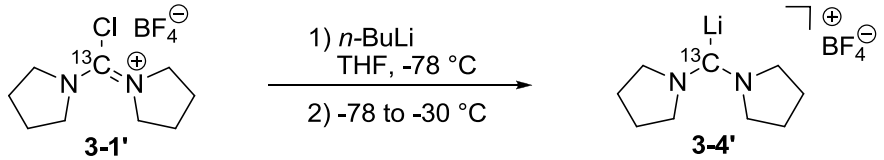

(3-3)

In the 2D gHMBC spectrum, the carbene carbon (232.9 ppm) displayed couplings with two protons at 3.47 and 3.66 ppm. The gDQCOSY spectrum revealed the sequence 3.47–1.89–1.76–3.66. The carbons carrying these protons were detected in the gHMQC spectrum at 48.4, 26.5, 24.5 and 55.8 ppm, respectively. Therefore, the two proton resonances at 3.47 and 3.66 ppm can be assigned to the two protons at the C2 position of pyrrolidine, and this gHMBC spectrum is consistent with the proposed carbene intermediate structure.

Binding Diaminocarbenes to Transition Metals and Boron

The evidence from thiourea formation and NMR experimental studies gave solid proof of carbenoid generation, and the practical application of this methodology was sought. The

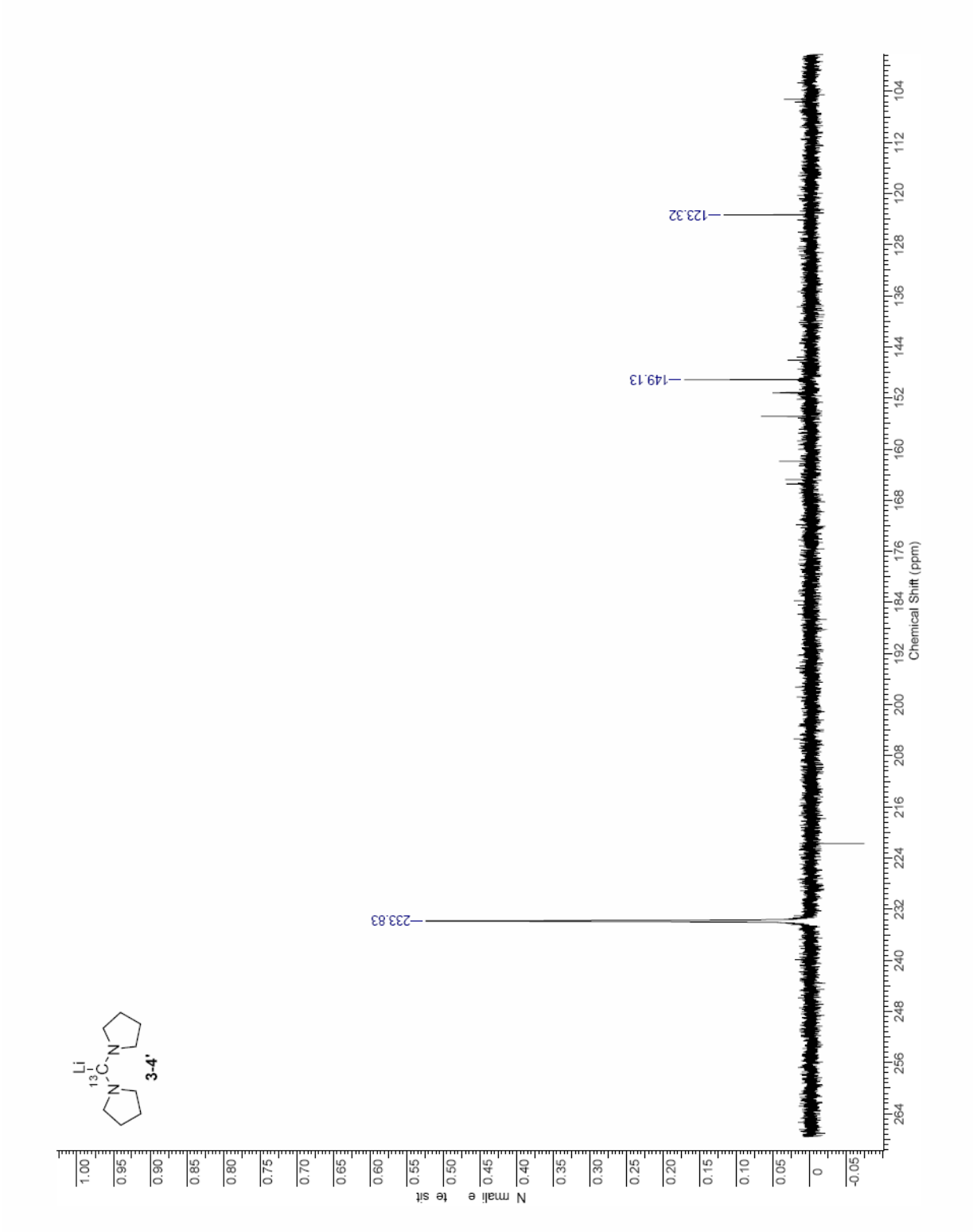

Figure 3-4. ^{13}C-NMR spectrum of lithiated carbene intermediate **3-4´** produced through lithium-halogen exchange.

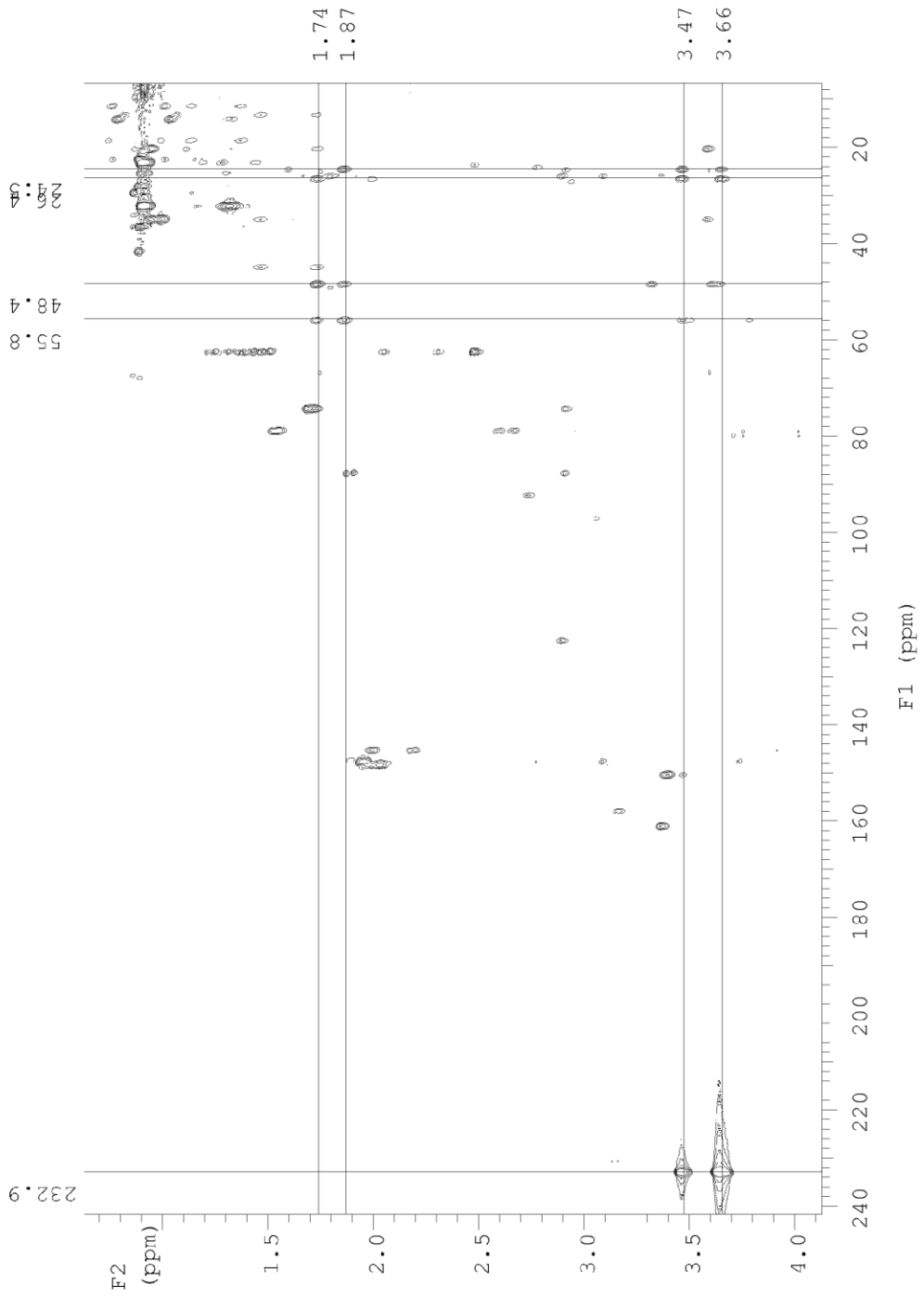

Figure 3-5. 2D gHMBC spectrum of lithiated carbene intermediate **3-4′** produced through lithium-halogen exchange.

synthesis of potential catalysts was desired, and the formation of transition metal catalysts and boron carbene adducts was attempted.

First, Group 9 metals were explored using $[Rh(COD)Cl]_2$ and $[Ir(COD)Cl]_2$ precursors. Chloroamidinium **3-1** was added to a flame dried Schlenk flask in a glovebox under argon atmosphere, and after removing the flask from the glovebox, THF was added. The suspension was cooled to -78 °C and followed by the addition of 1.05 equivalents of *n*-BuLi. After one hour, either $[Rh(COD)Cl]_2$ or $[Ir(COD)Cl]_2$ was added, and the solution was slowly warmed to room temperature, followed by a reaction period of twelve hours. The rhodium and iridium complexes were purified through dissolution in ethyl acetate or dichloromethane respectively, and then impurities were precipitated out of solution through the addition of hexanes. The rhodium complex was isolated in 65% yield while the iridium complex was isolated in 71% yield (Figure 3-6). It is important to note that the counter-ion identity proved to be important because the chloride salt of chloroamidinium **3-1** did not react productively under the lithium-halogen conditions. The metal complexes were fully characterized by NMR and high resolution mass spectrometry, and proof of the assigned structure was demonstrated by X-ray analysis (Figures 3-8 and 3-9).

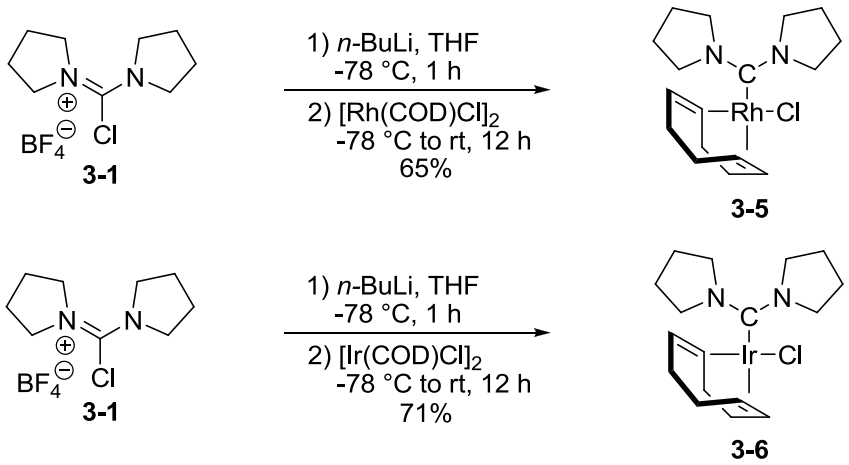

Figure 3-6. Formation of rhodium and iridium ADC complexes from chloroamidinium **3-1**.

The lithium-halogen exchange methodology was expanded in scope to include commercially available chloroimidazolium salt **3-7**. Upon treatment of chloroimidazolium **3-7** with *n*-BuLi, introduction of rhodium or iridium metals led to transition metal complexes (Figure 3-7). In this case, the chloride salt performed better than the BF_4 salt. The metal complexes were fully characterized by NMR and high resolution mass spectrometry, and proof of the assigned structure was demonstrated by X-ray analysis (Figure 3-10).

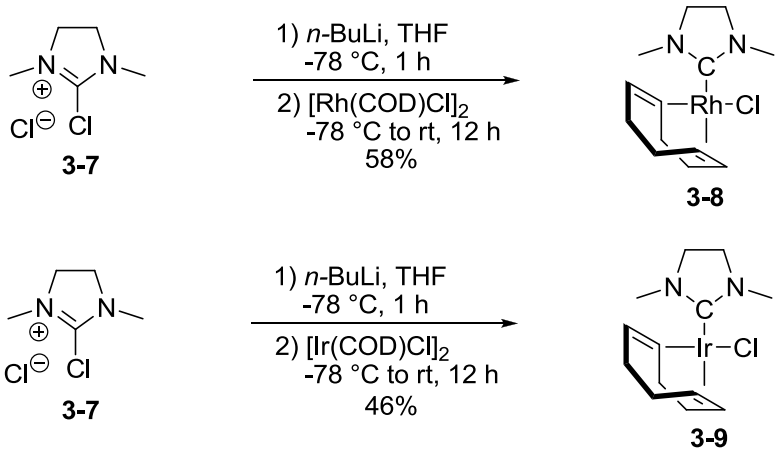

Figure 3-7. Formation of rhodium and iridium NHC complexes from chloroamidinium **3-7**.

Not surprisingly, the ADC complexes **3-5** and **3-6** showed larger N—C—N bond angles of 117.9(2)° and 118.4(4)° respectively as compared to the carbene bond angle of 108.6(6)° for NHC complex **3-9**. Also, the carbene bond length between carbon and transition metal was longer for the ADCs when compared to the NHC iridium complex. ADC-Ir complex **3-6** showed a carbene metal bond length of 2.045(5)Å, and NHC-Ir complex **3-9** showed a carbene metal bond length of 2.028(7)Å suggesting that the ADC might be more sterically demanding than the NHC. Where the imadazole ring is nearly flat, the ADC ligand in complexes **3-5** and **3-6** is not planar. Instead the pyrrolidine rings are twisted showing torsion angles of approximately 26° in complex **3-5**.

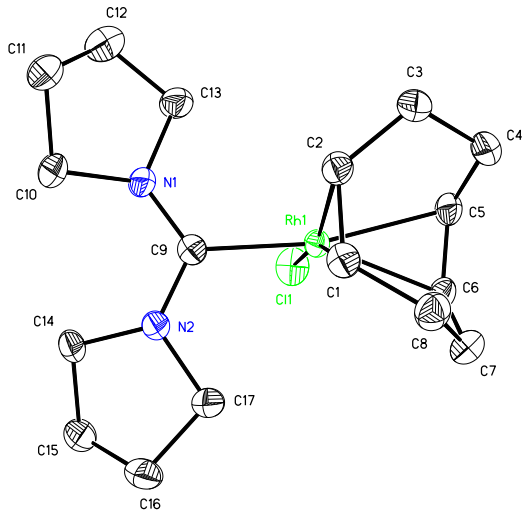

Figure 3-8. Molecular structure of complex **3-5**. Thermal ellipsoids are drawn at the 50% probability level. Selected bond lengths (Å) and angles (°): Rh1-C9 2.022(2), Rh1-Cl1 2.3855(6), Rh1-C1 2.110(2), Rh1-C2 2.104(2), Rh1-C5 2.241(2), Rh1-C6 2.197(2), N1-C9-N2 117.90(18), N2-C9-N1-C10 25.68(32), N1-C9-N2-C14 26.69(30).

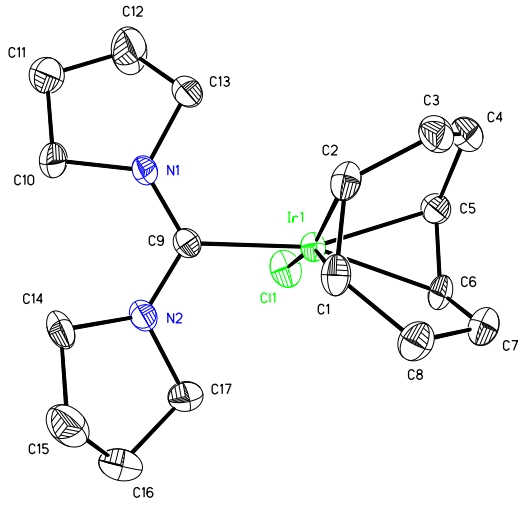

Figure 3-9. Molecular structure of complex **3-6**. Thermal ellipsoids are drawn at the 50% probability level. Selected bond lengths (Å) and angles (°): Ir1-C9 2.045(5), Ir1-Cl1 2.3713(11), Ir1-C1 2.101(4), Ir1-C2 2.104(4), Ir1-C5 2.173(5), Ir1-C6 2.189(4), N1-C9-N2 118.4(4), N2-C9-N1-C10 16.84(62), N1-C9-N2-C14 30.48(63).

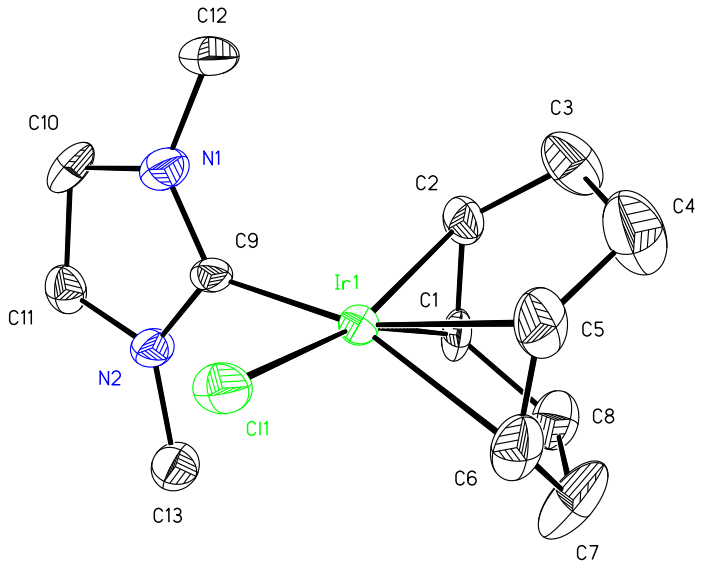

Figure 3-10. Molecular structure of complex **3-9**. Thermal ellipsoids are drawn at the 50% probability level. Selected bond lengths (Å) and angles (°): Ir1-C9 2.028(7), Ir1-Cl1 2.3570(17), Ir1-C1 2.113(7), Ir1-C2 2.097(7), Ir1-C5 2.197(7), Ir1-C6 2.189(7), N1-C9-N2 108.6(6).

Table 3-1. Crystal data and structure refinement for **3-5**.

Empirical formula	C17 H28 Cl N2 Rh	
Formula weight	398.77	
Temperature	173(2) K	
Wavelength	0.71073 Å	
Crystal system	Monoclinic	
Space group	P21/n	
Unit cell dimensions	a = 6.5715(6) Å	α= 90°.
	b = 18.7963(18) Å	β= 94.439(2)°.
	c = 13.7990(13) Å	γ = 90°.
Volume	1699.3(3) $Å^3$	
Z	4	
Density (calculated)	1.559 Mg/m^3	
Absorption coefficient	1.158 mm^{-1}	
F(000)	824	
Crystal size	0.26 x 0.13 x 0.07 mm^3	
Theta range for data collection	1.83 to 27.50°.	

Index ranges	$-8 \leq h \leq 8$, $-21 \leq k \leq 24$, $-16 \leq l \leq 17$
Reflections collected	11259
Independent reflections	3899 [R(int) = 0.0697]
Completeness to theta = 27.50°	99.7 %
Absorption correction	Numerical
Max. and min. transmission	0.9233 and 0.7528
Refinement method	Full-matrix least-squares on F^2
Data / restraints / parameters	3899 / 0 / 222
Goodness-of-fit on F^2	1.048
Final R indices [I>2sigma(I)]	R1 = 0.0313, wR2 = 0.0795 [3490]
R indices (all data)	R1 = 0.0351, wR2 = 0.0816
Largest diff. peak and hole	1.034 and -0.948 e.$Å^{-3}$

Table 3-2. Crystal data and structure refinement for **3-6**.

Empirical formula	C17 H28 Cl Ir N2	
Formula weight	488.06	
Temperature	173(2) K	
Wavelength	0.71073 Å	
Crystal system	Monoclinic	
Space group	P2(1)/c	
Unit cell dimensions	a = 9.8235(9) Å	α= 90°.
	b = 14.9332(14) Å	β= 91.616(2)°.
	c = 23.221(2) Å	γ = 90°.
Volume	3405.0(5) $Å^3$	
Z	8	
Density (calculated)	1.904 Mg/m^3	
Absorption coefficient	7.995 mm^{-1}	
F(000)	1904	
Crystal size	0.34 x 0.23 x 0.17 mm^3	
Theta range for data collection	1.62 to 27.50°.	
Index ranges	$-12 \leq h \leq 9$, $-12 \leq k \leq 19$, $-30 \leq l \leq 29$	
Reflections collected	21406	
Independent reflections	7805 [R(int) = 0.0360]	
Completeness to theta = 27.50°	99.8 %	
Absorption correction	Integration	
Max. and min. transmission	0.3435 and 0.1719	

Refinement method	Full-matrix least-squares on F^2
Data / restraints / parameters	7805 / 0 / 379
Goodness-of-fit on F^2	1.224
Final R indices [I>2sigma(I)]	R1 = 0.0323, wR2 = 0.0747 [7041]
R indices (all data)	R1 = 0.0370, wR2 = 0.0766
Largest diff. peak and hole	0.933 and -1.257 e.$Å^{-3}$

Table 3-3. Crystal data and structure refinement for **3-9**.

Empirical formula	C13 H22 Cl Ir N2	
Formula weight	433.98	
Temperature	173(2) K	
Wavelength	0.71073 Å	
Crystal system	Orthorhombic	
Space group	P2(1)2(1)2(1)	
Unit cell dimensions	a = 7.2770(15) Å	α= 90°.
	b = 12.449(3) Å	β= 90°.
	c = 15.738(3) Å	γ = 90°.
Volume	1425.7(5) $Å^3$	
Z	4	
Density (calculated)	2.022 Mg/m^3	
Absorption coefficient	9.534 mm^{-1}	
F(000)	832	
Crystal size	0.20 x 0.02 x 0.01 mm^3	
Theta range for data collection	2.09 to 27.50°.	
Index ranges	-9≤h≤9, -16≤k≤16, -20≤l≤12	
Reflections collected	9737	
Independent reflections	3271 [R(int) = 0.0628]	
Completeness to theta = 27.50°	99.9 %	
Absorption correction	Integration	
Max. and min. transmission	0.9107 and 0.2515	
Refinement method	Full-matrix least-squares on F^2	
Data / restraints / parameters	3271 / 0 / 154	
Goodness-of-fit on F^2	1.046	
Final R indices [I>2sigma(I)]	R1 = 0.0296, wR2 = 0.0652 [3128]	
R indices (all data)	R1 = 0.0320, wR2 = 0.0659	
Absolute structure parameter	-0.021(13)	

Largest diff. peak and hole	1.197 and -0.918 e.Å^{-3}

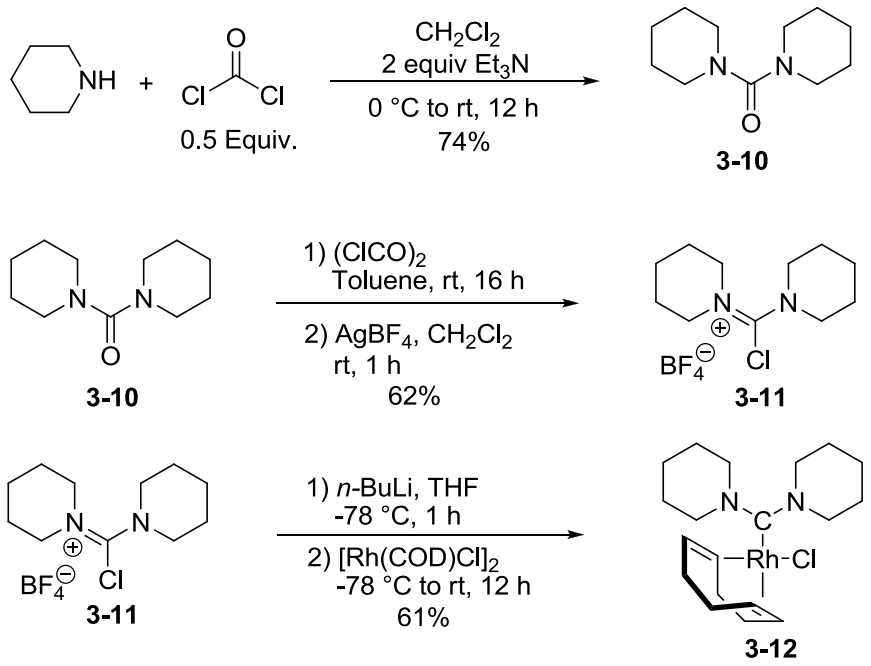

Figure 3-11. Formation of piperidine based ADC-rhodium complex **3-12**.

In addition to the pyrrolidine based ADC ligand and the *N*-methyl substituted NHC, several other ADC ligands were attached to rhodium. Piperidine based chloroamidinium **3-11** was synthesized and used as an ADC synthon after treatment with *n*-BuLi. Rhodium complex **3-12** was obtained in 61% isolated yield (Figure 3-11).

Chiral chloroamidiniums **2-11** and **3-14** were also used as ADC precursors to further demonstrate the scope of the new methodology (Figure 3-12). The usual method of carbene formation from *n*-BuLi was utilized. Because $[Rh(COD)Cl]_2$ was left after reaction, simple precipitation of impurities was insufficient to purify ADC metal complexes **3-13** and **3-15**.

Resultantly, silica gel chromatography on a short column was employed starting with a 3:1 mixture of hexanes to ethyl acetate and then quickly shifting to pure ethyl acetate as the rhodium complex is slightly unstable on a silica gel column. After column chromatography, the desired product was dissolved in dichloromethane and remaining impurities were precipitated

with hexanes. After filtration and evaporation of the filtrate, complexes **3-13** and **3-15** were obtained in 65% and 60% yield. The metal complexes were fully characterized by NMR and high resolution mass spectrometry, and proof of the assigned structure **3-13** was demonstrated by X-ray analysis (Figure 3-13).

Using the lithium-halogen exchange method for preparing carbenes in place of the oxidative addition of chloroamidiniums results in several advantages of note. Most importantly, sterically demanding ligands previously not accessible through the oxidative addition route become available as seen in compound **3-15**. The oxidative addition route requires the use of bulky phosphines that intrude into the space occupied by the NHC and ADC ligands as seen in the crystal structure of compound **2-15** that resulted in lengthened carbene metal bonds. Chiral centers were repositioned toward the back of the metal complex indicating that this positioning was more favorable than the opposite location which directs the substituents toward the metal. Palladium complexes stemming from chloroamidinium **2-12** could not be isolated most likely due to extreme steric constraints. Without the incorporation of bulky phosphine, ligands coming from **2-12** become feasible suggesting the lithium-halogen exchange route is amenable to a greater variety of ligands than those obtained through oxidative addition.

The second point of interest relates to the first point and involves the repositioning of the chiral substituents so that they are oriented toward the metal center instead of distal to the coordination sphere. When examining the crystal structure of **3-13**, this repositioning is noticed, again insinuating the decreased steric restraints operating upon the square planar rhodium system. By reorienting the chiral centers, there is a greater chance the ligands can transfer their chirality to substrates.

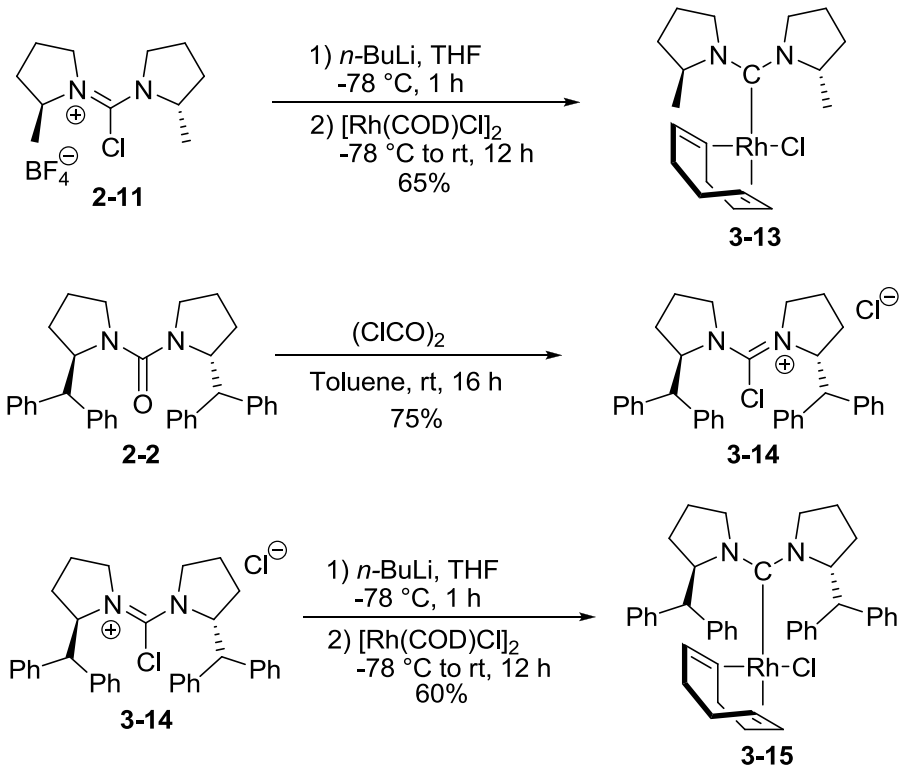

Figure 3-12. Synthesis of chiral ADC rhodium complexes **3-13** and **3-15**.

As mentioned previously, a major goal of this research effort was to develop a methodology providing a more general route to divergent metal complexes than possible through the oxidative addition pathway. With this in mind, the research moved beyond Group 9 metals and into Group 10. Chloroamidinium **3-1** was transformed into a carbene species with use of *t*-BuLi in place of *n*-BuLi, and then dimeric palladacycle **3-17** was added to the THF solution (Figure 3-14).[25] The use of *n*-BuLi led to lower yields. The resultant suspension was allowed to slowly warm to room temperature and then was stirred for twelve hours. At the end of the reaction time, compound **3-18** was first purified by silica gel chromatography using pure ethyl acetate as the eluent and then followed by 5% methanol in dichloromethane. The ensuing solid was further purified by precipitating the product from ethyl acetate with hexanes, giving **3-18** in 45% yield.

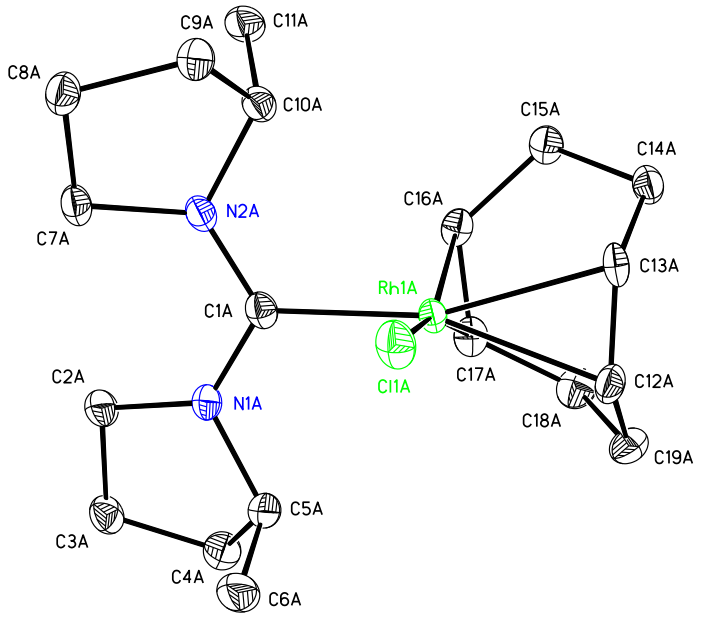

Figure 3-13. Molecular structure of complex **3-13**. Thermal ellipsoids are drawn at the 50% probability level. Selected bond lengths (Å) and angles (°): Rh1A-C1A 2.052(3), Rh1A-Cl1A 2.3928(7), Rh1A-C16A 2.105(3), Rh1A-C17A 2.136(3), N1A-C1A-N2A 117.8(2), C7A-N2A-C1A-N1A 34.0(4), C2A-N1A-C1A-N2A 20.1(4).

Table 3-4. Crystal data and structure refinement for **3-13**.

Empirical formula	C19 H32 Cl N2 Rh	
Formula weight	426.83	
Temperature	100(2) K	
Wavelength	0.71073 Å	
Crystal system	Monoclinic	
Space group	P2(1)	
Unit cell dimensions	a = 10.4422(9) Å	α= 90°.
	b = 11.9880(10) Å	β= 93.8320(10)°.
	c = 15.3266(13) Å	γ = 90°.
Volume	1914.3(3) $Å^3$	
Z	4	
Density (calculated)	1.481 Mg/m^3	
Absorption coefficient	1.033 mm^{-1}	
F(000)	888	
Crystal size	0.41 x 0.20 x 0.09 mm^3	

Theta range for data collection	1.33 to 27.50°.
Index ranges	-13≤h≤10, -15≤k≤15, -19≤l≤19
Reflections collected	13908
Independent reflections	8304 [R(int) = 0.0176]
Completeness to theta = 27.50°	99.1 %
Absorption correction	Numerical
Max. and min. transmission	0.9127 and 0.6755
Refinement method	Full-matrix least-squares on F^2
Data / restraints / parameters	8304 / 1 / 467
Goodness-of-fit on F^2	1.034
Final R indices [I>2sigma(I)]	R1 = 0.0260, wR2 = 0.0649 [8132]
R indices (all data)	R1 = 0.0265, wR2 = 0.0652
Absolute structure parameter	0.03(2)
Largest diff. peak and hole	1.667 and -0.982 e.Å^{-3}

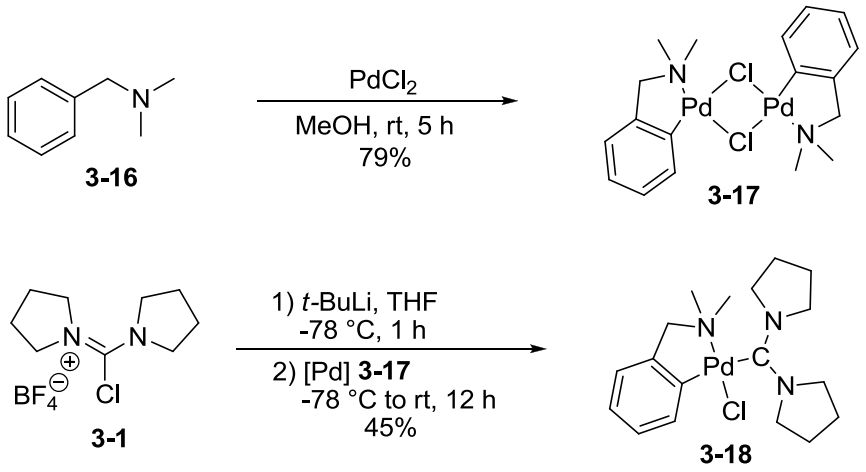

Figure 3-14. Synthesis of ADC palladium complex **3-18**.

Several metal precursors were explored before ultimately finding that dimeric palladacycle **3-17** was suitable for catalyst synthesis. Difficulty was experienced in trying to form either Pd^0 or Pd^{II} complexes because as explained by Herrmann and co-workers, Pd^0 has little electron affinity for very strong σ-donors, and ADCs act as effective reducing agents for Pd^{II}, forming ill defined Pd^0 species.[6b] $[Pd(allyl)]_2$, $PdCl_2$, $Pd(MeCN)_4(BF_4)_2$, $Pd(PPh_3)_2Cl_2$, $Pd(dba)_2$, and

phospha-palladacycle **3-25** were investigated, but none led to the desired ADC palladium species.

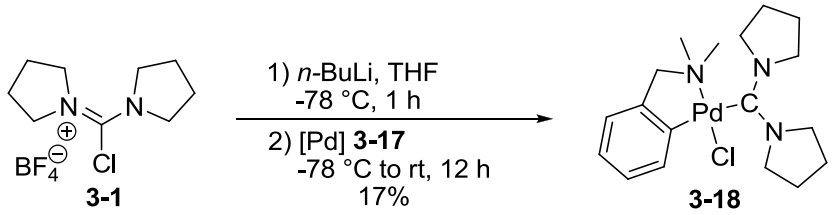

(3-4)

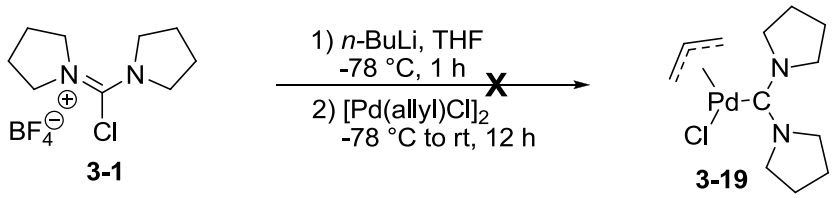

(3-5)

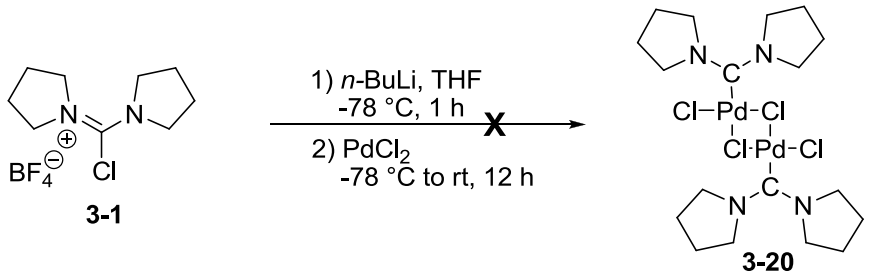

(3-6)

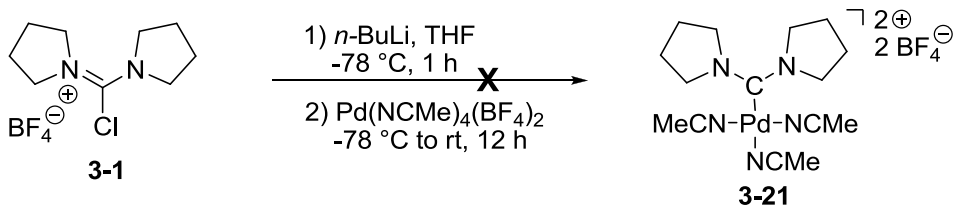

(3-7)

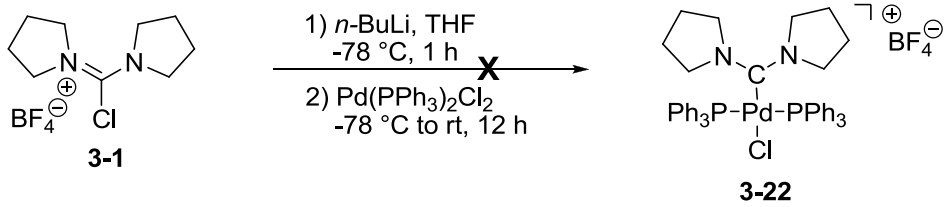

(3-8)

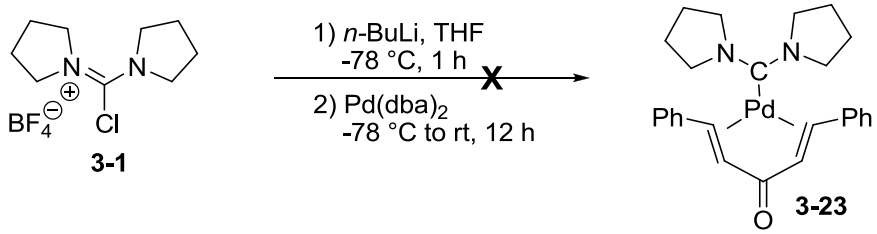

(3-9)

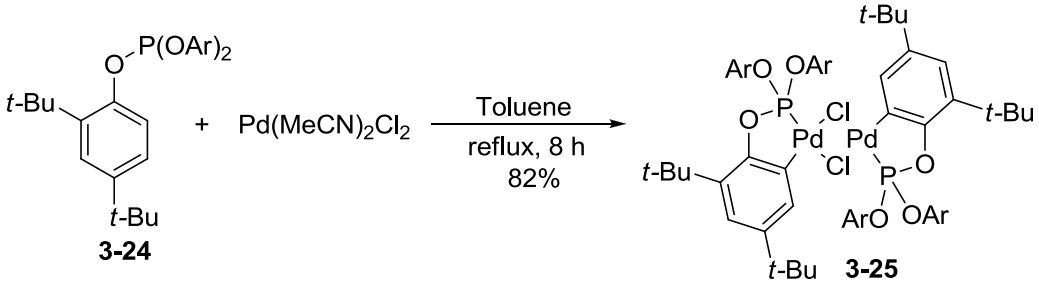

(3-10)

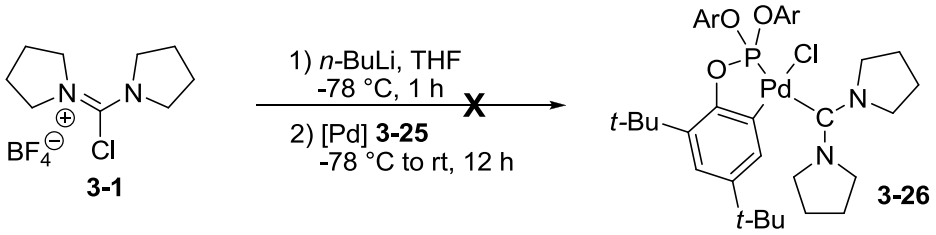

(3-11)

Ruthenium complexes with ADCs were desired, but they proved to be difficult to isolate. First, catalyst synthesis was attempted by displacement of a tricyclohexyl phosphine ligand from Grubbs First Generation metathesis catalyst (Equation 3-12). Lithiated carbene was generated from n-BuLi, and then Grubbs catalyst was added to the solution. Upon warming the reaction mixture to room temperature, the color changed from purple to an orangish-brown color as expected, but quickly, a black sludge was formed. Only decomposition products were detected by NMR in a result similar to that obtained by Herrmann and co-workers when working with ruthenium and ADC ligands.[6d] Other complex formation was attempted with precursors other than Grubbs First Generation by Hwimin Seo, a group member; however none of these trials resulted in successful isolation of an ADC ruthenium complex.

ADC adducts were able to be formed with main group elements in addition to transition

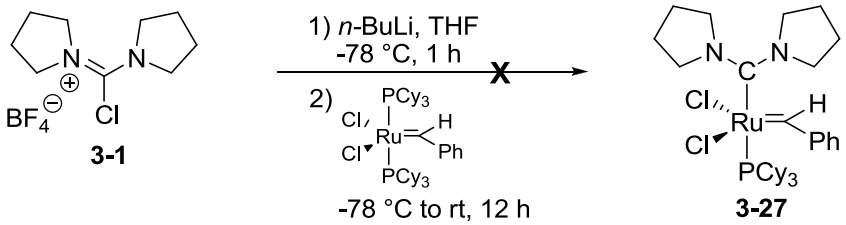

(3-12)

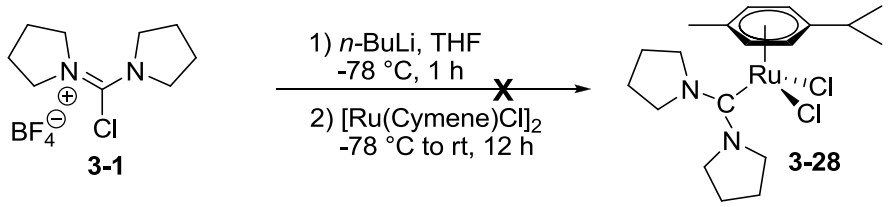

(3-13)

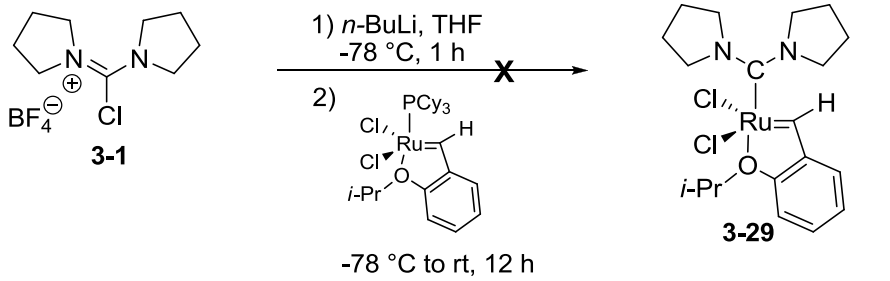

(3-14)

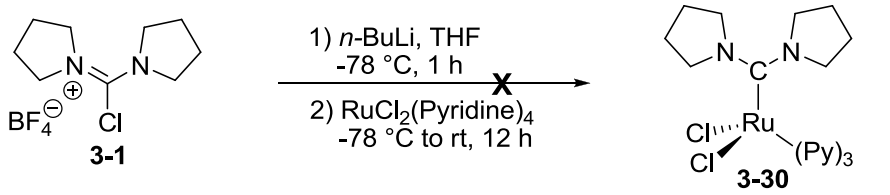

(3-15)

metals. After generation of ADC **3-4** from chloroamidinium, the electrophilic boron trifluoride etherate was introduced to the reaction mixture. The ADC easily complexed with boron, and the ensuing product was purified on a short silica gel column with a 1:1 mixture of hexanes and ethyl acetate, giving the adduct in 81% (Equation 3-16). Compound **3-31** was characterized by ^{1}H and ^{13}C NMR as well as elemental analysis and mass spectrometry. Transmetalation of the carbene from boron to rhodium was attempted, but it was not successful (Table 3-5). ADC boron compound **3-31** was recovered after the reaction showing the stability of the carbene boron bond.

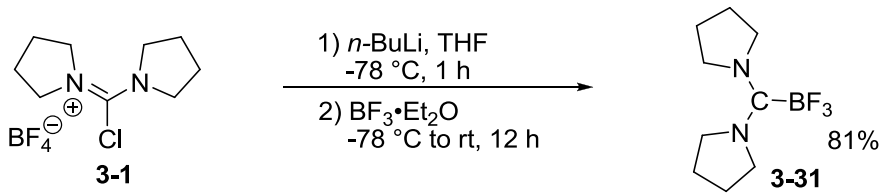

(3-16)

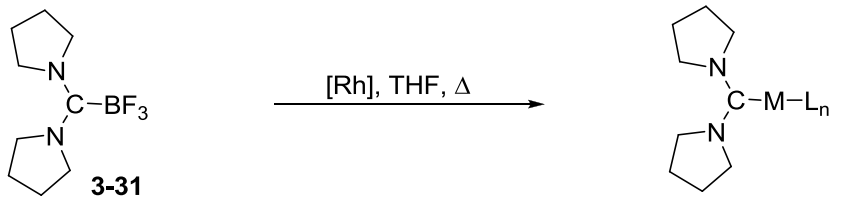

(3-17)

Table 3-5. Attempts at transmetalating ADC ligand to rhodium.

Entry	Metal Precursor	Temperature	Additive	Yield
1	$[Rh(COD)Cl]_2$	70	-	NR
2	$[Rh(COD)Cl]_2$	110	-	NR
3	$[Rh(COD)Cl]_2$	110	Ag_2O	NR
4	$[Rh(COD)OH]_2$	110	-	NR

The work of Tamm and colleagues showed that NHCs acting in conjunction with tris(pentafluorobenzene) borate functioned to activate small molecules like diatomic hydrogen through dissociation of the carbene boron bond.[26] Steric repulsion caused by the joining of **3-32** and **3-33** creates a frustrated Lewis pair (Figure 3-15). With the idea that this type of boron carbene molecule might be a useful species for transferring an ADC to a transition metal through transmetalation, the synthesis of compound **3-34** from tris(pentafluorobenzene) borate was attempted, but it was not accessed. It was believed that if formed, compound **3-34** might behave similarly to **3-32** and **3-33**, with the dissociation of the carbene boron bond in the presence of a metal source leading to a metal carbene bond.

Other Ligands Explored in Carbene Formation from the Lithium-Halogen Exchange

Success was observed when conducting metal complexation with ADC and NHC ligands featuring a low degree of functionality and mostly alkyl substituents. Ligand structure was varied more drastically, however, to understand the scope of methodology for carbene generation from chlorinated precursors, and unfortunately several classes of ligands did not fare well. This section details these efforts.

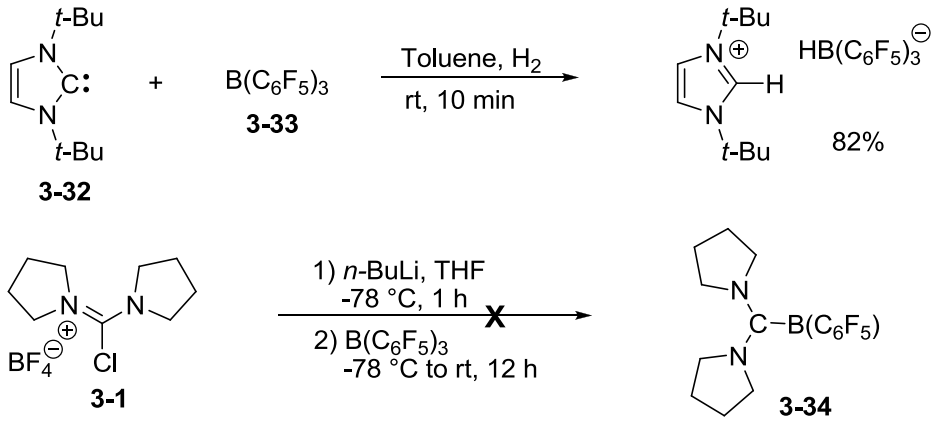

Figure 3-15. Attempt to create a frustrated Lewis pair with an ADC.

First, the identity of the chloroamidinium's counter-ion is important but for what reason is not clear. Bis(pyrrolidine) chloroamidinium **3-36** was synthesized in the laboratory, but anion exchange was not performed so that the counter-ion remained as chloride. Attempts at formation of rhodium complex **3-5** failed from this precursor (Figure 3-16). After converting **3-36** to the tetrafluoroborate salt, synthesis of **3-5** succeeded. ^{13}C labeled chloroamidinium **3-36´** was used in an NMR experiment to understand why the chloride version of **3-1** did not form the rhodium

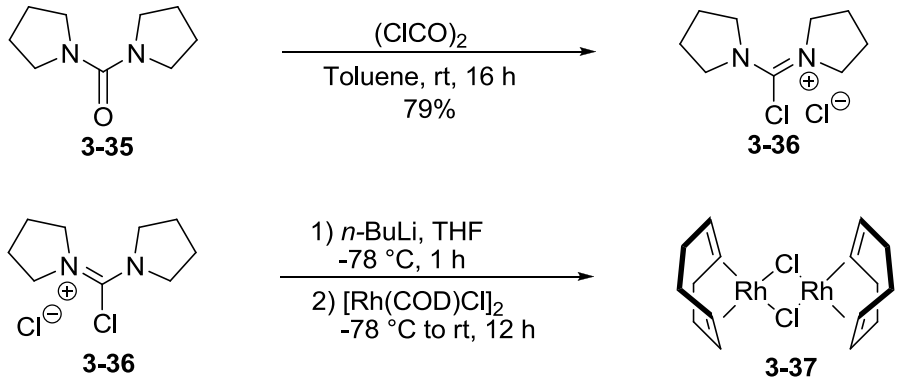

Figure 3-16. Attempts at synthesis of ADC rhodium catalyst using chloroamidinium **3-36**.

catalyst, and it was seen that the carbene was not formed under these circumstances (Figure 3-17). A similar dependence on the identity of the counter-ion was observed when working with NHC precursor **3-38**. In this instance, however, the chloride anion was preferential to tetrafluoroborate (Figure 3-18).

Some seemingly simple alkyl-based diaminocarbenes did not perform well under the lithium-halogen exchange conditions. Neither bis(dimethyl) chloroamidinium **3-39** nor bis(morpholine) chloroamidinium **3-40** showed evidence of binding to rhodium. Both reactions were run twice, and after twelve hours of reaction time, $[Rh(COD)Cl]_2$ was recovered in quantitative amounts. Based on data from Alder and co-workers,[6b] it was believed that the carbene stemming from **3-39** might quickly dimerize even at low temperature. After all, the successful ligand stemming from **3-1** dimerizes within three hours in THF at -78 °C.[27] Likewise, a chiral chloroamidinium with a low degree of functionality developed by a co-worker, Hwimin Seo, failed to ligate to a rhodium center under the identical lithium-halogen exchange conditions.

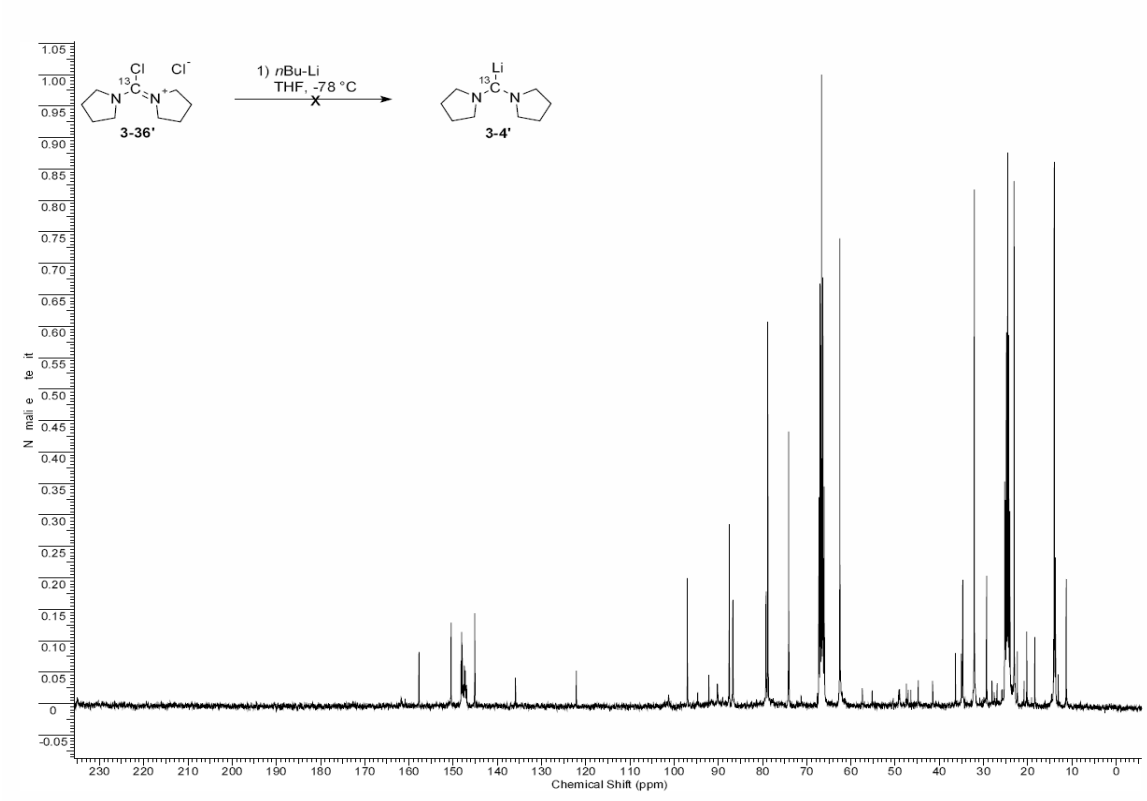

Figure 3-17. NMR taken at -60 ˚C of chloride salt **3-36´** under Li-X exchange conditions.

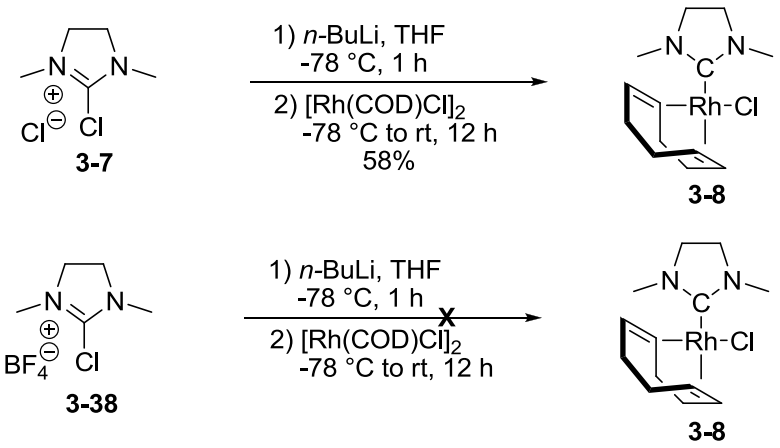

Figure 3-18. Observed differences in reactivity based upon counter-ion identity.

Iron catalysts exhibit an abundance of dative bonds to nitrogen containing ligands, and so the potential of pyridine-based ADCs was of special interest.[28] Chloroamidinium

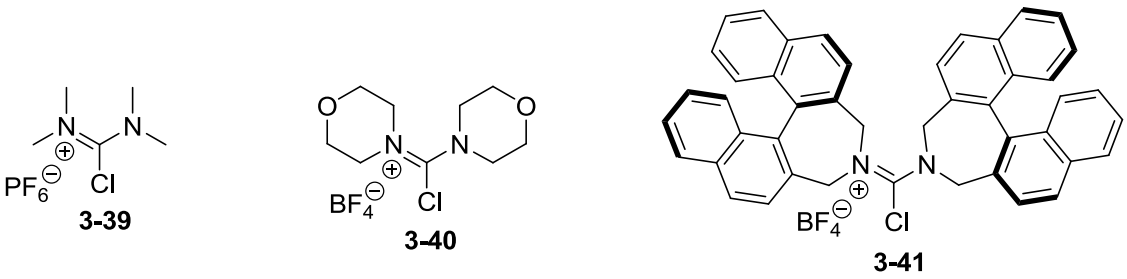

Figure 3-19. Diaminocarbene precursors which were unsuccessful in attempts to complex with rhodium using lithium-halogen exchange methodology.

3-42 was previously noted for its simple preparation and isolation. Treatment of **3-42** with *n*-BuLi followed by addition of $[Rh(COD)Cl]_2$ did not yield the desired product, however (Figure 3-20). Initially, the chloride salt was used because the chloroamidinium was simple to obtain as a nice, white solid, whereas the tetrafluoroborate salt was a nearly intractable, colorless oil. Resultantly, when **3-42** failed to give the proper product, tetrafluoroborate salt **3-44** was examined, but it also did not yield the rhodium complex.

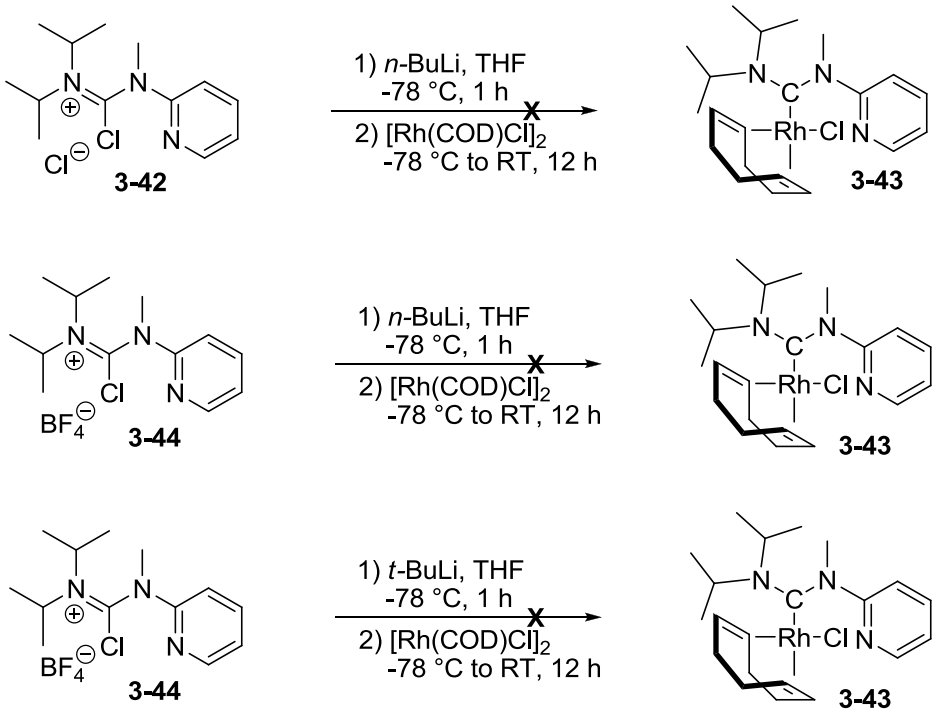

Figure 3-20. Attempts at synthesis of a mixed pyridine-ADC rhodium complex.

In an attempt to pinpoint the problem with catalyst formation, the reaction was dissected into two halves, as either the lithium-halogen exchange or the metal binding might be problematic. After addition of *n*-BuLi to **3-44** in THF and thirty minutes of stirring, sulfur was added to the reaction mixture. Thiourea **3-45** was not isolated. In a separate trial, trifluoroborane diethyletherate was also used as an electrophile to trap the ADC after generation with *n*-BuLi, but again, the expected product was not observed (Figure 3-21). This led us to believe that the problem with rhodium complex formation lay with the lithium-halogen exchange.

One possible scenario was that a lithium aggregate was formed, diminishing the reactivity of the lithiated carbene. Clustered organo-lithium species are known to lower reactivity, and breaking the aggregate is a common method for increasing rate of reaction.[29] HMPA is one of the most effective additives to deconstruct the tetrameric phenyl-lithium structure, and so it was

used in conjunction with the lithiation of pyridine based chloroamidinium **3-44**. The addition of HMPA did not prove to be effective in the formation of borate **3-46** (Equation 3-18).

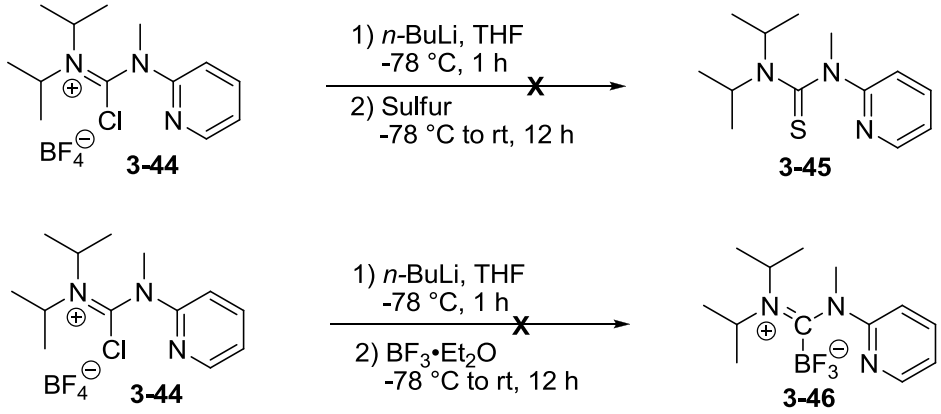

Figure 3-21. Trials to determine whether *n*-BuLi is effective in generation of carbene intermediacy with precursor **3-44**.

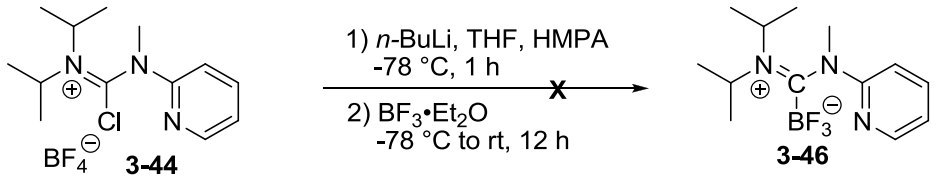

(3-18)

In previous projects, formation of sterically hindered tetra-substituted ureas was found to be very challenging, and this has been observed in other research groups as well.[14] A potential strategy to circumvent this obstacle is to pursue *N,X* carbenes instead of diaminocarbenes, where *X* equals sulfur or oxygen. The use of divalent sulfur or oxygen would effectively eliminate the strain observed in the ADC ligands, and this methodology might allow the use of 2,5 *trans*-diphenylpyrrolidine or other C_2-symmetric amines as chiral building blocks.

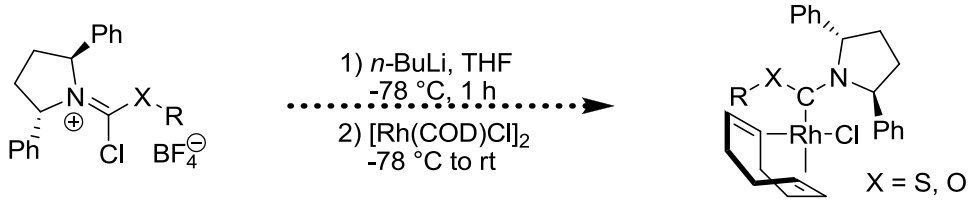

(3-19)

N,S carbene precursors **3-49** and **3-50** were synthesized quite easily from the nucleophilic attack on carbon disulfide by a secondary amine. After isolation of the dithiocarbamate salt, ethyl iodide was added to give the alkylated product in high yield (Figure 3-22). Thiocarbamate **3-54** leading to a possible *N,O* carbene was made by addition of pyrrolidine to phenyl chlorothionoformate (Figure 3-23). All of these molecules were easily chlorinated by adding oxalyl chloride to a solution of the dithiocarbamate or thiocarbamate in toluene and stirring the reaction mixture at room temperature for twenty four hours.

The first carbene synthons investigated were chlorinated dithiocarbamates **3-51** and **3-52**. Both were subjected to *n*-BuLi in THF at -78 °C, which was followed by the addition of $[Rh(COD)Cl]_2$. At the end of the reaction period, quantitative amounts of the rhodium precursor were recovered (Equations 3-20 and 3-21). A switch from the tetrafluoroborate anion to the chloride anion was explored but did not produce an affirmative result.

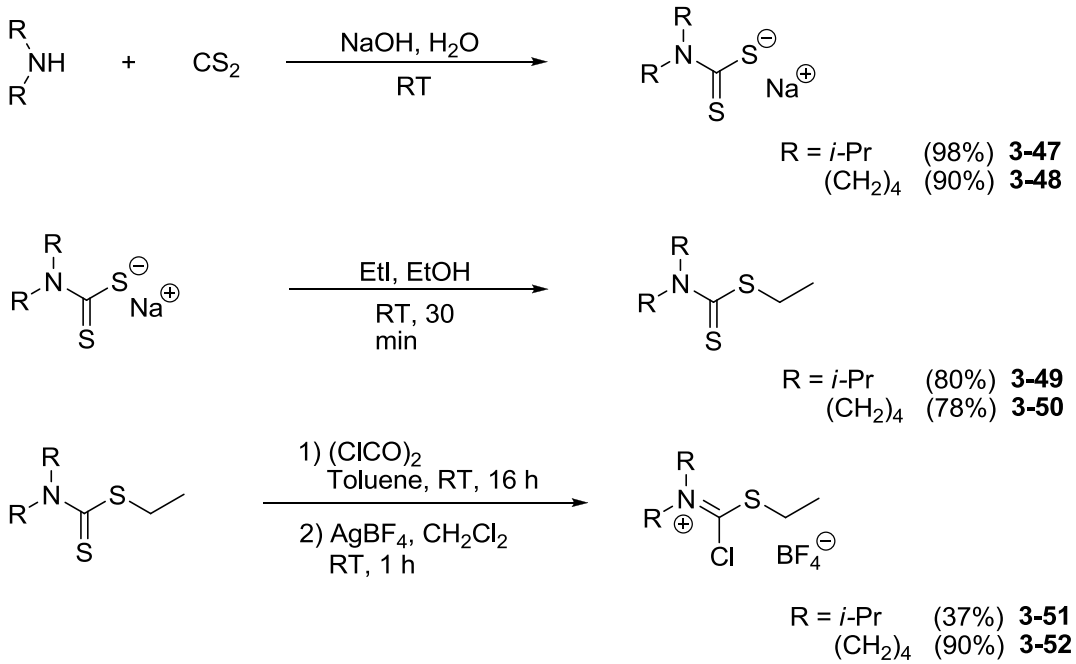

Figure 3-22. Formation of chlorinated dithiocarbamate tetrafluoroborate salts **3-51** and **3-52**.

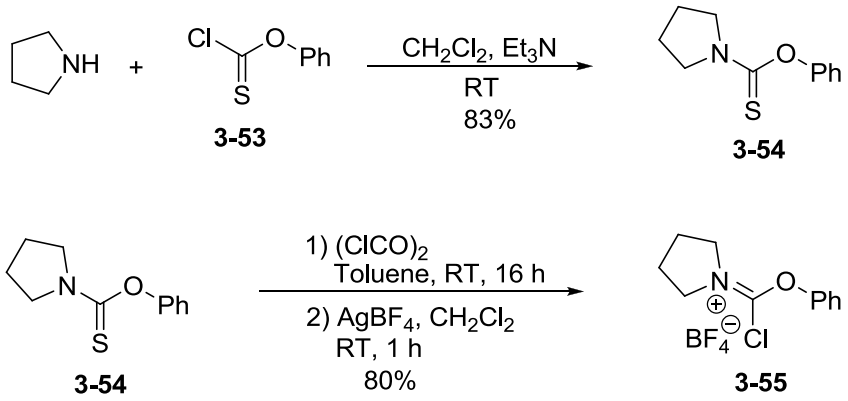

Figure 3-23. Formation of chlorinated thiocarbamate tetrafluoroborate salt **3-55**.

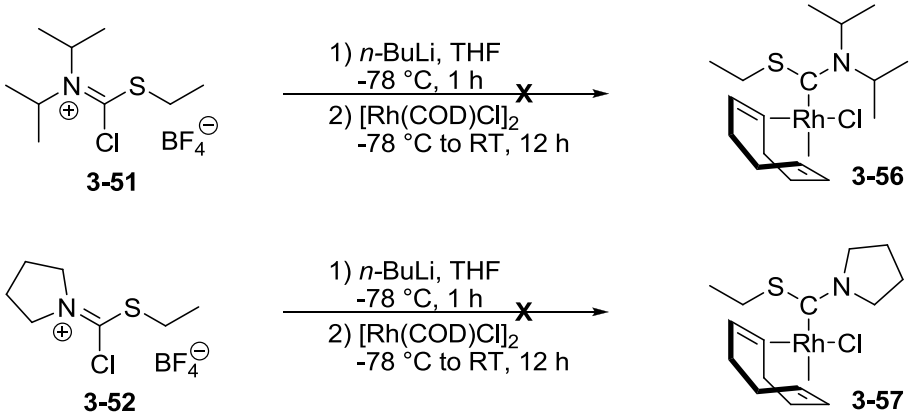

(3-20)

(3-21)

Next, attention was paid to the chlorinated carbamate, **3-55**. Again, treatment with *n*-BuLi followed by addition of $[Rh(COD)Cl]_2$ failed to produce the desired rhodium complex, and salts with the tetrafluoroborate or chloride counter-ion were both investigated (Figure 3-24). Two different fragments of the carbamate appear upon isolation of the reaction byproducts. One featured a pyrrolidine unit without any aromatic signal in ^1H NMR, whereas the other product showed only aromatic peaks, looking quite similar to phenol. Based on this information it seemed as though the *n*-BuLi might be attacking the chlorinated molecule with phenoxide ejected as a suitable leaving group. With this hypothesis in hand, *t*-BuLi was substituted as the reducing agent, but no complex was isolated. Thiocarbamate formation was tested with the chlorinated carbamate to test the efficacy of lithium-halogen exchange, but addition of elemental

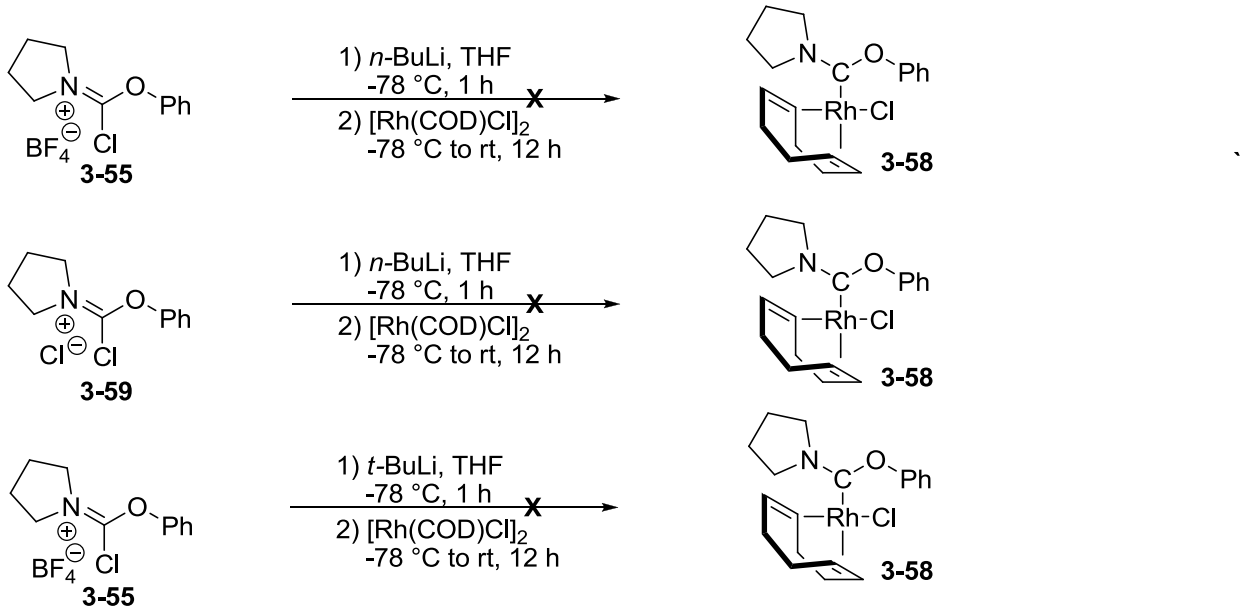

Figure 3-24. Attempts at synthesis of rhodium complex **3-58** by changing counter-ion identity and lithiation source.

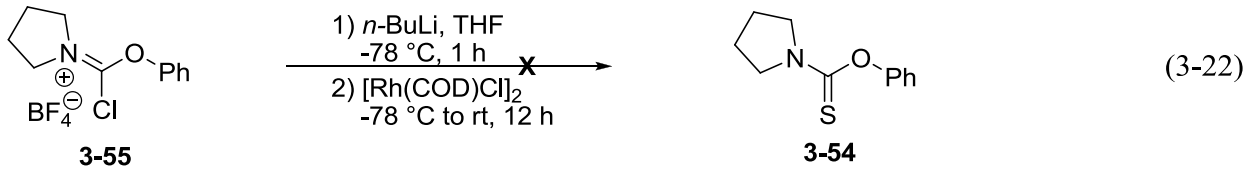

(3-22)

sulfur to the putative lithio-carbene species did not produce the desired product (Equation 3-22).

With some of the difficulties in obtaining a usable carbene, a different method for reduction of the carbon—chlorine bond was sought. One such possibility involved the application of metallic lithium and naphthalene to create a radical anionic naphthalene species (Figure 3-25).[18] Crucial to production of the radical anion was activation of the lithium granules by crushing with a spatula once inside the Schlenk flask. If activated outside an inert atmosphere, the freshly exposed surface quickly oxidized giving a sluggish lithium species. The initially dark green lithio-naphthalene solution was added to the simple chloroamidinium **3-1**, and although the green color disappeared, the chloroamidinium never dissolved. The presence of the chloroamidinium was somewhat troubling since normally the chloroamidinium dissolves as it

transforms into a carbenoid species. Not unexpectedly, complex **3-5** was not isolated after addition of $[Rh(COD)Cl]_2$.

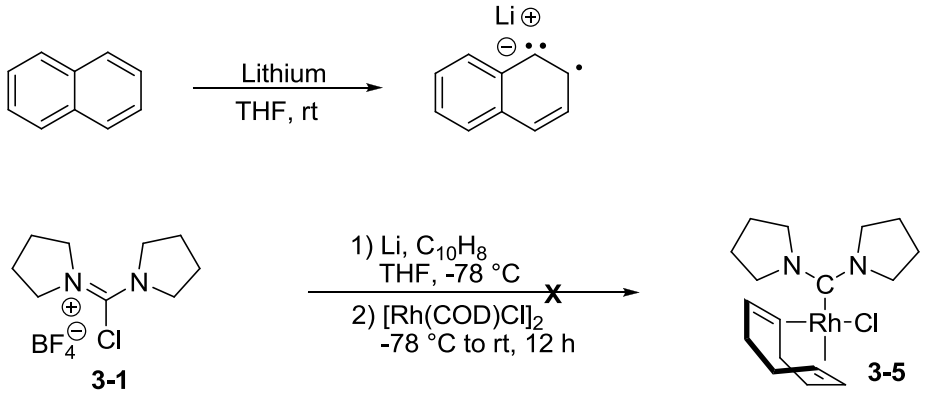

Figure 3-25. Use of a lithio-naphthalene solution to generate compound **3-5**.

Catalytic Activity of Rhodium Complexes Accessed Through Lithium-Halogen Exchange

Rhodium complexes function as diverse catalysts capable of a range of transformations effective in C—C and C—X bond formation (Figure 3-26).[30] Among these reactions rhodium is especially known for its ability to effect cycloadditions,[30,31] afford carbenoids from diazonium ylides,[32] and promote C—H activation.[33] Recently, rhodium has also gained attention for insertion reactions such as 1,4 conjugate addition[34,35] and 1,2 migratory insertion.[36,37] The 1,4 conjugate addition is particularly effective due to the high degree of enantioselectivity, low catalyst loadings, and mild conditions employed in catalysis, with the work of Hayashi and co-workers playing a large role in the achievements.

Catalysis with rhodium was explored since access to these complexes along with iridium was most straightforward. With the rhodium complexes, catalysis involving transmetalation of a boronic acid seemed to work well, and conjugate addition of boronic acids to enones was explored first using cyclohexenone **3-60** as the standard substrate (Equation 3-23). Rhodium ADC complex **3-5**, boronic acid, and potassium hydroxide were added to a Schlenk flask under

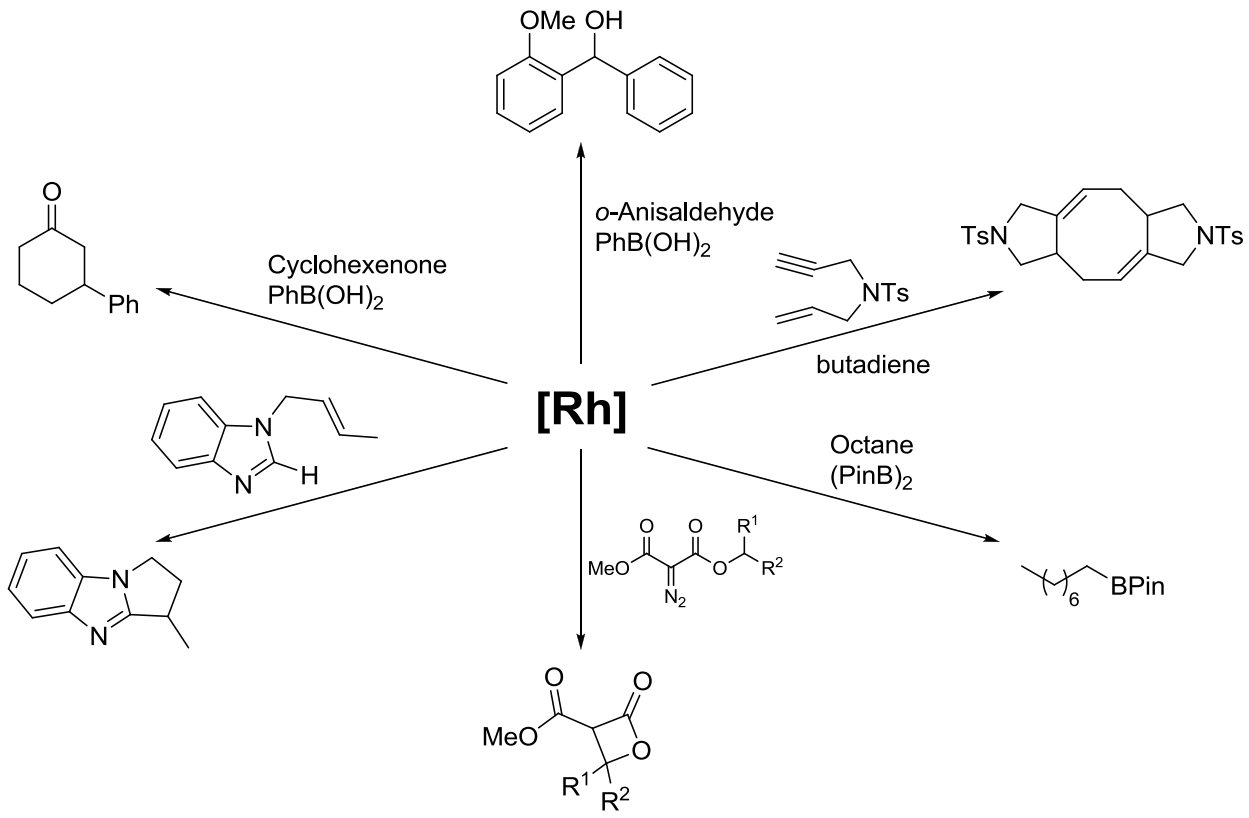

Figure 3-26. Examples of catalysis with rhodium including cycloadditions, borylations, carbenoid chemistry, C—H activation, 1,4 conjugate addition, and 1,2 addition to aldehydes.

argon atmosphere, followed by a 10:1 mixture of THF and water respectively. After addition of the solvent, distilled and degassed cyclohexenone was added to the solution. The yellowish reaction mixture was heated to 40 °C for thirty minutes, and as it neared completion, the aqueous phase separated from the organic layer. The solvent was evaporated and the residue was purified by silica gel column chromatography using a 4:1 mixture of hexanes to ethyl acetate.

Arylboronic acids functioned very well under these conditions (Table 3-6, entries 1-6), giving product in excellent yields and short reaction times. With a vinylboronic acid (entry 7), a longer reaction time was necessary, and the yield was not as high. This might be expected however, as the enone could be regenerated easily to make a highly conjugated product. Extension of the methodology to include alkylboronic acids (entry 8) did not result in successful

isolation of the product. The catalyst was investigated with a more challenging heterocyclic substrate, **3-69**. The reaction was run under conditions similar to those used for conjugate addition to cyclohexenone; however, more time was needed (Equation 3-24).

ADC complex **3-5** also fared well in another reaction involving transmetalation, the 1,2 addition of arylboronic acids to aldehydes (Table 3-7). Under an inert atmosphere of argon, the catalyst, aldehyde, boronic acid, and base were combined, and then a 3.5:1 mixture of 1,2-dimethoxyethane and water was added. The reaction was heated at 80 °C for varying times before purification by silica gel chromatography.

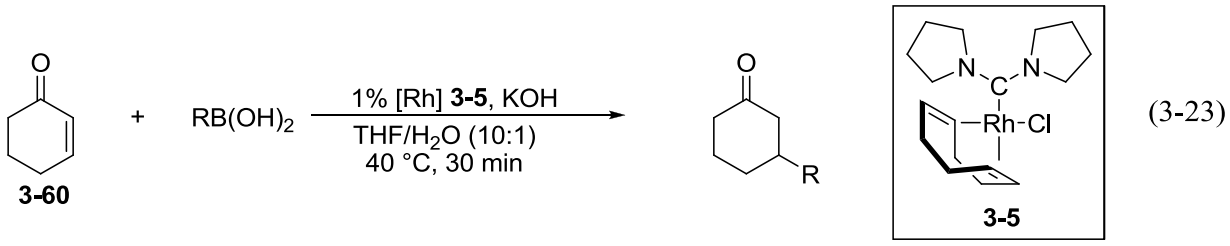

(3-23)

Table 3-6. 1,4 Conjugate Addition of Boronic Acids to Cyclohexenone

Entry	$ArB(OH)_2$	Time	Isolated Yield (%)
1	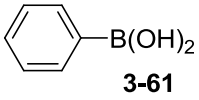 **3-61**	20 min	98
2	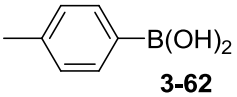 **3-62**	20 min	96
3	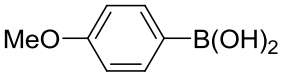 **3-63**	30 min	90
4	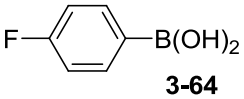 **3-64**	20 min	98
5	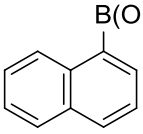 **3-65**	30 min	98
6	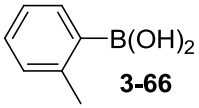 **3-66**	20 min	97

7	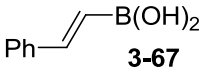 **3-67**	12 h	59
8	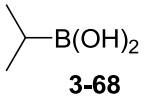 **3-68**	12 h	0

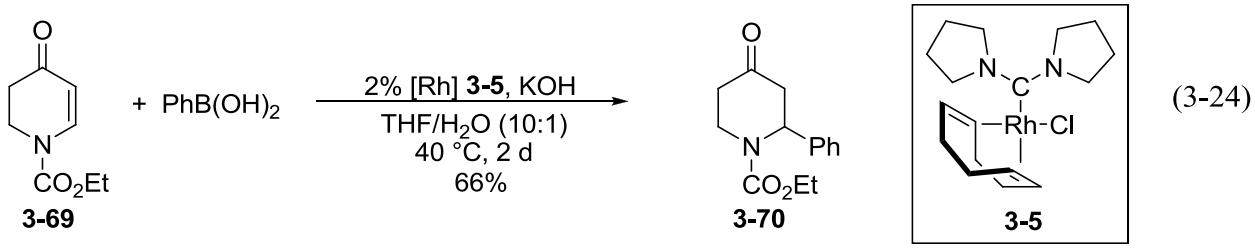

(3-24)

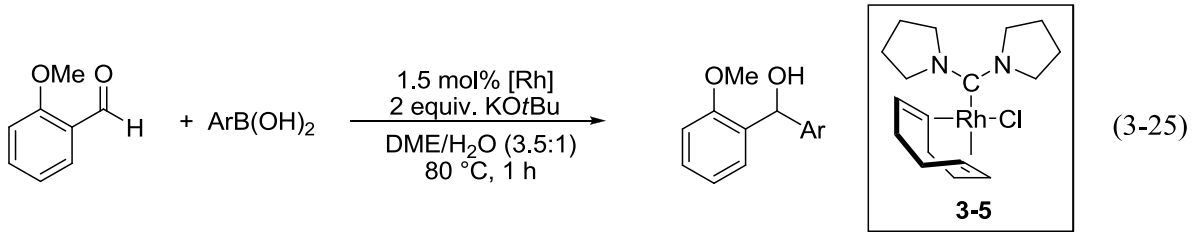

(3-25)

Table 3-7. 1,2 Addition of arylboronic acids to *o*-anisaldehyde.

Entry	Catalyst	Aldehyde	Boronic Acid	Yield (%)
1	$[Rh(COD)Cl]_2$	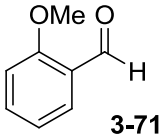 **3-71**	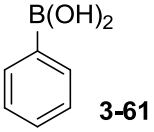 **3-61**	62
2	Rh(IMes)(COD)Cl			80
3	**3-5**			92
4	**3-5**		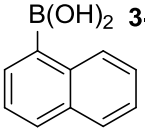 **3-65**	96
5	**3-5**		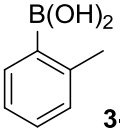 **3-66**	92
6	**3-5**		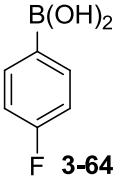 **3-64**	83

7	**3-5**	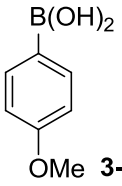 **3-63**	83

The effectiveness of the bis(pyrrolidine) ADC as a ligand was compared directly to IMes and 1,4-cyclooctadiene (COD) and showed a higher level of catalytic activity (entries 1-3). In conjunction with 2-methoxybenzaldehyde, **3-5** afforded product in 92% yield while Rh(IMes)(COD)Cl and $[Rh(COD)Cl]_2$ gave 80% and 62% yield respectively. While COD was easily the best ligand in 1,4 conjugate addition reactions, it did not compete as successfully in the 1,2 addition. This result demonstrates the potential of ADCs as viable ligands and alternates to NHCs and phosphines.

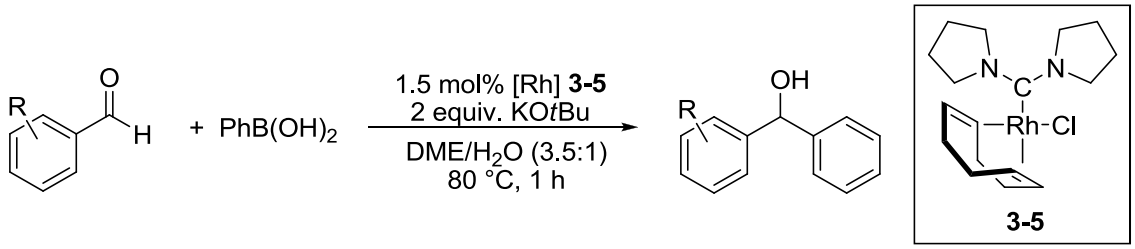

(3-26)

Table 3-8. 1,2 Addition of phenylboronic acid to arylaldehydes.

Entry	Benzaldehyde	Boronic Acid	Time	Yield (%)
1	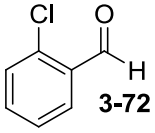 **3-72**	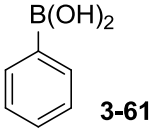 **3-61**	1 h	95
2	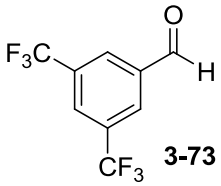 **3-73**		1 h	41
3	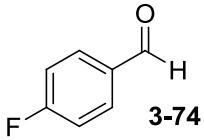 **3-74**		7 h	87

4	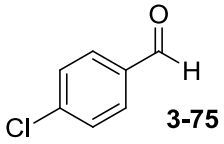 **3-75**	8 h	46
5	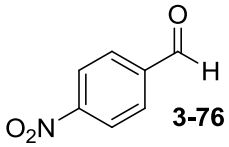 **3-76**	7 h	0
6	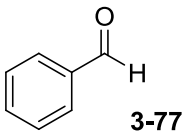 **3-77**	7 h	0

The insertion worked with a variety of boronic acids as coupling partners. Both electron deficient and rich aryl rings transferred with the same efficacy (entries 6 and 7), and mono-*ortho*-substituted aryl rings reacted with excellent activity (entries 4 and 5). The aldehyde proved to be the most sensitive variable examined (Table 3-8). A substituent in the *ortho*-position capable of coordinating to a metal center or alternatively an electron withdrawing group seemed to promote success. For example, simple benzaldehyde and 4-methoxybenzaldehyde did not react under the catalytic conditions investigated; however, the broad scope of boronic acid tolerance helps to overcome this limitation in the synthesis of diaryl methanol products.

A plausible catalytic cycle is shown below and based on the thoroughly investigated cycle for 1,4 conjugate addition (Figure 3-27).[30] Presumably, the first step is exchange of chloride for an alkoxide.[38] Formation of a rhodium hydroxo or alkoxo intermediate has proven crucial in the acceleration of reaction rates.[38a] It is believed that the transmetalation preferentially proceeds from the hydroxo or alkoxo complex due to the oxophilic nature of the boronic acid. Following ligand exchange is transmetalation, coordination of the aldehyde, and insertion of the aryl group into the aldehyde. The newly formed alkoxide undergoes either protonolysis or remains on the metal to start the next catalytic cycle.

It is of interest to note that there is precedent for the transmetalation step to be initiated from an intermediate involving η-6 coordination of the boronic acid.[39] Electron rich metal complexes bind olefins tighter and at a quicker rate than less electron rich metal centers.[40] Potentially, the ADC complex is more active in the 1,2 addition of arylboronic acids to aldehydes because it is more efficient in the transmetalation step. Alternatively, the difference in reactivity between the ADC and NHC metal complex might be attributed to a quicker rate of exchange of chloride for *t*-butoxide. In examining the structures of ADC-Ir complex **3-6** and NHC-Ir complex **3-9**, it is seen that the Ir—Cl bond is longer in the ADC complex, ostensibly because the greater electron density coming from the ADC weakens the Ir—Cl bond, making exchange for *t*-butoxide more facile.

The 2-bis(alkylpyrrolidino)methylidine ligands were briefly tested in the asymmetric 1,2 addition to aldehydes (Table 3-5). The most active substrates, *o*-anisaldehyde and 1-naphthylboronic acid, were used since **3-15** tends to exhibit sluggish reactivity. With both **3-13** and **3-15** slightly lower yields were obtained, and catalyst **3-15** imparted 12% ee. With NHC ligands, the highest selectivity observed thus far is 38% ee to the best of my knowledge.[37d,41]

The aforementioned results demonstrate the viability of ADC-Rh complex **3-5** in catalysis involving insertion of aryl groups into double bonds. Because transition metals bind alkenes more tightly when they are electron rich, it seemed reasonable to infer that an ADC metal complex might work well in catalysis with olefinic substrates such as 2,3-dihydrofuran **3-78** that do not bind well to metal centers. To understand the boundaries and capabilities of catalysis with the ADC complex, the unprecedented Rh-catalyzed 1,2 addition of naphthylboronic acid to 2,3-dihydrofuran was tested (Equation 3-28). The catalyst was not active enough to promote the reaction in conditions favoring either reformation of the double

bond or protonolysis. The synthesis of the bis(ethylene) and bis(cyclooctene) versions of **3-5** were attempted in order to make a more active metal center; however, neither complex was able to be isolated (Figure 3-28).

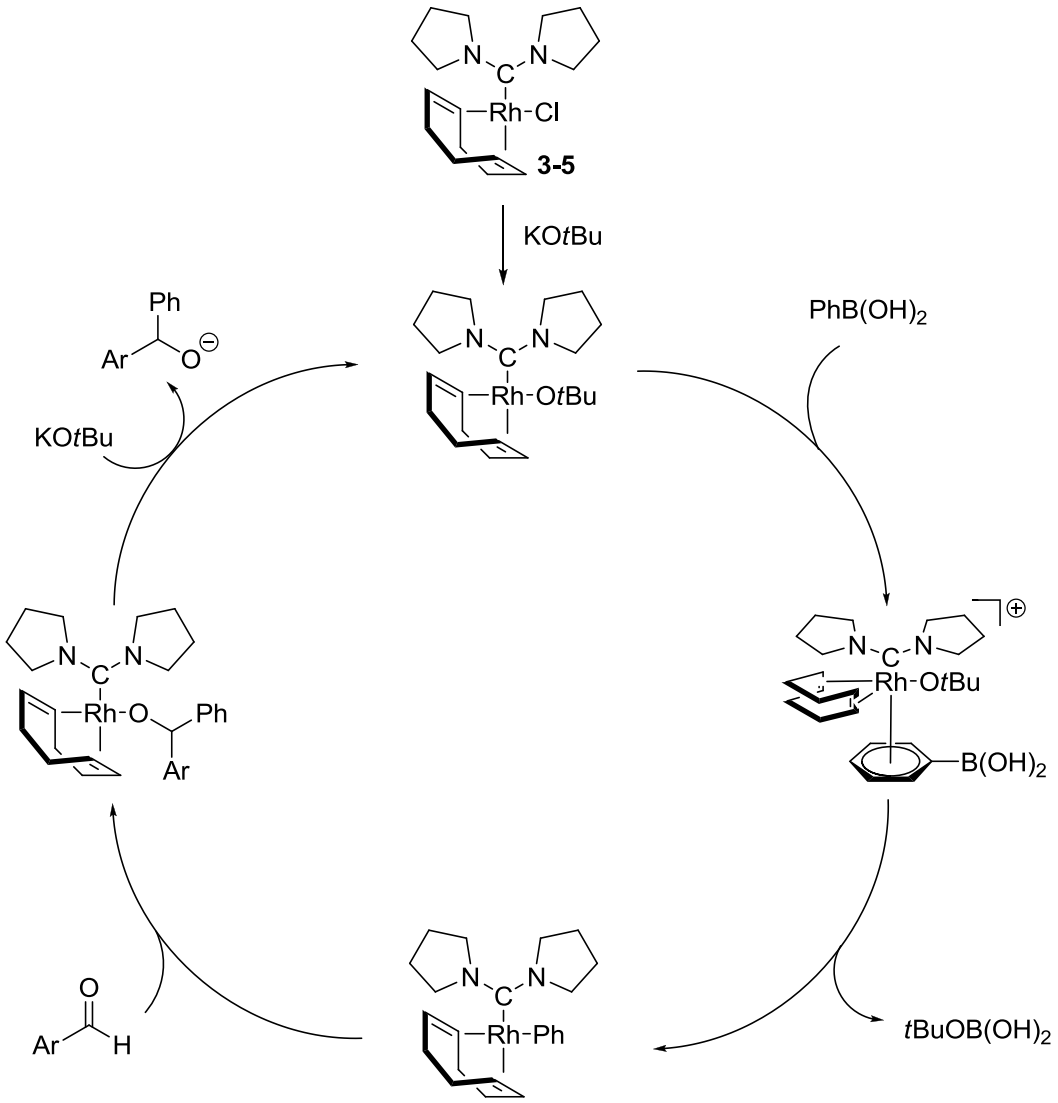

Figure 3-27. A plausible catalytic cycle for the 1,2 addition of aryboronic acids to aldehydes.

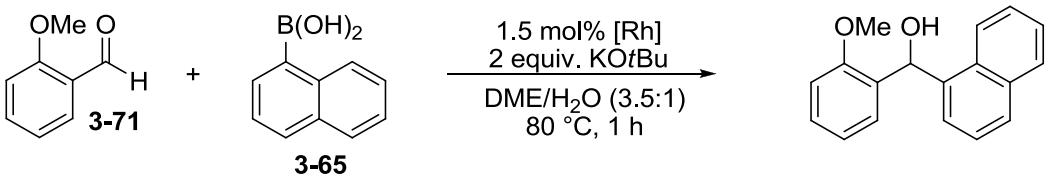

(3-27)

Table 3-9. 1,2 Asymmetric addition of 1-naphthylboronic acid to *o*-anisaldehyde.

Entry	Catalyst	Time	Yield (%)	ee (%)
1	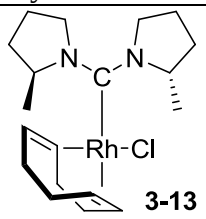 **3-13**	1 h	71	2
2	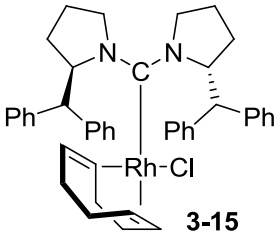 **3-15**	16 h	75	12

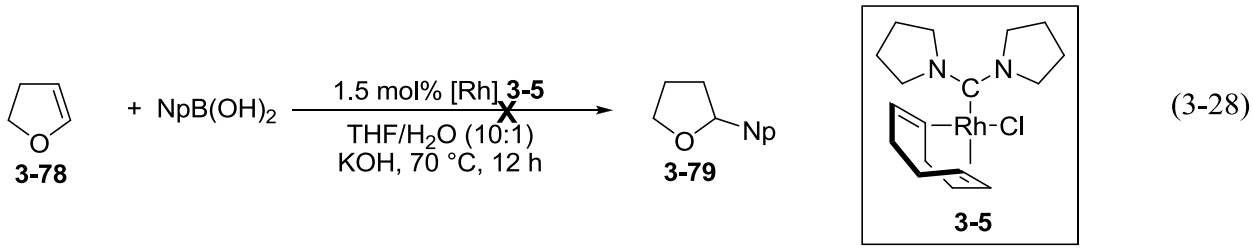

(3-28)

With the electron rich ADC, **3-5** might be expected to perform exceptionally well in catalytic cycles involving oxidative addition. As such, low-pressure hydrogenation was investigated (Equation 3-29).[42] **3-5** and coumarin **3-82** were loaded into a Schlenk flask under an argon atmosphere. Dichloromethane was added and the argon was exchanged for hydrogen at one atmosphere of pressure by bubbling the gas through the CH_2Cl_2 solution. The reaction proceeded overnight, but isolation of starting material showed that the enone failed to be reduced.

Recently, a report appeared covering the cross-coupling of aryltosylates with arylboronic acids. Wu and co-workers nicely demonstrated that electron-rich, Rh(NHC)(COD) complexes catalyzed the reaction, which makes use of readily available phenols with a functional group less

sensitive than triflate.[43] Since ADCs are even more donating than NHCs, we believed they might be more effective in the cross-coupling.

Rhodium compound **3-5**, an aryltosylate, a boronic acid, and cesium fluoride were combined in a Schlenk flask. Anhydrous toluene under an argon atmosphere was added to the solids, and the suspension was then heated to 120 °C and stirred for thirty hours. After purifying the products of the reaction mixture by silica gel chromatography, the aryltosylate was recovered in quantitative yields, giving evidence that a reaction did not take place (Equation 3-30).

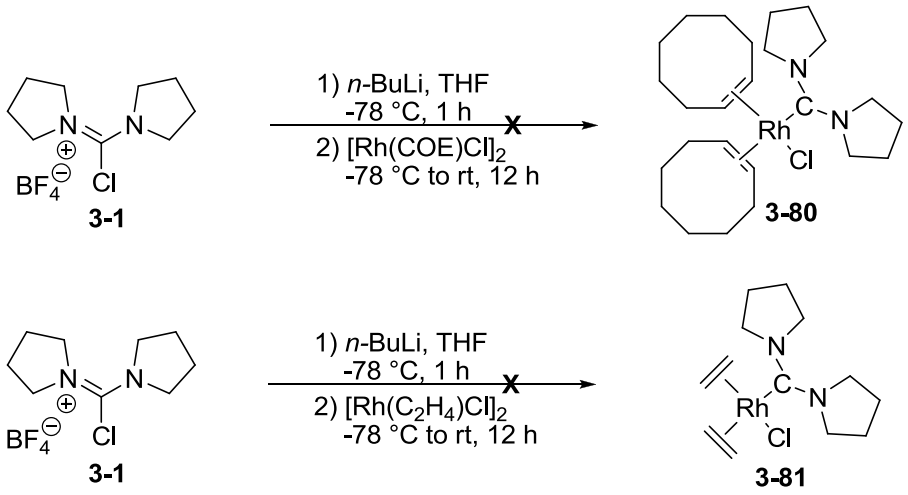

Figure 3-28. Attempts at synthesis of complexes **3-80** and **3-81** which might be expected to show greater activity toward insertion reactions with olefins.

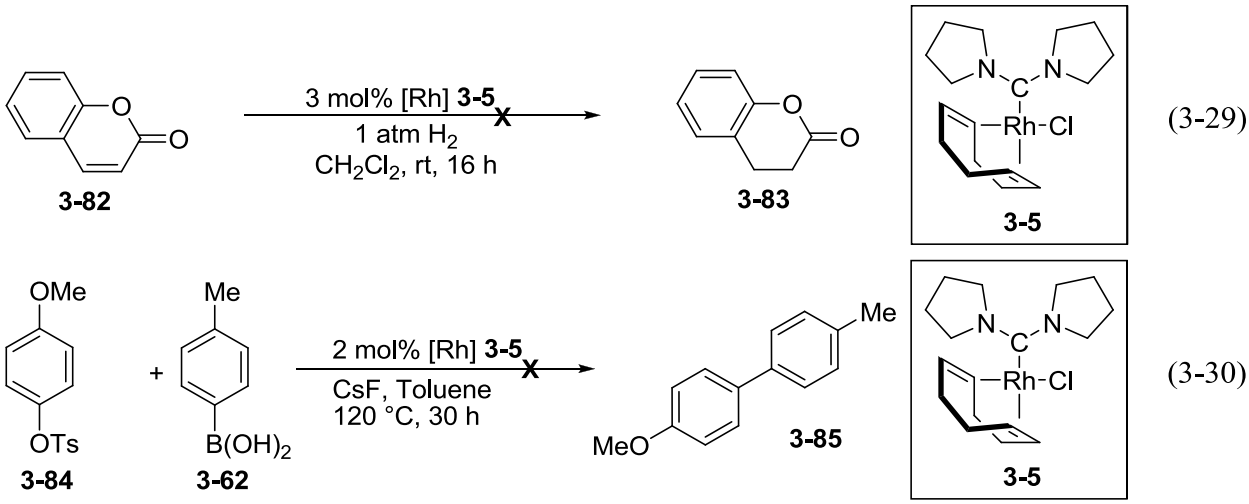

ADC-Pd Complex 3-18 in the Suzuki Cross-Coupling

Although palladacycles of type **3-18** are not typically used in the Suzuki cross-coupling reaction, it was investigated to see the effects of the ADC ligand in the absence of triphenyl phosphine. With toluene at reflux, the conditions employed when using **2-15** and **2-26**, low yield of the binaphthyl product was obtained. Using the harsher conditions developed by Iyer and co-workers, **3-87** was formed in 78% yield (Figure 3-29).[44]

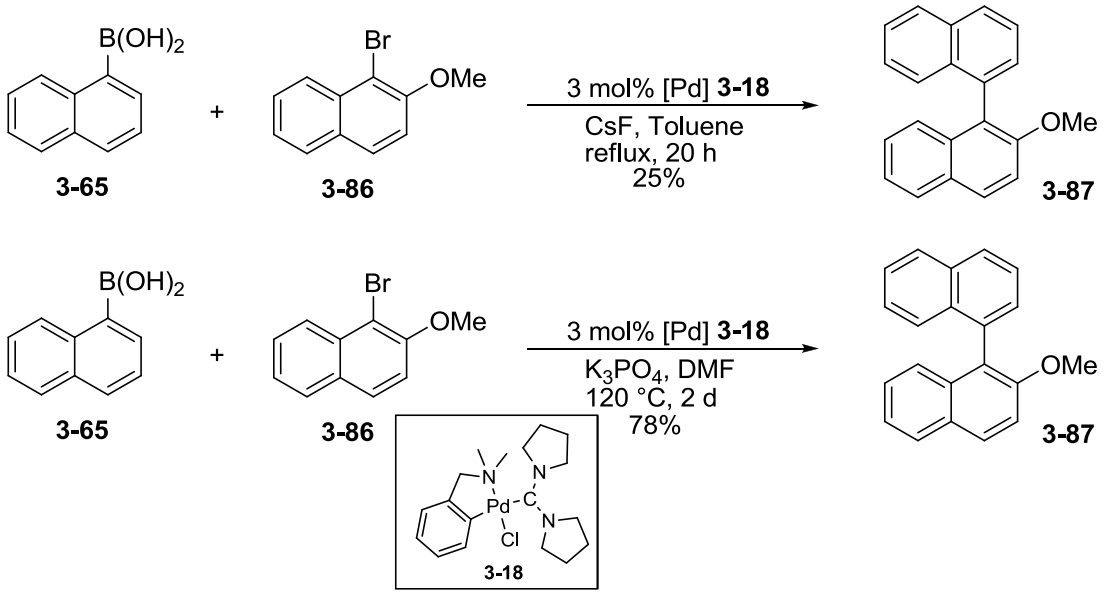

Figure 3-29. Suzuki coupling to form triortho-substituted product using catalyst **3-18**.

Steric and Electronic Measurements of ADC and NHC Compounds

Iridium complexes **3-6** and **3-9** were further characterized using cyclic voltametry to measure the diaminocarbenes' donor properties. As discussed by Plenio and co-workers, electrochemistry and the measurement of reduction potentials gives a more precise understanding of electronic characteristics than measurement of υ(CO) of M(NHC)$(CO)_2$Cl complexes and calculation of the Tolman electronic parameter (TEP) since most NHCs fall within a 3 cm^{-1} range.[45] Lower reduction potentials indicate stronger donor ligands, as more electron rich ligands ease the oxidation of the iridium center from Ir^{I} to Ir^{II}. ADC iridium complex **3-6** exhibited an $E_{1/2}$ of

0.422 V and NHC iridium complex showed a $E_{1/2}$ of 0.765 V, clearly demonstrating the superior donor properties of the ADC ligand. Plenio and co-workers synthesized a variety of NHC ligands, and when bound to metal, these complexes yielded $E_{1/2}$ values spanning from 0.591 to 0.920 V, clearly delineating the electronic spectrum of carbene ligands (Table 3-10). ADCs fall well below the range observed for even the most donating NHC. The electronic properties for bis(diisopropylamino)carbene were previously reported;[6d] however donor power only accounts for half of the puzzle when determining carbene properties.

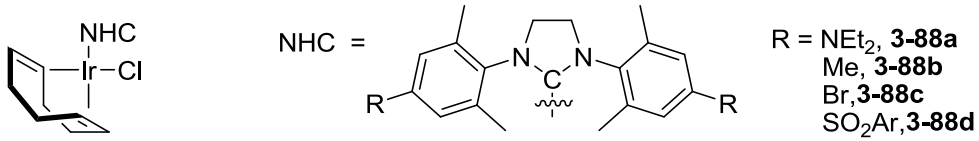

Figure 3-30. Variable NHC ligands used in Plenio's study of electronic influence of aromatic substituents.

Table 3-10. Redox half potentials for some Ir(L)(COD)Cl complexes in CH_2Cl_2 (scan rate 100mVs^{-1}).

Complex	$E_{1/2}$ [V]	Complex	$E_{1/2}$ [V]
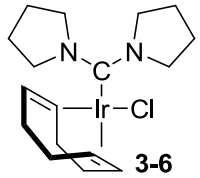 **3-6**	0.422	**3-88b**, R = Me	0.735
		3-88c, R = Br	0.838
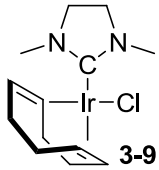 **3-9**	0.765	**3-88d**, R = SO_2Ar	0.910
3-88a, R = NEt_2	0.591	$Ir(PCy_3)(COD)Cl$	0.948

Thus far, steric parameters of ADCs have not been disclosed. Cavallo and co-workers developed an excellent model aiding the determination of a ligand's steric bulk. It is known as percent volume buried, or % V_{Bur} and is a metric for how much of a ligand lies within a set radius representing the coordination sphere of a metal (Figure 3-31).[46]

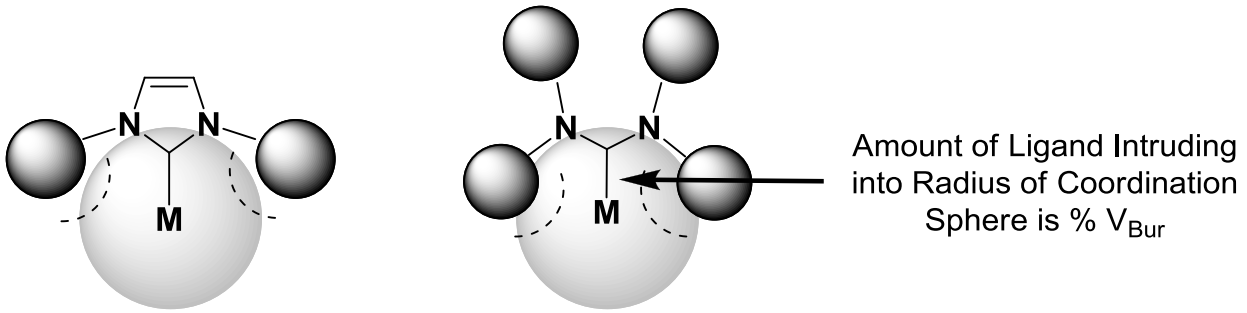

Figure 3-31. Graphical illustration of % V_{Bur}.

Table 3-11. Calculated % V_{Bur} values for ADC ligands in complexes **3-5**, **3-6**, **3-9**, and **3-13**. Calculated with Bondi radii scaled by 1.17, 3.5Å radius of the sphere, and 2.1Å distance of the ligand from the sphere. NHC values reported by Cavallo.[46]

Ligand	% V_{Bur}	Ligand	% V_{Bur}
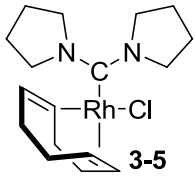 **3-5**	27.9	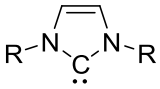 R = Me(saturated)	25.4
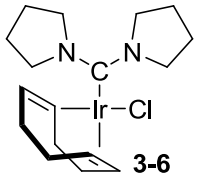 **3-6**	28.0	R = Et	26.0
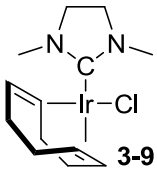 **3-9**	25.3	R = IMes	31.6
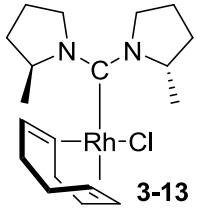 **3-13**	29.7	R = DIPr	33.6
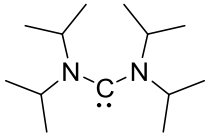	30.1	R = Adamantyl	36.1

One might expect that the larger carbene bond angle of ADCs might cause them to have higher % V_{Bur} values than NHCs. With the ADCs explored thus far; however, the % V_{Bur} has

been considerably lower than typical NHCs. This could reasonably be expected since the pyrrolidine rings exhibit a low degree of substitution. Complexes **3-6**, **3-9**, and **3-13** show % V_{Bur} values of 28.0, 25.3, and 29.7 % respectively, while IMes possesses a percentage of 31.6 (Table 3-11).

Conclusions and Summary

The methodology developed provides a solid platform for the synthesis and exploration of ADC ligands. Despite the benefits of the lithium-halogen exchange, several drawbacks still exist. The process as of now is not applicable to all chloroamidinium precursors. Particularly, functionalized molecules and *N,X* type carbenes were not formed, and alkyl-based ureas tend to fare best.

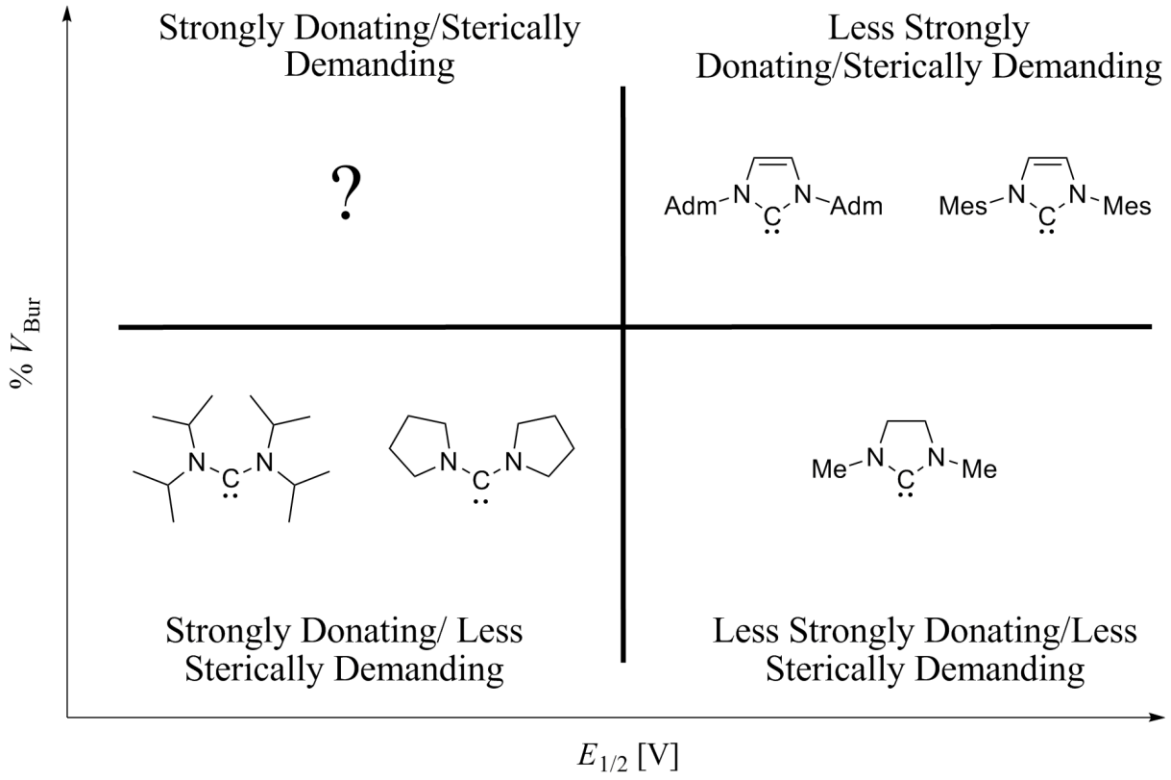

Figure 3-32. Plot of redox potential vs. % V_{Bur}. Carbenes that are both strongly donating and sterically demanding are as of yet uninvestigated.

ADC structures have only just begun to be investigated, and measurement of reduction potentials and % V_{Bur} give a logical means of tuning ADC properties. The combined information from cyclic voltametry and % V_{Bur} data paints a picture of a ligand possessing quite distinct characteristics from those of the well-known NHC basis set. Promising results showing the potential of ADCs has been demonstrated, but truly exceptional catalytic activity has not yet been achieved. Perhaps one needs to draw deeper into the well of available catalytic reactions and further from those known to work well with NHCs to realize the desired outcomes of ADCs. Clearly by expanding into other quadrants of the graph in Figure 3-32, through single factor variation of either sterics or electronics, considerable changes in catalytic reactivity might be observed.

CHAPTER 4
EXPERIMENTAL SECTION

General Remarks

All reactions were conducted in flame-dried glassware under an inert atmosphere of dry argon. THF, CH_2Cl_2, and Et_2O were passed through two packed columns of neutral alumina under positive pressure of dry nitrogen prior to use. Toluene was passed through an alumina column and a copper (II) oxide column under positive pressure of dry nitrogen prior to use. All other chemicals were commercially available and were used as received without further purification. NMR spectra were recorded using a FT-NMR machine, operating at 300 MHz for ^{1}H NMR and at 75.4 MHz for ^{13}C NMR. All chemical shifts for ^{1}H and ^{13}C NMR spectroscopy were referenced to residual signals from $CDCl_3$ (^{1}H) 7.27 ppm and (^{13}C) 77.23 ppm. High resolution mass spectra were recorded on a GC/MS spectrometer or a TOF-LC/MS spectrometer.

General Procedure for Formation of Ureas Based on 2-Substituted Pyrrolidines.

A pyrrolidine derivative (8.82 mmol), triethyl amine (26.4 mmol), and CH_2Cl_2 (17.6 mL) were added to a flame dried Schlenk flask, and the solution was stirred and cooled to 0 °C. Phosgene (4.4 mmol, 2.32 mL) was slowly added in the form of a 20 wt% solution in toluene, and the Schlenk flask was sealed to prevent loss of gaseous phosgene. The reaction was vigorously stirred for 4 hours at which point extra phosgene (2.2 mmol, 1.16 mL) was added to ensure complete reaction of the amine. Stirring continued for an additional 4 hours, and then the reaction was quenched with water. The aqueous layer was extracted with CH_2Cl_2 (20 mL x 3), dried with $MgSO_4$, and concentrated. The crude product was purified by silica gel column chromatography (hexanes, ethyl acetate, 1:1) to give the pure urea.

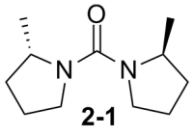

2-1

Bis(2*S*)-Methylpyrrolidine Urea. ^{1}H NMR (300 MHz, $CDCl_3$) δ = 1.15 (d, *J* = 6.30 Hz, 3H), 1.36-1.43 (m, 1H), 1.61-1.74 (m, 1H), 1.76-1.83 (m, 1H), 2.01-2.12 (m, 1H), 3.23-3.37 (m, 2H), 3.89- 4.02 (m, 1H); ^{13}C NMR ($CDCl_3$, 75 MHz) δ = 21.0, 25.5, 49.7, 54.0, 161.5; HRMS Calcd. for $C_{11}H_{20}N_2O$ $[M+H]^+$: 197.1648, Found: 197.1643.

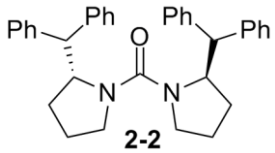

2-2

Bis(2*R*)-Diphenylmethylpyrrolidine Urea. ^{1}H NMR (300 MHz, $CDCl_3$) δ = 1.45 - 1.72 (m, 4 H), 1.70 - 2.01 (m, 4 H), 2.45 - 2.65 (m, 2 H), 2.98 - 3.21 (m, 2 H), 3.99 (d, *J* = 10 Hz, 2 H), 5.19 - 5.36 (m, 2 H), 5.38 - 5.86 (m, 1 H), 7.04 - 7.46 (m, 20 H). ^{13}C NMR (75 MHz, $CDCl_3$) δ = 14.5, 24.0, 28.6, 55.5, 69.6, 127.7, 127.9, 128.5, 128.6, 129.0, 129.1, 129.2, 139.3, 140.3, 152.5. HRMS Calcd. for $C_{35}H_{36}N_2Cl$ $[M+H]^+$: 519.2562, Found: 519.2585.

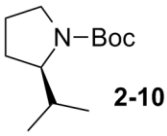

2-10

(2*R*)-(Isopropyl)-*N*-(*tert*-Butyloxycarbonyl)pyrrolidine. To a flame dried 3-neck round bottom flask, pyrrolidinone **2-9** (15.7 mmol, 2.0 g) and THF (78 mL) were added. The solution was cooled to 0 °C, and lithium aluminum hydride (31.4 mmol, 1.195 g) was added portion wise over 10 minutes. The reaction mixture was stirred at this temperature for half an hour before warming to room temperature. After an additional 30 minutes, the reaction was heated to reflux and stirred for 3.5 hours. The reaction was quenched with 1.2 mL of water followed by 2.4 mL of a 10 % NaOH solution, and lastly 3 mL of water was added. Lithium salts were removed by filtering over a celite bed. Boc_2O was added to the THF filtrate, and the solution was stirred overnight. Volatiles were removed and the crude product was purified by column chromatography (hexanes/ethyl acetate, 4:1) to give **2-10** (3.24 g, 97%). ^{1}H NMR (300 MHz,

$CDCl_3$) δ = 0.76 (d, *J* = 6.9 Hz, 3H), 0.83 (d, *J* = 7.2 Hz, 3H), 1.42 (s, 9H), 1.63-1.79 (m, 4H), 1.94-2.23 (m, 1H), 3.14-3.22 (m, 1H), 3.36-3.70 (m, 2H). ^{13}C NMR (75 MHz, $CDCl_3$) δ = 17.4, 20.0, 23.8, 24.5, 26.0, 26.9, 28.8, 30.2, 31.1, 47.2, 62.5, 78.6, 154.5. HRMS Calcd. for $C_{12}H_{23}NO_2$ $[M+Na]^+$: 236.1621, Found: 236.1606.

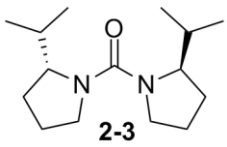

2-3

Bis(2*R*)-Diphenylmethylpyrrolidine Urea. Boc-protected amine **2-10** (4.69 mmol, 1.00 g) and ether (1 mL) were added to a flame dried Schlenk flask and cooled to 0 °C. Slowly, 4M HCl in dioxane (23.5 mmol, 5.87 mL) was added to the vigorously stirred solution. The reaction was stirred at room temperature for 3 hours, and a white salt precipitated out of solution. Solvent was removed in situ, and the solid was washed twice with ether. The solid was dried in vacuo, and the general procedure described above was used for formation of urea **2-3** (0.271 g, 46 %). ^{1}H NMR (300 MHz, $CDCl_3$) δ = 0.78 (d, *J* = 7 Hz, 3 H), 0.86 (d, *J* = 7 Hz, 3 H), 1.44 - 1.95 (m, 4 H), 1.95 - 2.18 (m, 1 H), 3.21 (m, 1 H), 3.28 - 3.47 (m, 1 H), 3.91 - 4.14 (m, 1 H). ^{13}C NMR (75 MHz, $CDCl_3$) δ = 13.6, 16.5, 19.7, 25.7, 30.3, 50.9, 62.6, 162.4. HRMS Calcd. for $C_{12}H_{23}NO_2$ $[M+H]^+$: 253.2274, Found: 253.2264.

General Procedure for the Formation of Chloroamidinium Ions.

Urea **2-1** (2.09 mmol, 0.400 g) was mixed with toluene (10.45 mL) in a flame dried Schlenk flask. To this solution was added oxalyl chloride (2.51 mmol, 0.212 mL), and the reaction mixture was heated to 60 °C. The reaction was stirred overnight at which point, a brown, oily residue precipitated out of solution. The reaction was cooled to room temperature and the toluene was siphoned off. The oily residue was washed twice with ether, dissolved in CH_2Cl_2 (12 mL), and $AgBF_4$ (2.09 mmol, 0.407 g) was added. The reaction was stirred for 1

hour. After this time, the CH_2Cl_2 was filtered off into a dry Schlenk flask under an argon atmosphere. Volatiles were removed resulting in an off white solid (0.4445 g, 70%).

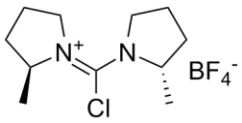

2-11

Bis(2*S*)-Methylpyrrolidine Chloroamidinium Tetrafluoroborate 2-11. ^{1}H NMR (300 MHz, $CDCl_3$) δ = 1.39 (d, 6 H), 1.63 - 1.88 (m, 2 H), 2.11 (dd, *J* = 5, 1 Hz, 4 H), 2.25 - 2.56 (m, 2 H), 3.68 - 3.90 (m, 2 H), 3.90 - 4.13 (m, 2 H), 4.20 - 4.56 (m, 2 H). ^{13}C NMR (75 MHz, $CDCl_3$) δ = 20.3, 25.4, 33.5, 55.9, 62.4, 152.7. HRMS Calcd. for $C_{11}H_{20}N_2Cl$ $[M+H]^+$: 215.1310, Found: 215.1310.

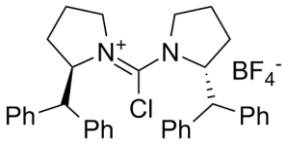

2-12

Bis(2*R*)-Diphenylmethylpyrrolidine Chloroamidinium Tetrafluoroborate 2-12. ^{1}H NMR (300 MHz, $CDCl_3$) δ = 1.45 - 1.72 (m, 4 H), 1.70 - 2.01 (m, 4 H), 2.45 - 2.65 (m, 2 H), 2.98 - 3.21 (m, 2 H), 3.99 (d, *J* = 10 Hz, 2 H), 5.19 - 5.36 (m, 2 H), 5.38 - 5.86 (m, 1 H), 7.04 - 7.46 (m, 20 H). ^{13}C NMR (75 MHz, $CDCl_3$) δ = 14.5, 24.0, 28.6, 55.5, 69.6, 127.7, 127.9, 128.5, 128.6, 129.0, 129.1, 129.2, 139.3, 140.3, 152.5. HRMS Calcd. for $C_{35}H_{36}N_2Cl$ $[M+H]^+$: 519.2562, Found: 519.2585.

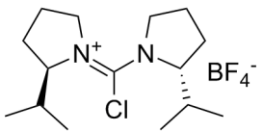

2-13

Bis(2*R*)-Isopropylpyrrolidine Chloroamidinium Tetrafluoroborate 2-13. ^{1}H NMR (300 MHz, $CDCl_3$) δ = 0.82 (br. s., 3 H), 0.91 (br. s., 3 H), 1.32 (br. s., 1 H), 2.09 (br. s., 4 H), 3.68 (br. s., 2 H), 4.27 (br. s., 1 H). ^{13}C NMR (75 MHz, $CDCl_3$) δ = 13.12, 16.04, 19.46, 24.98,

25.38, 30.56, 49.13, 57.65, 58.24, 71.73, 153.48, 156.42. HRMS Calcd. for $C_{15}H_{28}N_2Cl$ $[M+H]^+$: 271.1936, Found: 271.1928.

General Procedure for the Formation of Palladium Complexes.

Amidinium chloride **2-11** (0.140 mmol, 0.0408 g) was added to a flame dried Schlenk flask along with toluene (10 mL). To the suspension was added $Pd(PPh_3)_4$ (0.140 mmol, 0.1623 g). The yellow solution was heated to 100 °C and quickly turned deep red in color. The reaction was stirred for two hours at which point, a yellow solid precipitated from solution. The mixture was allowed to cool to room temperature, and the toluene was evaporated. Pentane was added to the resulting solid (10 mL x 2) which was stirred for 1 hour before being decanted. CH_2Cl_2 was used to dissolve the product and insoluble salts were filtered off. Pentane was layered on top of the filtrate to purify the product by recrystallization (0.078 g, 65 %).

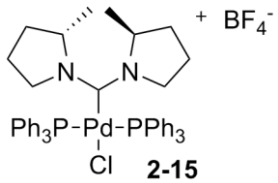

2-15

Bis(Triphenylphosphine)-(2*S*)-Methylpyrrolidinecarbene Palladium Chloride 2-15.

^{1}H NMR (300 MHz, $CDCl_3$) δ = 0.54 (d, *J* = 7 Hz, 1 H), 0.76 - 0.96 (m, 5 H), 1.21 - 1.34 (m, 1 H), 1.42 - 1.60 (m, 2 H), 1.60 - 1.79 (m, 2 H), 1.79 - 2.01 (m, 1 H), 3.70 - 4.07 (m, 3 H), 4.85 (q, *J* = 9 Hz, 1 H), 7.06 - 7.28 (m, 2 H), 7.28 - 7.51 (m, 2 H), 7.53 - 7.81 (m, 25 H). ^{13}C NMR (75 MHz, $CDCl_3$) δ = 14.0, 20.2, 20.9, 21.7, 22.6, 22.9, 30.0, 32.1, 34.3, 57.1, 59.0, 129.2, 129.3, 129.3, 129.8, 130.0, 132.0, 132.2, 134.6, 187.2. HRMS Calcd. for $C_{47}H_{40}N_2P_2ClPd$ $[M+H]^+$: 845.2181, Found: 845.2152.

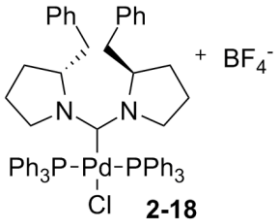

2-18

Bis(Triphenylphosphine)-(2*R*)-Methylpyrrolidinecarbene Palladium Chloride 2-15.

^{1}H NMR (300 MHz, $CDCl_3$) δ = 1.00 - 1.51 (m, 4 H), 1.53 - 2.13 (m, 5 H), 2.49 - 2.72 (m, 2 H), 2.96 (dd, *J* = 14, 5 Hz, 2 H), 3.66 - 3.85 (m, 2 H), 4.28 - 4.48 (m, 2 H), 5.49 (ddd, *J* = 11, 6, 6 Hz, 2 H), 6.81 - 7.85 (m, 40 H). ^{13}C NMR (75 MHz, $CDCl_3$) δ = 22.8, 25.9, 40.0, 54.4, 71.5, 126.8, 128.5, 128.8, 129.1, 130.2, 131.6, 132.4, 134.3, 134.7, 135.3, 137.1, 185.8.

General Procedure for Suzuki Cross-Coupling Reaction

Boronic acid **2-23** (0.269 mmol, 0.0464 g), aryl bromide **2-24** (0.221 mmol, 0.524 g), palladium complex **2-15** (0.0066 mmol, 0.0060 g), and CsF (0.619 mmol, 0.0940 g) were added to a flame dried Schlenk flask. THF (3.5 mL) was added to the solids and the reaction was heated at reflux for 16 hours. After this time, the reaction mixture was diluted with water and extracted with ethyl acetate (3.5 mL x 3). The organic layers were combined, dried with $MgSO_4$, and concentrated. The crude product was purified by column chromatography (hexanes/ethyl acetate, 50:1) resulting in pure biaryl (0.0619 g, 99%) with spectra that match those reported in the literature. ^{1}H NMR ($CDCl_3$, 300 MHz) δ = 3.79 (s, 3H), 7.2-7.4 (m, 5H), 7.46-7.54 (m, 3H), 7.67 (t, *J* = 6.9 Hz, 1H), 7.92 (d, *J* = 6.3 Hz, 1H), 7.98- 8.04 (m, 3H). ^{13}C NMR (75 MHz, $CDCl_3$) δ = 154.54, 134.51, 134.21, 133.65, 132.91, 129.42, 128.94, 128.39, 128.17, 127.76, 127.67, 126.34, 126.12, 125.8 1, 125.64, 125.52, 125.43, 123.50, 113.71, 56.61. HRMS Calcd. for $C_{21}H_{16}O$ $[M+H]^+$: 284.1201, found, 284.1225.

General Procedure for the Formation of Ureas from Carbamoyl Chlorides

Chiral amine **2-37 (**0.672 mmol, 0.150 g), triethyl amine (1.345 mmol, 0.188 mL), pyrrolidine carbamoyl chloride (1.01 mmol, 0.111 mL), and CH_2Cl_2 (1.2 mL) were mixed in a flame dried Schlenk flask. The solution was warmed to 60 °C and heated overnight. The reaction was diluted with water and extracted with CH_2Cl_2 (3 mL x 3). The organic fractions were collected, dried with $MgSO_4$, and concentrated. The crude product was purified by column chromatography (hexanes/ethyl acetate, 2:1) to give **2-41** (0.152 g, 70%).

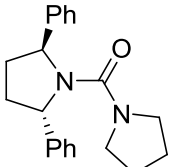

2-41

(2*S*, 5*S*)-Diphenylpyrrolidine Pyrrolidine Urea 2-41. ^{1}H NMR (300 MHz, $CDCl_3$) δ = 1.40-1.56 (m, 2H), 1.62-1.74 (m, 2H), 1.76-1.83 (m, 2H), 2.38-2.50 (m, 2H), 3.08-3.38 (m, 4H), 5.35-5.39 (m, 2H), 7.18-7.36 (m, 10H); ^{13}C NMR (75 MHz, $CDCl_3$) δ = 25.1, 25.5, 34.2, 34.5, 63.5, 63.8, 125.5, 125.8, 126.7, 127.0, 128.3, 128.4, 128.6, 144.5, 144.8, 159.1.

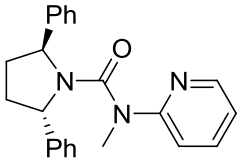

2-49

***N*,*N*-Methyl,Pyridine-(2*S*, 5*S*)-Diphenylpyrrolidine Urea 2-49.** ^{1}H NMR (300 MHz, $CDCl_3$) δ = 8.32 (br. s., 1 H), 7.72 - 7.45 (m, 1 H), 7.25 (br. s., 10 H), 7.02 - 6.78 (m, 1 H), 6.67 (d, *J* = 7.6 Hz, 1 H), 5.27 (br. s., 1 H), 5.01 (br. s., 2 H), 2.84 (br. s., 3 H), 2.58 - 2.29 (m, 2 H), 1.85 (br. s., 2 H). ^{13}C NMR (75MHz, $CDCl_3$) δ = 158.7, 156.3, 148.0, 144.0, 137.4, 128.7, 127.3, 126.2, 117.4, 114.5, 64.3, 34.9

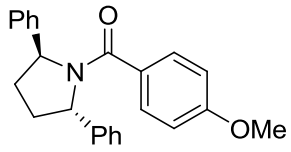

2-50

Anisoyl (2*S*, 5*S*)-Diphenylpyrrolidine Amide 2-50. ^{1}H NMR (300 MHz, $CDCl_3$) δ = 1.89-2.01 (m, 2H), 2.57-2.87 (m, 2H), 3.81 (s, 3H), 5.44 (d, *J* = 6.3 Hz, 1H), 5.82 (d, *J* = 5.7 Hz, 1H), 6.77 (d, *J* = 8.7 Hz, 2H), 7.12 (d, *J* = 7.5 Hz, 2H), 7.21-7.59 (m, 10H); ^{13}C NMR (75 MHz, $CDCl_3$) δ = 31.8, 34.2, 55.6, 62.3, 65.1, 133.5, 125.9, 127.2, 128.8, 130.5, 143.9, 144.5, 160.6, 171.4.

General Procedure for the Formation of Tri-Substituted Ureas from Isocyanates

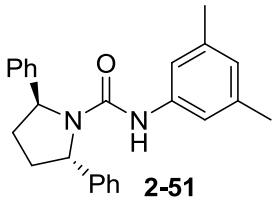

2-51

3,5-Dimethylaniline (2*S*, 5*S*)-Diphenylpyrrolidine Urea 2-51. 3,5-dimethylphenyl isocyanate (0.448 mmol, 0.063 mL) and MTBE (2 mL) were added to a flame dried Schlenk flask. To this solution was added drop wise chiral amine **2-37** (0.448 mmol, 0.100 g) dissolved in MTBE (2 mL). After five minutes, a white precipitate formed, and the reaction was stirred for 5 hours. The reaction was quenched with water and extracted with CH_2Cl_2 (3 mL x 3). The organic layers were collected, dried with $MgSO_4$, and concentrated. The crude product was purified by column chromatography (hexanes/ethyl acetate 4:1) to give the pure urea (0.148 g, 89%) as a white solid. ^{1}H NMR (300 MHz, $CDCl_3$) δ = 1.79-1.84 (m, 2H), 2.16 (s, 6H), 2.51-2.60 (m, 2H), 5.12-5.60 (br. s., 2H), 6.01 (s, 1H), 6.57 (s, 1H), 6.72 (s, 2H), 7.25-7.44 (m, 10H); ^{13}C NMR (75 MHz, $CDCl_3$) δ = 21.5, 62.2, 117.1, 124.7, 129.3, 138.6, 138.9, 153.5.

General Procedure for the Methylation of Tri-Substituted Ureas

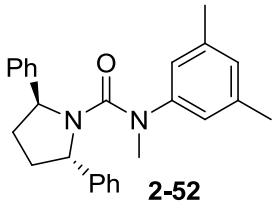

2-52

***N,N*-Methyl-3,5-Dimethylaniline (2*S*, 5*S*)-Diphenylpyrrolidine Urea 2-52.** Urea **2-51** (0.329 mmol, 0.122 g) was combined with DMF (3.3 mL) in a flame dried Schlenk flask. Sodium hydride (0.494 mmol, 0.0197 g) was added to this solution and it was stirred at room temperature for 45 minutes. After this point, methyl iodide (0.494 mmol, 0.031 mL) was added, the reaction was heated to 40 °C, and the reaction mixture was stirred overnight. The reaction was quenched with water and extracted with CH_2Cl_2. The organic fractions were combined, dried with $MgSO_4$, and concentrated. The crude product was purified by column chromatography (hexanes/ethyl acetate, 4:1) to afford the pure product (0.119 g, 94%). ^{1}H NMR (300 MHz, $CDCl_3$) δ = 1.62-1.68 (m, 2H), 2.23-2.40 (s, 8H), 2.80 (s, 3H), 6.38 (s, 2H), 6.84 (s, 1H), 7.11-7.38 (m, 10H); ^{13}C NMR (75 MHz, $CDCl_3$) δ = 21.4, 38.9, 63.5, 123.5, 126.2, 127.1, 128.5, 138.8, 145.1, 145.4, 159.7.

General Procedure for Formation of Carbene 3-4

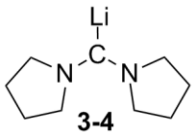

3-4

Lithium-Bis(Pyrrolidine)Carbene 3-4. To a Schlenk flask in a glovebox, 100 mg (0.364 mmol) of chloroamidinium **3-1** was added, and the flask was connected to a Schlenk line outside the glovebox. THF (2 mL) was added, and the suspension was cooled to -78 °C with a dry-ice/acetone bath. After cooling, 2.5M *n*-BuLi in hexanes (0.153mL) was added. After 5 minutes, the suspension turned to a clear and slightly yellowish solution upon formation of

carbene. The solution proceeded to stir at -78 °C for a total of 1 hour. ^{1}H NMR (300MHz, THF-d_8) δ = 3.56 (br. s., 8 H), 1.70 (br. s., 8 H). ^{13}C NMR (75MHz, THF-d_8) δ = 233.8.

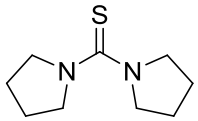

Bis(Pyrrolidine)thiourea 3-2. Carbene generation was followed as described above. After formation of carbene, 100 mg (3.125 mmol) of sulfur was added, and the reaction was allowed to slowly warm to room temperature. The resulting suspension stirred for 12 hours, diluted with ether, and filtered over a bed of celite. The filtrate was concentrated and purified by silica-gel chromatography (2:1 hexanes/ethyl acetate). After removal of solvent, 45 mg (0.245 mmol) of a colorless crystal resulted (68% yield). ^{1}H and ^{13}C NMR matched the values found in literature.[47]

General Procedure for Rhodium and Iridium Complex Formation

Generation of carbene as described for **3-4** was followed. After stirring for 1 hour at -78 °C, $[M(COD)Cl]_2$ (0.5 equiv.) was added, and the reaction slowly warmed to room temperature. Stirring at room temperature proceeded for 12 hours, at which point, solvent was evaporated. To remove any remaining $[M(COD)Cl]_2$, the product was purified by chromatography on a very short pad of silica-gel. Columns were run starting with a mixture of 2:1 hexanes/ethyl acetate and then transferring to pure ethyl acetate. The complexes showed very slight decomposition on silica gel, so the product was further purified by dissolving the product in ethyl acetate and then precipitating impurities with addition of hexanes. The product is sufficiently soluble in hexanes.

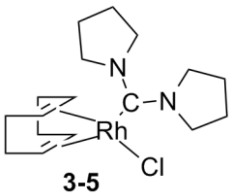

3-5

Chloro(η^4-1,5-cyclooctadiene)-bis(pyrrolidinecarbene)rhodium(I) 3-5. ^{1}H NMR (300MHz, $CDCl_3$) δ = 4.80 (br. s., 4 H), 4.44 (br. s., 2 H), 3.40 (br. s., 4 H), 3.18 (m, 2 H), 2.52 - 2.17 (m, 4 H), 2.10 - 1.71 (m, 12 H). ^{13}C NMR (75MHz, $CDCl_3$) δ = 216.8, 216.2, 96.7, 96.6, 68.3, 68.1, 55.7, 51.9, 32.8, 28.9, 26.5, 24.9. HRMS Calcd. for $C_{17}H_{28}N_2Rh$ $[M\text{-}Cl]^+$: 363.1302, Found: 363.1312.

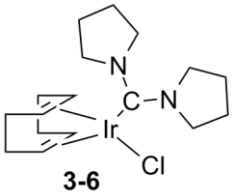

3-6

Chloro(η^4-1,5-cyclooctadiene)-bis(pyrrolidinecarbene)iridium(I) 3-6. ^{1}H NMR (300MHz, $CDCl_3$) δ = 4.53 (br. s., 2 H), 4.35 (br. s., 4 H), 4.23 (br. s., 2 H), 3.48 (br. s., 4 H), 3.03 - 2.68 (m, 2 H), 2.40 - 2.00 (m, 4 H), 1.86 (br. s., 8 H), 1.71 - 1.40 (m, 4 H). ^{13}C NMR (75MHz, $CDCl_3$) δ = 211.7, 81.4, 54.7, 52.0, 33.4, 29.5, 25.7. HRMS Calcd. for $C_{34}H_{56}N_4Ir_2Cl$ $[2M+Cl]^+$: 941.3436, Found: 941.3376.

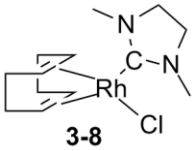

3-8

Chloro(η^4-1,5-cyclooctadiene)-(1,3-dimethylimidazolidin-2-ylidene)iridium(I) 3-8. ^{1}H NMR (300MHz, $CDCl_3$) δ = 4.92 (br. s., 2 H), 4.64 (br. s., 2 H), 3.54 - 3.43 (m, 8 H), 3.33 - 3.18 (m, 2 H), 2.47 - 2.19 (m, 4 H), 2.00 - 1.74 (m, 4 H). ^{13}C NMR (75MHz, $CDCl_3$) δ = 213.2, 212.6, 99.2, 99.1, 68.3, 68.1, 51.7, 37.4, 33.1, 28.9. HRMS Calcd. for $C_{13}H_{22}N_2Rh$ $[M\text{-}Cl]^+$: 309.0833, Found: 309.0834.

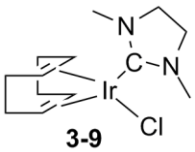

3-9

Chloro(η^4-1,5-cyclooctadiene)-(1,3-dimethylimidazolidin-2-ylidene)iridium(I) 3-9. ^{1}H NMR (300MHz, $CDCl_3$) δ = 4.51 (br. s., 2 H), 3.55 (br. s., 4 H), 3.40 (s, 6 H), 2.98 (br. s., 2 H), 2.16 (br. s., 4 H), 1.78 - 1.54 (m, 4 H). ^{13}C NMR (75MHz, $CDCl_3$) δ = 207.9, 85.0, 52.0, 52.0, 37.2, 33.6, 29.5. HRMS Calcd. for $C_{26}H_{44}N_4Ir_2Cl$ $[2M+Cl]^+$: 833.2495, Found: 833.2419.

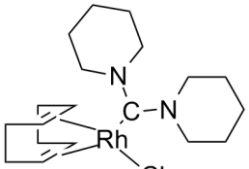

3-12

Chloro(η^4-1,5-cyclooctadiene)-bis(piperidinecarbene)rhodium(I) 3-12. ^{1}H NMR (300MHz, $CDCl_3$) δ = 4.81 (br. s., 2 H), 3.88-3.82 (m, 8 H), 3.17 (br. s., 2 H), 2.27 (br. s., 4 H), 1.82 (m, 4 H), 1.62 (br. s., 12 H). ^{13}C NMR (75MHz, $CDCl_3$) δ = 222.3, 221.7, 97.7, 97.6, 68.1, 67.9, 54.0, 32.8, 28.9, 26.7, 24.5. HRMS Calcd. for $C_{19}H_{32}N_2Rh$ $[M-Cl]^+$: 391.1615, Found: 391.1612.

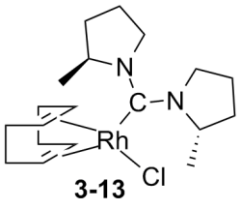

3-13

Chloro(η^4-1,5-cyclooctadiene)-bis((S)-2-methylpyrrolidine)rhodium(I) 3-13. ^{1}H NMR (300MHz, $CDCl_3$) δ = 6.42 (br. s., 1 H), 5.93 (br. s., 1 H), 5.57 (br. s., 0.4 H), 5.09 - 4.62 (m, 2.3 H), 4.23 - 3.70 (m, 1.4 H), 3.28 (br. s., 5 H), 1.82 (br. s., 22 H). ^{13}C NMR (75MHz, $CDCl_3$) δ = 97.0, 97.0, 68.6, 68.4, 66.9, 66.7, 63.3, 61.9, 51.2, 50.9, 34.9, 33.2, 33.0, 32.6, 31.6, 31.1, 29.8, 29.3, 28.6, 28.3, 25.0, 23.3, 23.0, 21.0, 20.5, 14.3. HRMS Calcd. for $C_{19}H_{32}N_2Rh$ $[M-Cl]^+$: 391.1615, Found: 391.1616. $[\alpha]_D^{26}$ -182.6 (*c* 8.3 mg/mL $CHCl_3$).

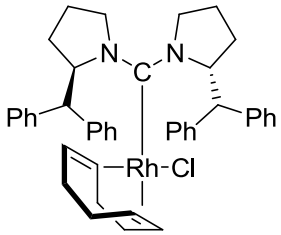

3-15

Chloro(η^4-1,5-cyclooctadiene)-bis((*R*)-2-diphenylmethylpyrrolidine)rhodium(I) 3-15. ^{1}H NMR (300MHz, $CDCl_3$) δ = 7.53 (d, *J* = 7.3 Hz, 2 H), 7.47 - 7.11 (m, 12 H), 6.96 (t, *J* = 6.6 Hz, 1 H), 6.69 - 6.51 (m, 1 H), 5.71 (d, *J* = 3.8 Hz, 1 H), 4.81 (br. s., 2 H), 4.36 (d, *J* = 6.2 Hz, 1 H), 3.20 - 2.99 (m, 2 H), 2.93 (dd, *J* = 5.3, 10.0 Hz, 1 H), 2.83 - 2.60 (m, 2 H), 2.49 - 2.12 (m, 3 H), 2.12 - 1.84 (m, 3 H), 1.84 - 1.40 (m, 7 H), 1.39 - 1.13 (m, 4 H). ^{13}C NMR (75MHz, $CDCl_3$) δ = 222.5, 221.9, 143.3, 143.2, 142.8, 142.6, 142.0, 141.6, 131.0, 129.9, 129.4, 129.3, 129.1, 129.0, 128.8, 128.6, 128.5, 128.4, 128.3, 128.0, 127.5, 127.4, 127.3, 127.1, 126.8, 126.7, 126.5, 126.2, 126.2, 98.1, 98.0, 97.8, 97.7, 78.6, 70.8, 69.5, 69.3, 69.1, 67.7, 67.5, 60.6, 60.0, 56.1, 55.8, 54.5, 54.1, 53.3, 49.0, 32.9, 32.8, 31.2, 31.2, 28.7, 28.6, 28.1, 26.7, 26.0, 25.8, 24.9, 23.8, 21.3, 14.4. HRMS Calcd. for $C_{43}H_{48}N_2Rh$ $[M\text{-}Cl]^+$: 695.2867, Found: 695.2868.

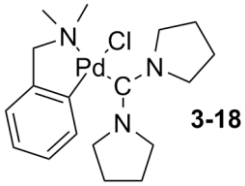

3-18

Chloro(η^2-*N*,*N*-dimethylbenzylamine)-bis(pyrrolidinecarbene)palladium(II) 3-18. To a Schlenk flask in a glovebox, 0.055 g (0.2 mmol) of chloroamidinium **3-1** was added, and the flask was connected to a Schlenk line outside the glovebox. THF (2 mL) was added, and the suspension was cooled to -78 °C with a dry-ice/acetone bath. After cooling, 1.7M *t*-BuLi in hexanes (0.235 mL) was added. After 5 minutes, the suspension turned to a clear and slightly yellowish solution upon formation of carbene. The solution proceeded to stir at -78 °C for a total of 1 hour. After stirring for 1 hour at -78 °C, 0.055 g (0.1 mmol) palladium(η^2-*N*,*N*-

dimethylbenzylamine)chloride dimer was added, and the reaction slowly warmed to room temperature. Stirring at room temperature proceeded for 12 hours, at which point, solvent was evaporated. To remove any remaining metal precursor, the product was purified by chromatography on a short pad of silica-gel. Columns were run starting with ethyl acetate and then transferring to 2.5% MeOH in DCM. ^{1}H NMR (300MHz, $CDCl_3$) δ = 6.93 (br. s., 2 H), 6.82 (m, 1 H), 6.64 (d, *J* = 7.0 Hz, 1 H), 3.74 (br. s., 10 H), 2.66 (s, 6 H), 1.85 (br. s., 8 H). ^{13}C NMR (75MHz, $CDCl_3$) δ = 204.3, 150.3, 148.6, 135.2, 125.8, 123.6, 122.3, 71.9, 50.0, 25.8. HRMS Calcd. for $C_{18}H_{28}N_3Pd$ $[M]^+$: 392.1320, Found: 392.1328.

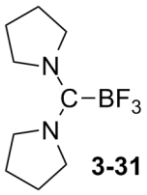

3-31

***N,N,N′,N′*-bis(tetramethylene)-2-formamidinium trifluoroborate 3-31.** Generation of carbene as described for **3-4** was followed with 0.50g (1.82 mmol) of chloroamidinium **3-1**. After stirring for 30 minutes at -78 °C, 0.23 mL (1.82 mmol) of BF_3•Et_2O was added, and the reaction slowly warmed to room temperature. Stirring at room temperature proceeded for 12 hours, at which point, solvent was evaporated. The product was purified by silica gel chromatography (1:1 hexanes:ethyl acetate). ^{1}H NMR (300MHz, $CDCl_3$) δ = 3.59 (br. s., 8 H), 1.73 (br. s., 8 H). ^{13}C NMR (75MHz, $CDCl_3$) δ = 180.3, 52.8, 25.4. ^{19}F NMR (282MHz, $CDCl_3$) δ = 138.95 (q, *J* = 45 Hz). Anal Calcd for $C_9H_{16}N_2BF_3$: C, 49.13; H, 7.33; N, 12.73. Found: C, 49.374; H, 7.528; N, 12.591.

General Procedure for 1,4 Conjugate Addition

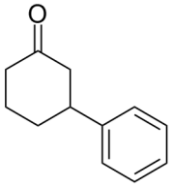

3-Phenyl Cyclohexanone. To a flame dried Schlenk flask under argon, 126 mg (1.04 mmol) of phenyl boronic acid, 29 mg (0.52 mmol) of potassium hydroxide, and 2 mg (0.0052 mmol) of rhodium catalyst **3-5** were added. 1 mL of THF and 0.1 mL of water was added, and to the reaction mixture, 50 mg (0.52 mmol) of cyclohexenone was added. The solution was heated to 40 °C. The mixture was stirred for thirty minutes and monitored by TLC (R_f 0.63, 2:1 hexanes/ethyl acetate). The solution was diluted with 10 mL of diethyl ether and washed twice with a 10% aqueous solution of NaOH. The organic layer was dried and concentrated, and then purified by silica-gel chromatography (4:1 hexanes/ethyl acetate) to isolate the product as a clear oil in 98% yield. Spectroscopic values matched those reported in the literature.[48] ^{1}H NMR (300MHz, $CDCl_3$) δ = 7.39 - 7.28 (m, 2 H), 7.28 - 7.15 (m, 3 H), 3.12 - 2.89 (m, 1 H), 2.66 - 2.26 (m, 4 H), 2.25 - 1.99 (m, 2 H), 1.95 - 1.65 (m, 2 H). ^{13}C NMR (75MHz, $CDCl_3$) δ = 211.3, 144.6, 128.9, 126.9, 126.8, 49.2, 45.0, 41.4, 33.0, 25.8.

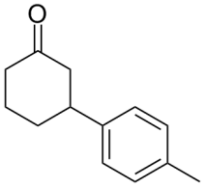

3-(*p*-Tolyl)-Cyclohexanone. Spectroscopic values matched those reported in the literature.[4] ^{1}H NMR (300MHz, $CDCl_3$) δ = 7.27 - 7.01 (m, 4 H), 3.16 - 2.86 (m, 1 H), 2.69 - 2.39 (m, 4 H), 2.35 (s, 4 H), 2.23 - 2.02 (m, 2 H), 1.93 - 1.68 (m, 2 H). ^{13}C NMR (75MHz, $CDCl_3$) δ = 211.3, 141.7, 136.4, 129.6, 126.7, 49.3, 44.6, 41.4, 33.1, 25.8, 21.2.

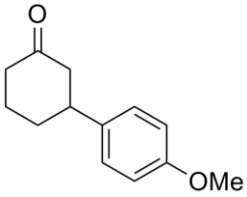

3-(*p*-Anisoyl) Cyclohexanone. Spectroscopic values matched those reported in the literature.[4] ^{1}H NMR (300MHz, $CDCl_3$) δ = 7.22 - 7.04 (d, *J* = 7.6 Hz, 2 H), 6.96 - 6.75 (d, *J* = 7.6 Hz, 2 H), 3.77 (s, 3 H), 3.06 - 2.81 (m, 1 H), 2.64 - 2.24 (m, 4 H), 2.22 - 1.93 (m, 2 H), 1.91 - 1.61 (m, 2 H). ^{13}C NMR (75MHz, $CDCl_3$) δ = 211.4, 158.5, 136.8, 127.7, 114.2, 55.5, 49.4, 44.2, 41.4, 33.2, 25.7.

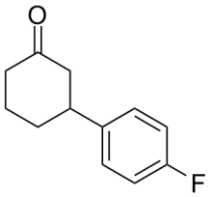

3-(*p*-Fluorophenyl) Cyclohexanone. Spectroscopic values matched those reported in the literature.[4] ^{1}H NMR (300MHz, $CDCl_3$) δ = 7.25 - 7.06 (m, 2 H), 6.97 (t, *J* = 8.2 Hz, 2 H), 3.08 - 2.86 (m, 1 H), 2.63 - 2.24 (m, 4 H), 2.21 - 1.93 (m, 2 H), 1.90 - 1.66 (m, 2 H). ^{13}C NMR (75MHz, $CDCl_3$) δ = 210.9, 163.3, 160.1, 140.3, 128.3, 128.2, 115.7, 115.5, 49.2, 44.2, 41.3, 33.1, 25.6.

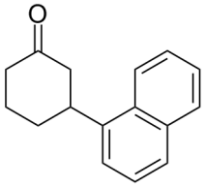

3-(1-Naphthyl) Cyclohexanone. Spectroscopic values matched those reported in the literature.[49] ^{1}H NMR (300MHz, $CDCl_3$) δ = 8.05 (d, *J* = 7.9 Hz, 1 H), 7.88 (d, *J* = 7.6 Hz, 1 H), 7.77 (d, *J* = 7.9 Hz, 1 H), 7.63 - 7.30 (m, 4 H), 3.86 (t, *J* = 11.1 Hz, 1 H), 2.82 - 2.73 (m, 1 H), 2.71 - 2.40 (m, 3 H), 2.36 - 2.10 (m, 2 H), 1.98 (t, *J* = 10.8 Hz, 2 H). ^{13}C NMR (75MHz, $CDCl_3$)

δ = 211.5, 140.3, 134.2, 131.1, 129.3, 127.5, 126.5, 125.9, 125.8, 123.0, 122.7, 48.8, 41.7, 39.6, 32.5, 25.8.

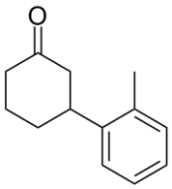

3-*(o*-Tolyl)-Cyclohexanone. Spectroscopic values matched those reported in the literature.[50] ^{1}H NMR (300MHz, $CDCl_3$) δ = 7.43 - 7.03 (m, 4 H), 3.23 (d, *J* = 8.8 Hz, 1 H), 2.61 - 2.36 (m, 4 H), 2.34 (s, 3 H), 2.18 (td, *J* = 2.5, 6.5 Hz, 1 H), 2.09 - 1.95 (m, 1 H), 1.93 - 1.73 (m, 2 H). ^{13}C NMR (75MHz, $CDCl_3$) δ = 211.4, 142.6, 135.3, 130.9, 126.7, 126.6, 125.3, 48.6, 41.5, 40.5, 32.2, 26.0, 19.5.

General Procedure for Formation of Biaryl Methanols

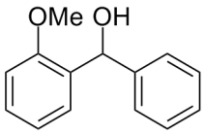

2-Methoxyphenyl-Phenyl-methanol. To a flame dried Schlenk flask under argon, 50 mg (0.364 mmol) of *o*-anisaldehyde, 89 mg (0.728 mmol) of phenyl boronic acid, 83 mg (0.728 mmol) of potassium *tert*-butoxide, and 2 mg (0.0052 mmol) of rhodium catalyst **3-5** were added. 1.22 mL of DME and 0.33 mL of water were added, and the solution was heated to 40 °C. The mixture was stirred for one hour and monitored by TLC (R_f 0.38, 4:1 hexanes/ethyl acetate). The solution was diluted with 10 mL of diethyl ether and 10 mL of water and was then extracted three times. The organic layer was dried and concentrated, and then purified by silica-gel chromatography (8:1 hexanes/ethyl acetate) to isolate the product as a clear oil in 92% yield. Spectroscopic values matched those reported in the literature.[51] ^{1}H NMR (300MHz, $CDCl_3$) δ = 7.49 - 7.11 (m, 8 H), 7.07 - 6.82 (m, 2 H), 6.07 (s, 1 H), 3.78 (s, 3 H), 3.32 (br. s., 1 H). ^{13}C

NMR (75MHz, $CDCl_3$) δ = 156.9, 143.5, 132.2, 129.7, 129.0, 128.4, 128.1, 127.4, 126.8, 121.1, 115.6, 111.0, 72.4, 55.7. HRMS Calcd. for $C_{14}H_{13}O$ $[M\text{-}OH]^+$: 197.0989, Found: 197.0994.

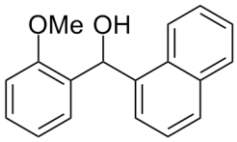

2-Methoxyphenyl-Naphthalen-1-yl Methanol. ^1H NMR (299MHz, $CDCl_3$) δ = 8.05 (d, *J* = 7.4 Hz, 1 H), 7.96 - 7.79 (m, 2 H), 7.71 (d, *J* = 7.1 Hz, 1 H), 7.60 - 7.39 (m, 3 H), 7.37 - 7.22 (m, 1 H), 7.11 - 6.78 (m, 4 H), 3.91 (s, 3 H), 3.22 (br. s., 1 H). ^{13}C NMR (75MHz, $CDCl_3$) δ = 157.2, 138.4, 134.0, 131.6, 131.3, 129.2, 128.9, 128.7, 128.3, 126.2, 125.7, 124.6, 124.5, 121.1, 110.8, 68.6, 55.8. HRMS Calcd. for $C_{18}H_{15}O$ $[M\text{-}OH]^+$: 247.1177, Found: 247.1176.

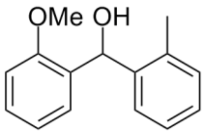

2-Methoxyphenyl-*o*-Tolyl Methanol. ^1H NMR (299MHz, $CDCl_3$) δ = 7.66 - 7.46 (m, 1 H), 7.43 - 7.13 (m, 4 H), 7.12 - 6.83 (m, 3 H), 6.32 (s, 1 H), 3.88 (s, 3 H), 3.00 (br. s., 1 H), 2.27 (s, 3 H). ^{13}C NMR (75MHz, $CDCl_3$) δ = 157.3, 140.8, 135.8, 131.5, 130.4, 129.1, 128.1, 127.5, 126.8, 126.2, 121.0, 110.7, 68.5, 55.7, 19.5. HRMS Calcd. for $C_{15}H_{15}O$ $[M\text{-}OH]^+$: 211.1176, Found: 211.1185.

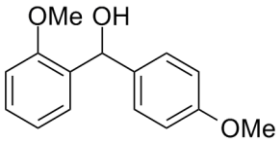

2-Methoxyphenyl-4-Methoxyphenyl Methanol. ^1H NMR (300MHz, $CDCl_3$) δ = 7.60 - 7.17 (m, 4 H), 7.11 - 6.73 (m, 4 H), 6.05 (s, 1 H), 3.79 (s, 6 H), 3.30 (br. s., 1 H). ^{13}C NMR (75MHz, $CDCl_3$) δ = 159.0, 156.9, 136.0, 132.6, 128.8, 128.1, 127.8, 121.0, 113.8, 111.0, 71.7, 55.6, 55.5. HRMS Calcd. for $C_{15}H_{14}O_2$ $[M\text{-}OH]^+$: 226.0994, Found: 226.0987.

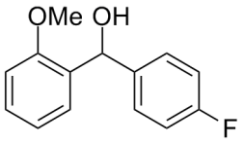

4-Fluorophenyl-2-Methoxyphenyl Methanol. ^{1}H NMR (300MHz, $CDCl_3$) δ = 7.55 - 7.19 (m, 4 H), 7.13 - 6.79 (m, 4 H), 6.03 (br. s., 1 H), 3.80 (s, 3 H), 3.27 (br. s., 1 H). ^{13}C NMR (75MHz, $CDCl_3$) δ = 163.8, 160.6, 156.8, 139.4, 139.4, 132.1, 129.1, 128.5, 128.4, 127.8, 121.1, 115.3, 115.0, 111.0, 71.7, 55.6. HRMS Calcd. for $C_{14}H_{13}O_2F$ $[M]^+$: 232.0900, Found: 232.0886.

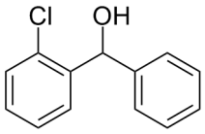

2-Chlorophenyl-Phenyl Methanol. Spectroscopic values matched those reported in the literature. ^{1}H NMR (299MHz, $CDCl_3$) δ = 7.62 (dd, *J* = 1.4, 7.6 Hz, 1 H), 7.51 - 7.11 (m, 8 H), 6.37 - 6.05 (m, 1 H), 2.88 - 2.58 (m, 1 H). ^{13}C NMR (75MHz, $CDCl_3$) δ = 142.5, 141.3, 132.7, 129.8, 129.0, 128.7, 128.3, 128.0, 127.4, 127.2, 72.9. HRMS Calcd. for $C_{13}H_{10}Cl$ $[M\text{-}OH]^+$: 201.0446, Found: 201.0472.

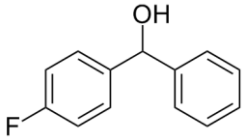

4-Fluorophenyl-Phenyl Methanol. Spectroscopic values matched those reported in the literature.[52] ^{1}H NMR (300MHz, $CDCl_3$) δ = 7.45 - 7.18 (m, 7 H), 7.09 - 6.85 (m, 2 H), 5.74 (s, 1 H), 2.63 (br. s., 1 H). ^{13}C NMR (75MHz, $CDCl_3$) δ = 164.0, 160.7, 143.8, 139.8, 139.7, 130.1, 128.8, 128.6, 128.5, 128.4, 127.9, 126.7, 115.6, 115.3, 75.8. HRMS Calcd. for $C_{13}H_9F$ $[M\text{-}OH]^+$: 185.0761, Found: 185.0772.

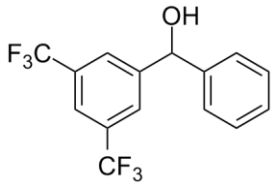

3,5-Bis(Trifluoromethyl)phenyl-Phenyl Methanol. ^{1}H NMR (300MHz, $CDCl_3$) δ = 7.87 (s, 2 H), 7.79 (s, 1 H), 7.55 - 7.19 (m, 5 H), 5.91 (s, 1 H), 2.50 (br. s., 1 H). ^{13}C NMR (75MHz, $CDCl_3$) δ = 146.3, 142.6, 132.1, 131.7, 129.3, 128.8, 126.9, 126.7, 121.7, 121.6, 75.5. HRMS Calcd. for $C_{15}H_{10}F_6$ $[M]^+$: 320.0636, Found: 320.0623.

NMR of Carbene Intermediate

The carbene was generated at -78 °C, in THF-d_8, and analyzed by NMR spectroscopy at -30 °C. First, gHMBC, gHMQC and gDQCOSY experiments were run in about 30 minutes, to quickly characterize the carbene, presumed unstable. The carbene carbon, at 232.9 ppm, displayed couplings in the gHMBC spectrum with two protons, at 3.47 and 3.66 ppm, both triplets. The gDQCOSY spectrum revealed the sequence 3.47–1.89–1.76– 3.66. The carbons carrying these protons were detected in the gHMQC spectrum at 48.4, 26.5, 24.5 and 55.8 correspondingly. The non-equivalence of the alpha positions in the tetrahydropyrrole moiety indicates restricted rotation about the carbene carbon – nitrogen bond.

NMR spectra were recorded on a Varian Inova spectrometer, operating at 500 MHz for ^{1}H and 125 MHz for ^{13}C, and equipped with a 5 mm indirect detection probe, with z-axis gradients. The ^{1}H and ^{13}C chemical shifts were referenced to internal tetramethylsilane. The solvent was THF-d_8, and the temperature -30 °C. The gHMBC experiment was run with the standard vnmr pulse sequence. 2048 points were acquired in f2, on a spectral window from 0.1 to 4.3 ppm. The acquisition time was 0.49 s, with a relaxation delay of 0.5 s. 512 increments were

acquired in f1, for a spectral window from 0 to 300 ppm, in 1 transient per increment. The total experiment time was 9 minutes.

The gHMQC experiment was run with the standard vnmr pulse sequence. 1024 points were acquired in f2, on a spectral window from 0.5 to 4.0 ppm. The acquisition time was 0.29 s, with a relaxation delay of 1 s. 256 increments were acquired in f1, for a spectral window from 10 to 80 ppm, in 1 transient per increment. The total experiment time was 6 minutes.

The gDQCOSY experiment was run with the standard vnmr pulse sequence. 2048 points were acquired in f2, on a spectral window from 0.64 to 3.64 ppm. The acquisition time was 0.64 s, with a relaxation delay of 1 s. 512 increments were acquired in f1, in 1 transient per increment. The total experiment time was 16 minutes.

LIST OF REFERENCES

1) (a) Kantchev, E. A. B.; O'Brien, C. J.; Organ, M. G. *Angew. Chem. Int. Ed*. **2007,** *46,* 2768-2813. (b) Clavier, H.; Nolan, S. P. *Annu. Rep. Prog. Chem.*, **2007,** *103,* 193-222. (c) Glorius, F. *Top. Organomet. Chem.* **2007,** *21,* 1-20. (d) Nolan, S. P., Ed. *N-heterocyclic Carbenes in Synthesis*; Wiley-VCH: Weinheim, Germany, 2006. (e) Garrison, J. C.; Youngs, W. J. *Chem. Rev.* **2005,** *105,* 3978-4008. (f) Peris, E. V.; Crabtree, R. H. *Coord. Chem. Rev.* **2004,** *248,* 2239-2246. (g) Crudden, C. M.; Allen, D. P. *Coord. Chem. Rev.* **2004,** *248,* 2247-2273. (h) Herrmann, W. A. *Angew. Chem. Int. Ed.* **2002,** *41,* 1290-1309. (i) Alder, R. W. "Diaminocarbenes: Exploring Structure and Reactivity," In *Carbene Chemistry, from Fleeting Intermediates to Powerful Reagents*; Bertrand, G. Ed.; Marcel Denker: New York, 2002, 153-230. (j) Bourissou, D.; Guerret, O.; Gabbai, F. P.; Bertrand, G. *Chem. Rev.* **2000,** *100,* 39-91. (k) Arduengo, A. J., III *Acc. Chem. Res*. **1999,** *32,* 913-921. (l) Arduengo, A. J., III; Harlow, R. L.; Kline, M. *J. Am. Chem. Soc.* **1991,** *113,* 361-363.

2) Green, J. C.; Scur, R. G.; Arnold, P. L.; Cloke, G. N. *Chem. Commun.* **1997,** 1963-1964.

3) (a) Diez-Gonzalez, S.; Nolan, S. P. *Coord. Chem. Rev.* **2007,** *251,* 874-883. (b) Crabtree, R. H. *J. Organomet. Chem.* **2005,** *690,* 5451-5457. (c) Alder, R. W.; Blake, M. E.; Chaker, L.; Harvey, J. N.; Paolini, F.; Schütz, J. *Angew. Chem. Int. Ed*. **2004,** *43,* 5896-5911.

4) (a) Rogers, M. M.; Stahl, S. S. *Top. Organomet. Chem.* **2007,** *21,* 21-46. (b) Chianese, A. R.; Kovacevic, A.; Zeglis, B. M.; Faller, J. W.; Crabtree, R. H. *Organometallics* **2004,** *23,* 2461-2468. (c) Chianese, A. R.; Li, X.; Janzen, M. C.; Faller, J. W.; Crabtree, R. H. *Organometallics* **2003,** *22,* 1663-1667.

5) (a) Trnka, T. M.; Morgan, J. P.; Sanford, M. S.; Wilhelm, T. E.; Scholl, M.; Choi, T. L.; Ding, S.; Day, M. W.; Grubbs, R. H. *J. Am. Chem. Soc.* **2003,** *125,* 2546-2558. (b) Sanford, M. S.; Love, J. A.; Grubbs, R. H. *J. Am. Chem. Soc.* **2001,** *123,* 6543-6549.

6) (a) Grey, G. D.; Herdtweck, E.; Herrmann, W. A. *J. Organomet. Chem.* **2006,** *691,* 2465-2478. (b) Frey, G. D.; Herrmann, W. A. *J. Organomet. Chem.* **2005,** *690,* 5876-5880. (c) Alder, R. W.; Blake, M. E.; Chaker, L.; Harvey, J. N.; Paolini, F.; Schatz, J. *Angew. Chem.,Int. Ed.* **2004,** *43,* 5896-5911. (d) Herrmann, W. A.; Ofele, K.; Preysing, D.; Herdtweck, E. *J. Organomet. Chem.* **2003,** *684,* 235-248. (e) Alder, R. W.; Blake, M. E.; Bufali, S.; Butts, C. P.; Orpen, A. G.; Schutz, J.; Williams, S. J. *J. Chem Soc., Perkin Trans. 1,* **2001,** 1586-1593. (f) Alder, R. W.; Allen, P. R.; Murray, M.; and Orpen, A. G. *Angew. Chem., Int. Ed.* **1996,** *35,* 1121-1123.

7) (a) Wanniarachchi, Y. A.; Slaughter, L. M. *Chem. Commun.* **2007,** 3294-3296. (b) Dhudshia, B.; Thadani, A. N. *Chem. Commun.* **2006,** 668-670. (c) Kremzow, D.; Seidel, G.; Lehmann, C. W.; Fürstner, A. *Chem. Eur. J.* **2005,** *11,* 1833-1853. (d) Fürstner, A.; Seidel, G.; Kremzow, D.; Lehmann, C. W. *Organometallics* **2003,** *22,* 907-909.

8) (a) McGuinness, D. S.; Cavell, K. J.; Yates, B. F.; Skelton, B. W.; White, A. H. *J. Am. Chem. Soc.* **2001,** *123,* 8317-8328. (b) Fraser, P. J.; Roper, W. R.; Stone, F. G. A. *J. Chem. Soc. Dalt. Trans. 1.* **1974,** 760-764.

9) (a) Altenhoff, G.; Goddard, R.; Lehmann, C. W.; Glorius, F. *J. Am. Chem. Soc.* **2004,** *126,* 15195-15201. (b) Altenhoff, G.; Goddard, R.; Lehmann, C. W.; Glorius, F. *Angew. Chem., Int. Ed.* **2003,** *42,* 3690-3693.

10) Kerr, M. S.; Read de Alaniz, J.; Rovis, T. *J. Org. Chem.* **2005,** *70,* 5725-5728.

11) (a) Marion, N.; Navarro, O.; Mei, J.; Stevens, E. D.; Scott, N. M.; Nolan, S. P. *J. Am. Chem. Soc.* **2006,** *128,* 4101-4111. (b) Christmann, U.; Vilar, R. *Angew. Chem., Int. Ed.* **2005,** *44,* 366-374. (c) Suzuki, A. *Proc. Jpn. Acad., Ser. B* **2004,** *80,* 359-371. (d) Bellina, F.; Carpita, A.; Rossi, R. *Synthesis* **2004,** *15, 2419-2440.*

12) (a) Genov, M.; Almorin, A.; Espinet, P. *Chem. Eur. J.* **2006,** *12,* 9346-9352. (b) Baudoin, O. *Eur. J. Org. Chem.* **2005,** 4223-4229. (c) Mikami, K.; Miyamoto, T.; Hatano, M. *Chem. Commun.* **2004,** 2082-2083. (d) Cammidge, A. N.; Crepy, K. V. L *Tetrahedron* **2004,** *60,* 4377-4386. (e) Jensen, J. F.; Johannsen, M. *Org. Lett.* **2003,** *5,* 3025-3028. (f) Castanet, A.; Colobert, F.; Broutin, P.; Orbringer, M. *Tetrahedron: Asymmetry* **2002,** *13,* 659-665. (g) Yin, J.; Buchwald, S. L. *J. Am. Chem. Soc.* **2000,** *122,* 12051-12052. (h) Cammidge, A. N.; Crepy, K. V. L. *Chem. Commun.* **2000,** 1723-1724.

13) Aldous, D. J.; Dutton, W. M.; Steel, P. G. *Tetrahedron: Asymmetry* **2000,** *11,* 2455-2462.

14) (a) Hernández-Rodríguez, M.; Avila-Ortiz, C. G.; del Campo, J. M.; Hernández-Romero, D.; Rosales-Hoz, M.; Juaristi, E. *Aust. J. Chem.* **2008,** *61,* 364-375. (b) Berg, S. S.; Cowling, T. *J. Chem. Soc. (C)* **1971,** 1653-1658.

15) (a) Würtz, S.; Glorius, F. *Acc. Chem. Res.* **2008,** *41,* 1523-1533. (b) Anderson, D. R.; Lavallo, V.; O'Leary, D. J. Bertrand, G.; Grubbs, R. H. *Angew. Chem., Int. Ed.* **2007,** *46,* 7262-7265.

16) (a) Snead, D. R.; Ghiviriga, I.; Abboud, K. A.; Hong, S. *Org. Lett.* **2009,** *ASAP*.

17) Rappoport, Z.; Marek, I., Eds. *The Chemistry of Organolithium Compounds;* John Wiley and Sons Ltd.: Chichester, England, 2004; Part 1 and 2 of Vol. 2.

18) (a) Najera, C.; Sansano, J. M.; Yus, M. *Tetrahedron* **2003,** *59,* 9255-9303. (b) Yus, M. *Chem. Soc. Rev.* **1996,** 155-161.

19) (a) Anctil, E. J.; Snieckus, V. in *Metal-Catalyzed Cross-Coupling Reactions* 2nd Ed.; de Meijere, A.; Diederich F. Eds; Wiley-VCH: Weinheim, Germany, 2004; pp 761-813. (b) Beak, P.; Johnson, T. A.; Kim, D. D.; Lim, S. H. *Top. Organomet. Chem.* **2003,** *5,* 139-176.

20) (a) Bailey, W. F.; Patricia, J. J. *J. Organomet. Chem.* **1988,** *352,* 1-46. (b) Jones, R. G.; Gilman, H. in *Organic Reactions;* Adams, R., Ed.; Wiley: New York, 1951; Vol. 6, pp 339-366.

21) (a) Pereyre, M.; Quintard, J.-P.; Rahm, A. *Tin in Organic Synthesis;* Butterworths: Stoneham, 1986. (b) Seyferth, D.; Weiner, M. A. *J. Org. Chem.* **1959,** *24,* 1395-1396.

22) (a) Köbrich, G.; Fischer, R. H. *Tetrahedron* **1968,** *24,* 4343-4346. (b) Dilling, W. L.; Edamura, F. Y. *J. Org. Chem.* **1967,** *32,* 3492-3499.

23) (a) Luu, T.; Morisaki, Y.; Cunningham, N.; Tykwinski, R. R. *J. Org. Chem.* **2007,** *72,* 9622-9629. (b) Fritsch, P. *Liebigs Ann. Chem.* **1894,** *279,* 319-323. (c) Buttenberg, W. P. *Liebigs Ann. Chem.* **1894,** *279,* 324-337. (d) Wiechell, H. *Liebigs Ann. Chem.* **1894,** *279,* 337-344.

24) Tapu, D.; Dixon, D. A.; Roe, C. *Chem. Rev.* **2009,** in press.

25) Cope, A. C.; Friedrich, E. C. *J. Am. Chem. Soc.* **1968,** *90,* 909-913.

26) (a) Holschumacher, D.; Bannenberg, T.; Hrib, C. G.; Jones, P. G.; Tamm, M. *Angew. Chem., Int. Ed.* **2008,** *47,* 7428-7432. (b) Phillips, A. D.; Power, P. P. *Acta Cryst.* **2005,** *C61,* 291-293. (c) Arduengo, A. J., III; Davidson, F.; Krafczyk, R.; Marshall, W. J.; Schmutzler, R. *Monatsh Chem.* **2000,** *131,* 251-265.

27) Alder, R. W.; Blake, M. E. *Chem. Commun.* **1997,** 1513-1514.

28) (a) Que, L.; Tolman, W. B.; *Nature* **2008,** 333-340. (b) Enthaler, S.; Junge, K.; Beller, M. *Angew. Chem., Int. Ed.* **2008,** *47,* 3317-3321. (c) Bolm, C.; Legros, J.; Le Paih, J.; Zani, L. *Chem. Rev.* **2004,** *104,* 6217-6254.

29) Reich, H. J.; Green, P.; Medina, M. A.; Goldenberg, W. S.; Gudmundsson, B.; Kykstra, R. R.; Phillips, N. H. *J. Am. Chem. Soc.* **1998,** *120,* 7201-7210.

30) (a) Evans, P. A., Ed. *Modern Rhodium-Catalyzed Organic Reactions* Wiley-VCH: Weinheim, Germany, 2005. (b) Fagnou, K.; Lautens, M. *Chem. Rev.* **2003,** *103,* 169-196.

31) (a) Trost, B. M.; McClory, A. *Angew. Chem., Int. Ed.* **2007,** *46,* 2074-2077. (b) Joo, J. M.; Yuan, Y.; Lee, C. *J. Am. Chem. Soc.* **2006,** *128,* 14818-14819. (c) Murakami, M. *Angew. Chem., Int. Ed.* **2003,** *42,* 718-720. (d) Varela, J. A.; Saa, C. *Chem. Rev.* **2003,** *103,* 3787-3801.

32) (a) Doyle, M. P.; McKervey, M. A.; Ye, T. *Modern Catalytic Methods for Organic Synthesis with Diazo Compounds: From Cyclopropanes to Ylides* Wiley: New York, NY, 1998. (b) Ye, T.; McKervey, A. *Chem. Rev.* **1994,** *94,* 1091-1160.

33) (a) Colby, D. A.; Bergman, R. G.; Ellman, J. A. *Chem. Rev.* **2009,** ASAP. (b) Lewis, J. C.; Bergman, R. G.; Ellman, J. A. *Acc. Chem. Res.* **2008,** *41,* 1013-1025. (c) Lawrence, J. D.; Takahashi, M.; Bae, C.; Hartwig, J. F. *J. Am. Chem. Soc.* **2004,** *126,* 15334-15335.

(d) Chen, H.; Schlecht, S.; Semple, T. C.; Hartwig, J. F. *Science* **2000,** *287,* 1995-1997. (e) Crabtree, R. H. *Dalton* **2001,** 2437-2450. (f) Kakiuchi, F.; Murai, S. *Top. Organomet. Chem.* **1999,** *3,* 47-79.

34) (a) Defieber, C.; Grutzmacher, H.; Carreira, E. M. *Angew. Chem., Int. Ed.* **2008,** *47,* 4482-4502. (b) Christoffers, J.; Koripelly, G.; Rosiak, A.; Roessle, M. *Synthesis*, **2007,** 1279-1300. (c) Yoshida, K.; Hayashi, T. In *Modern Rhodium-Catalyzed Organic Reactions*; Evans, P. A., Ed.; Wiley-VCH: Weinheim, Germany, 2005; pp 55-77. (d) Glorius, F. *Angew. Chem., Int. Ed.* **2004,** *43,* 3364-3366. (e) Hayashi, T.; Yamasaki, K. *Chem. Rev.* **2003,** *103,* 2829-2844.

35) (a) Okamoto, K.; Hayashi, T.; Rawal, V. H. *Org. Lett.* **2008,** *10,* 4387-4389. (b) Kina, A.; Iwamura, H.; Hayashi, T. *J. Am. Chem. Soc.* **2006,** *128,* 3904-3905. (c) Paquin, J.; Defieber, C.; Stephenson, C. R. J.; Carreira, E. M. *J. Am. Chem. Soc.* **2005,** *127,* 10850-10851. (d) Hayashi, T.; Takahashi, M.; Takaya, Y.; Ogasawara, M. *J. Am. Chem. Soc.* **2002,** *124,* 5052-5058.

36) (a) Miyaura, N. *Bull. Chem. Soc. Jpn.* **2008**, *81,* 1535-1553. (b) Darses, S.; Genet, J.-P. *Chem. Rev.* **2008,** *108,* 288-325. (c) Schmidt, F.; Stemmler, R. T.; Rudolph, J.; Bolm, C. *Chem. Soc. Rev.* **2006,** *35,* 454-470.

37) (a) Trindade, A. F.; Gois, P. M. P.; Veiros, L. F.; André, V.; Duarte, M. T.; Afonso, C. A. M.; Caddick, S.; Cloke, F. G. N. *J. Org. Chem.* **2008,** *73,* 4076-4086. (b) Jagt, R. B. C.; Toullec, P. Y.; de Vries, J. G.; Feringa, B. L.; Minnaard, A. J. *Org. Biomol. Chem.* **2006,** *4,* 773-775. (c) Duan, H.-F.; X. J.-H.; Shi, W.-J.; Zhang, Q.; Zhou, Q.-L. *Org. Lett.* **2006,** *8,* 1479-1481. (d) Focken, T.; Rudolph, J.; Bolm, C. *Synlett* **2005,** 429-436. (e) Pucheault, M.; Darses, S.; Genet, J.-P. *Chem. Commun.* **2005,** 4714-4716. (f) Imlinger, N.; Mayr, M.; Wang, D.; Wurst, K.; Buchmeiser, M. R. *Adv. Synth. Catal.* **2004,** *346,* 1836-1843. (g) Fürstner, A.; Krause, H. *Adv. Synth. Catal.* **2001,** *343,* 343-350. (h) Sakai, M.; Ueda, M.; Miyaura, N. *Angew. Chem., Int. Ed.* **1998,** *37,* 3279-3281.

38) (a) Hayashi, T.; Takahashi, M.; Takaya, Y.; Ogasawara, M. *J. Am. Chem. Soc.* **2002,** *124,* 5052-5058. (b) Grushin, V. V.; Kuznetsov, V. F.; Benimon, C.; Alper, H. *Organometallics* **1995,** *14,* 3927-3932. (c) Uson, R.; Oro, L. A.; Cabeza, J. A. *Inorg. Synth.* **1985,** *23,* 126-130.

39) (a)Albano, P.; Aresta, M.; Manassero, M. *Inorg. Chem.* **1980,** *19,* 1069-1072. (b)Schrock, R. R.; Osborn, J. A. *Inorg. Chem.* **1970,** *9,* 2339-2343. (c) Nolte, M. J.; Gafner, G.; Haines, L. M. *Chem. Commun.* **1969,** 1406-1407.

40) Johnson, J. B.; Rovis, T. *Angew. Chem., Int. Ed.* **2008,** *47,* 840-871.

41) Arao, T.; Sato, K.; Kondo, K.; Aoyama, T. *Chem. Pharm. Bull.* **2006,** *54,* 1576-1581.

42) Meier, N.; Hahn, F. E.; Pape, T.; Siering, C.; Waldvogel, S. R. *Eur. J. Inorg. Chem.* **2007,** 1210-1214.

43) Zhang, L.; Wu, J. *Adv. Synth. Catal.* **2008,** *350,* 2409-2413.

44) Iyer, S.; Jayanthi, A. *Synlett* **2003,** *8*, 1125-1128.

45) (a) Leuthäuβer, S.; Schwarz, D.; Plenio, H. *Chem. Eur. J.* **2007,** *13*, 7195-7203. (b) Süβner, M.; Plenio, H. *Angew. Chem., Int. Ed.* **2005,** *44*, 6885-6888. (c) Süβner, M.; Plenio, H. *Chem. Commun.* **2005,** 5417-5419.

46) (a) Poater, A.; Cosenza, B.; Correa, A.; Giudice, S.; Ragone, F.; Scarano, V.; Cavallo, L. *Eur. J. Inorg. Chem.* **2009,** 1759-1766. (b) http://www.molnac.unisa.it/OMtools.php (c) Kelly, R. A., III; Clavier, H.; Giudice, S.; Scott, N. M.; Stevens, E. D.; Bordner, J.; Samardjiev, I.; Hoff, C. D.; Cavallo, L.; Nolan, S. P. *Organometallics* **2008,** *27*, 202-210. (d) Dorta, R.; Stevens, E. D.; Scott, N. M.; Costabile, C.; Cavallo, L.; Hoff, C. D.; Nolan, S. P. *J. Am. Chem. Soc.* **2005,** *127*, 2485-2495. (e) Hillier, A. C.; Sommer, W. J.; Yong, B. S.; Petersen, J. L.; Cavallo, L.; Nolan, S. P. *Organometallics* **2003,** *22*, 4322-4326.

47) Yang, D.; Chen, Y.; Zhu, N. *Org. Lett.* **2004,** *6*, 1577-1580.

48) Lu, X.; Lin, S. *J. Org. Chem.* **2005,** *70*, 9651-9653.

49) Cho, C. S.; Motofusa, S.; Ohe, K.; Uemura, S.; Sang, C. *J. Org. Chem.* **1995,** *60*, 883-888.

50) Hayashi, T.; Tokunaga, N.; Yoshida, K.; Han, J. W. *J. Am. Chem. Soc.* **2002,** *124*, 12102-12103.

51) Kuriyama, M.; Shimazawa, R.; Enomota, T.; Shirai, R. . *J. Org. Chem.* **2008,** *73*, 6939-6942.

52) Trindade, A. F.; Gois, P. M. P.; Veiros, L. F.; Andre, V.; Duarte, M. T.; Afonso, C. A. M.; Caddick, S.; Cloke, F. G. N.. *J. Org. Chem.* **2008,** *73*, 4076-4086.

BIOGRAPHICAL SKETCH

David Snead was born in Charlotte, North Carolina on December 31st of 1982, and grew up in Raleigh, North Carolina. After graduating from St. Timothy's-Hale Episcopal High School in 2001, he attended the University of North-Carolina at Chapel Hill where he majored in chemistry. Upon graduation, David married Stephanie Leigh Elder on May 21st of 2005. David went on to pursue his PhD in organic chemistry at the University of Florida under the supervision of Dr. Sukwon Hong, and will pursue postdoctoral opportunities at MIT and Argonne National Laboratories in hopes of attaining a research professorship.